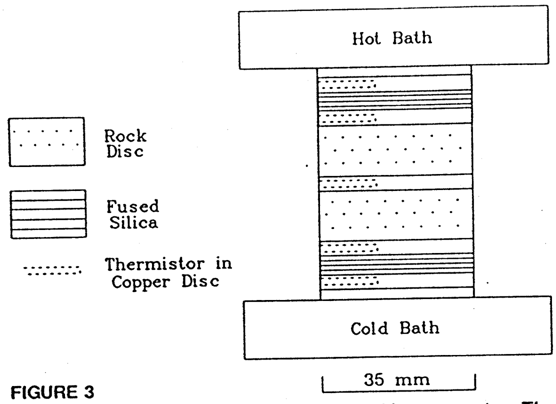

FIGURE 3
Diagrammatic representation of the divided bar apparatus. The whole system is lagged with cotton wool and styrofoam to minimise lateral heat loss and an axial pressure is applied with a hydraulic ram.

resistance. A contact fluid was not used unless explicitly stated (Table 2a) to avoid the possibility of the fluid or grease migrating into the sample. For those samples not measured with dry contacts household detergent was used as a contact medium in the dry state and Vaseline in the wet state. In all cases an axial pressure of 15–30 bars (1.5–3 MPa) was applied axially to the divided bar to improve the thermal contact. The discs were saturated by evacuation and reequilibration to atmospheric pressure under water. Weighing the samples before and after saturation allows the volume percentage of interconnected porespace to be estimated usually to within 1–2% (see table 2b). A slight increase in thickness was observed after saturation for some of the shales suggesting that water had been adsorbed and that the porosity estimates given here may be too high. However these samples had porosities less than 5% and the error is considered negligible. Some of the samples disintegrated during saturation and subsequently were not measured in the wet state. The system was calibrated with quartz discs cut perpendicular to the C optic axis and gave values to within 5% of those quoted by Ratcliffe (1959) (6.32 $Wm^{-1}K^{-1}$). Fused silica standards used during measurement were assumed to have a thermal conductivity of 1.37 $Wm^{-1}K^{-1}$ (Beck 1965). Each sample was measured at least twice to ensure repeatibility to within 5%.

Reduction of results

Fourier's law for the one-dimensional conduction of heat is:

$$Q = -K\, dT/dz \qquad (1)$$

where Q is the heat flux (Wm^{-2}), K the thermal conductivity ($Wm^{-1}K^{-1}$) and dT/dz the temperature gradient (Km^{-1}). The measured temperature difference across a sample (ΔT_o) can be expressed as the sum of the temperature difference due to the sample (ΔT_r) and that due to the contact resistance (ΔT_c) at the upper and lower surfaces and (1) can be restated in terms of the sample thickness (ΔZ_r) and the sample's thermal conductivity (K_t):

$$\Delta T_o/Q = 2\Delta T_c/Q - \Delta Z_r/K_t \qquad (2)$$

By using several discs of different thickness and plotting $\Delta T_o/Q$ against ΔZ_r, a least squares regression line may be calculated for which the contact resistance term ($2\Delta T_c/Q$) is given by the intercept and the true sample conductivity by the inverse of the slope. Neglecting the contact resistance would result in an underestimate of the true conductivity by an amount which increases as the sample thickness decreases (see Fig. 4 and Beck 1976). When only one or two discs were cut for a given sample a range of contact resistances was assumed to estimate the true conductivity. The appropriate ranges were chosen on the basis of grain size, lithology and length of time the samples were in the divided bar apparatus. The significance of the duration of the experiment for the wet measurements is discussed below. The measurements shown in Fig. 4 demonstrate the validity of the contact resistance interpretation.

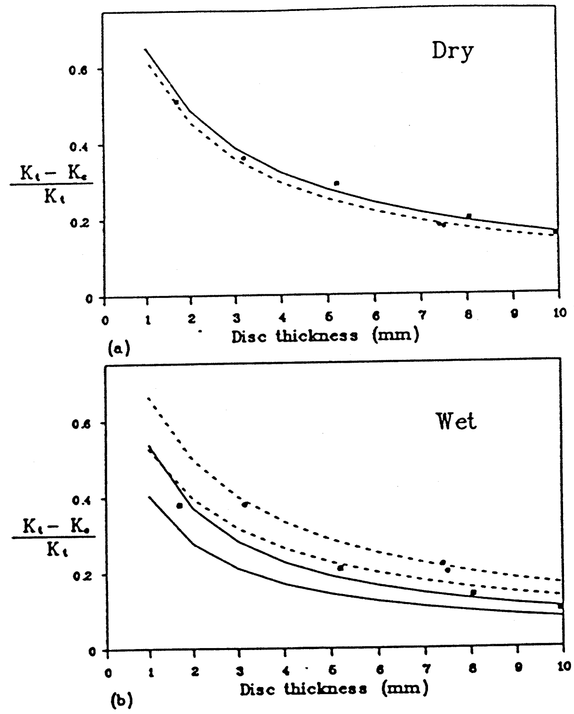

FIGURE 4
The relative error in measured thermal conductivity (K_e) due to neglect of the contact resistance term. K_t is the true sample thermal conductivity. Dullingari 1, depth 2592m: ———, ●, Burley 2, depth 2811 m :- - - - - - - -, ■ . The upper curve for each sample in (b) are calculated assuming dry contacts and the lower curves wet contacts. The curves in (a) assume dry contacts. The contact resistance term is assumed to be equal at both faces of the sample.

Steady state was assumed to have been attained when thermistor readings taken 5–10 minutes apart differed by less than 0.1%. The wet samples did not satisfy this condition after 45–60 minutes and several explanations for this observation were considered. The thermal time constant of the specimen assembly is estimated to be less than 5 minutes so in all cases thermal equilibrium should have been attained. Porous media convection was ruled out as (a) the temperature gradient is positive in the upward direction i.e. water in the samples would be stably stratified and (b) the permeabilities of the samples (measured on set B by Gravestock and Alexander 1986) are too low to allow convection. Some samples were left for up

TABLE 2a

Thermal conductivity (Kdry, Kwet) in $Wm^{-1}K^{-1}$ for sample set A. Observed values are calculated with a least squares regression fit to equation 2 where the inverse of the slope of the line is the true thermal conductivity and the intercept gives the contact resistance term ($2\Delta Tc/Q$). The range values are obtained by assuming a range for the contact resistance term. N is the number of discs, Φ is the measured porosity and Lith. is the lithology (Sd—sandstone, Si—siltstone, Sh—shale, Gr—granite, Bc—boulder clay). An asterix (*) indicates that a contact fluid was used (Vaseline in the wet state and detergent in the dry state). The numbers in brackets for the observed values are the 95% confidence limits on the least squares method estimate of the true thermal conductivity.

Location	Formation	Depth M	Lith.	N	Φ %	Kdry Observed	$2\Delta T_c/Q$	Kdry Range	$2\Delta T_c/Q$	Kwet Observed	$2\Delta T_c/Q$	Kwet Range	$2\Delta T_c/Q$
Innamincka 1	Patchawarra	2080	Sd	4	8.0	4.66 (1.40)	0.95	4.05-4.90	0.8-1.0	6.25 (0.85)	0.9	5.65-6.55	0.1-1.0
Innamincka 1	Patchawarra	2103	Sd	4	16.0	2.85 (0.48)	0.65	2.55-3.00	0.4-0.8	4.17 (0.92)	0.41	3.95-4.45	0.2-0.6
Gidgealpa 1	Nappamerri	2108	Sd	3	15.5	3.54 (1.12)	0.38	3.25-3.87	0.2-0.6	5.80 (0.76)	0.58	5.40-6.27	0.4-0.9
Dullingari 1	Patchawarra	2592	Si	3	6.5	2.50 (0.40)	0.68	2.20-2.68	0.4-0.9	3.10 (0.50)	0.55	2.95-3.40	0.4-0.8
Burley 1	Toolachee	2701	Si	3	4.0	3.56 (0.10)	0.40	3.40-3.80	0.3-0.6	4.50 (0.90)	0.30	4.28-4.95	0.2-0.6
Burley 1	Toolachee	2704	Si	3	6.0	2.77 (0.54)	0.34	2.65-3.20	0.2-0.6	3.20 (0.53)	0.39	2.80-3.65	0.2-0.6
Gidgealpa 2	Toolachee	2091	Sd	2	20.5	-	-	2.35-3.05	0.4-0.9	-	-	3.60-4.30	0.3-0.8
Tirrawarra 2	Patchawarra	2968	Sd	4	13.5	4.98 (1.50)	0.32	4.60-5.30	0.1-0.6	5.40 (0.58)	0.18	5.20-6.00	0.0-0.3
Moomba 1	Basement	2896	Gr	2	0.5	-	-	3.10-3.85	0.2-0.6	-	-	3.35-4.10	0.2-0.6
Burley 1	Toolachee	2698	Sh	3	1.5	2.54 (0.66)	0.76	2.40-2.75	0.6-0.9	2.42 (0.20)	0.50	2.30-2.80	0.4-0.7
Burley 2	Toolachee	2811	Sh	4	1.0	2.40 (0.80)	0.82	2.15-2.70	0.6-1.0	2.24 (0.10)	0.23	2.00 2.50	0.1-0.3
Innamincka 1	Patchawarra	2080	Sh	3	2.0	2.94 (0.70)	0.86	2.75-3.28	0.7-1.0	2.73 (0.20)	0.31	2.30-2.85	0.1-0.5
Tirrawarra 1*	Basement	3068	Sd	4	3.0	4.10 (0.97)	0.00	3.90-4.75	0.0-0.3	5.05 (0.90)	0.10	4.70-5.55	0.0-0.3
Gigdealpa 1*	Basement	2871	Sh	4	0.5	2.50 (0.13)	0.00	2.40-2.85	0.0-0.3	2.45 (0.20)	0.00	2.35-2.70	0.0-0.3
Innamincka 1	Allaru	623	Sh	1	19.0	-	-	1.10-1.30	0.1-2.0	-	-	1.70-2.20	0.1-1.2
Innnamincka 1	Cadna-Owie	1201	Sh	2	10.5	-	-	1.15-1.75	0.3-1.0	-	-	1.75-2.40	0.3-1.0
Innamincka 1	Cadna-Owie	1230	Sh	2	11.5	-	-	1.05-1.50	0.3-1.0	-	-	-	-
Innamincka 1	Nappamerri	1996	Sh	2	1.5	-	-	2.15-2.60	0.1-1.0	-	-	2.10-3.10	0.1-1.0
Dullingari 1	Winton	427	Sh	1	33.0	-	-	0.85-1.20	0.3-2.5	-	-	-	-
Dullingari 1	Wallumbilla	1210	Sh	1	15.5	-	-	1.55-1.85	0.3-1.0	-	-	1.85-2.35	0.3-1.0
Dullingari 1	Cadna-Owie	1375	Si	1	15.0	-	-	1.10-1.45	0.3-1.0	-	-	-	-
Dullingari 1	Nappamerri	2010	Sh	1	4.0	-	-	2.35-3.15	0.4-0.9	-	-	2.40-3.15	0.2-0.7
Dullingari 1	Toolachee	2106	Si	2	4.0	-	-	2.10-2.65	0.4-0.9	-	-	2.00-2.45	0.2-0.5
Dullingari 1	Roseneath	2281	Sh	2	2.5	-	-	1.95-2.55	0.4-0.9	-	-	2.15-2.75	0.2-0.6
Dullingari 1	Epsilon	2321	Si	1	2.0	-	-	2.30-2.85	0.2-0.9	-	-	2.75-3.50	0.2-0.7
Dullingari 1	Murteree	2409	Sh	1	1.5	-	-	2.20-2.55	0.3-0.9	-	-	2.35-2.85	0.2-0.7
Dullingari 1	Merrimelia	2743	Bc	2	2.0	-	-	2.65-3.25	0.4-0.9	-	-	2.60-3.35	0.2-0.7
Dullingari 1	Basement	2802	Sh	2	0.5	-	-	3.10-3.65	0.2-0.6	-	-	3.35-3.90	0.2-0.5
Dullingari 1	Basement	2948	Sh	2	0.5	-	-	3.40-3.85	0.2-0.6	-	-	3.55-4.15	0.2-0.5

TABLE 2b.
Thermal conductivity (Kdry, Kwet) in $Wm^{-1}K^{-1}$ for sample set B. Values are calculated for the dry samples using the values of the heat flux (Q) across the upper and lower standard discs. The wet values were calculated using only the lower value (i.e. lower standard). A correction factor of 1.944 was applied to the heat flux to allow for the smaller radius of the samples. ΦW is the porosity measured in this study and ΦHe the porosity measured by helium injection (Gravestock and Alexander 1986). Mu—Murta member, Na—Namur member.

Location	Formation	Depth M	Lith.	ΦW	ΦHe	Kdry	Kwet
Dullingari 35	Mooga (Mu)	1495	Si	7.5	10.0	3.97-4.02	4.22
Dullingari 35	Mooga (Mu)	1498	Sd	15.2	17.9	3.47-3.51	4.25
Dullingari 29	Mooga (Na)	1500	Sd	14.5	14.6	3.11-3.38	4.39
Dullingari 29	Mooga (Na)	1504	Si	6.6	6.5	2.40-2.42	3.61
Dullingari 29	Mooga (Na)	1513	Sd	22.1	20.3	3.15-3.28	4.60
Merrimelia 16	Mooga (Na)	1612	Sd	22.4	22.0	2.40-2.42	3.61
Merrimelia 16	Mooga (Na)	1602	Sd	19.3	19.6	3.46-3.62	3.59
Merrimelia 16	Mooga (Na)	1615	Sd	21.0	22.0	2.10-2.17	3.61
Gidgealpa 17	Hutton	1836	Sd	19.3	18.9	2.56-2.71	3.93
Gidgealpa 17	Hutton	1842	Sd	16.0	15.2	3.61-3.62	5.03
Gidgealpa 17	Hutton	1847	Sd	20.8	19.9	3.02-3.05	3.57
Strzelecki 4	Hutton	1705	Sd	15.4	15.0	4.12-4.21	5.35
Strzelecki 4	Hutton	1701	Sd	16.0	17.4	4.18-4.22	5.03
Srtzelecki 4	Hutton	1710	Sd	12.7	14.4	4.33-4.34	6.13
Strzelecki 4	Birkhead	1675	Si	5.4	7.6	3.47-3.50	4.10
Strezlecki 4	Birkhead	1694	Sd	13.3	13.9	3.56-3.57	5.55
Strezlecki 4	Birkhead	1686	Sd	19.2	20.6	2.92-2.96	4.64
Strezlecki 4	Birkhead	1684	Sd	14.6	15.3	4.04-4.05	5.60

to 6 hours in the divided bar and hourly readings were taken. Fig. 5 shows the results for one set of wet discs at several times. The slopes of the lines (i.e. the inverse of the conductivity) agree to 2%. However when the samples were

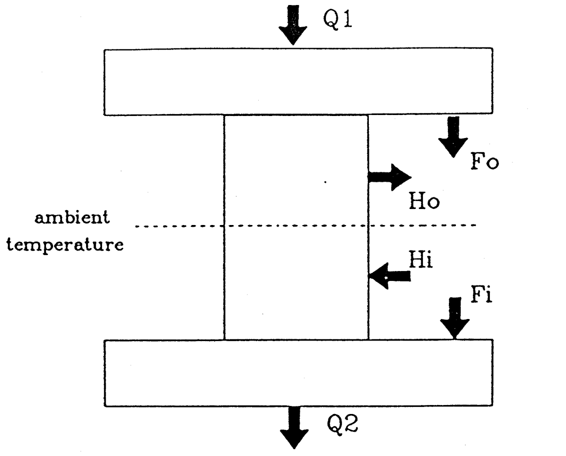

$$Q2 = Q1 - (Fo - Fi) - (Ho - Hi)$$

FIGURE 6
Difference in heat flow measurements at the upper and lower standards. Q1 and Q2 are the heat flow measurements at the upper and lower standards, Ho and Fo are heat losses through the outer face of the sample and the upper (hot) copper disc and Hi and Fi are heat gains through the sample and the lower (cold) copper disc. The ambient temperature controls the relative magnitudes of these heat gains and losses and thus the difference Q1 and Q2.

removed droplets of water were observed on the lower copper discs while the upper discs were dry indicating downward fluid migration. Beck and Beck (1958) noticed the same effect, although they stated that a steady state condition (i.e. cessation of fluid migration) should be reached after 5–10 minutes. The interpretation of this effect is that initially both surfaces of the sample were moist but with time the upper surface drys out, increasing the contact resistance.

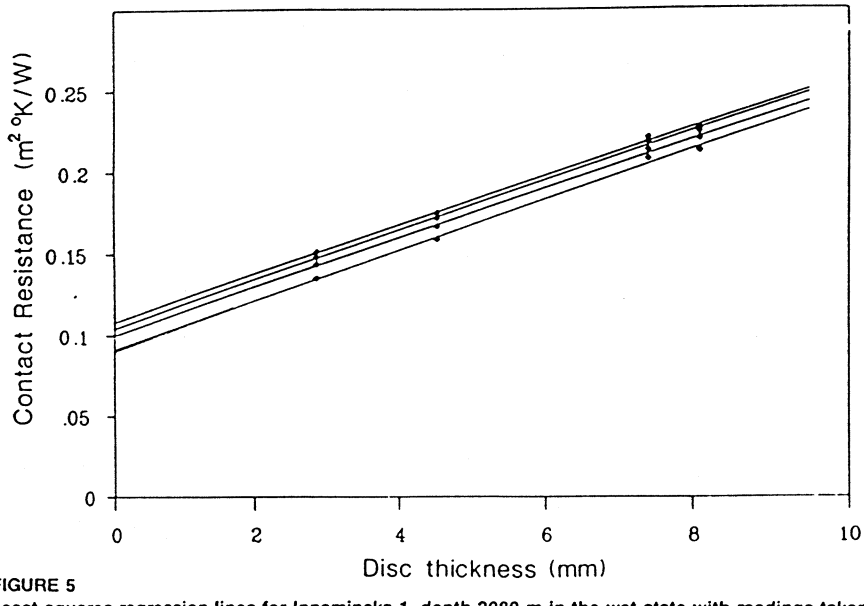

FIGURE 5
Least squares regression lines for Innamincka 1, depth 2080 m in the wet state with readings taken after 1 hour (lowest line), 2 hours, 4 hours and 5 hours (upper line). The slope of the line is constant but the intercept (i.e. contact resistance) increases with time due to drying out of the upper face.

Accordingly a qualitative adjustment may be made to the assumed contact resistance term.

As the samples in set B were longer than 30 mm the contact resistance was neglected. However other sources of uncertainty result from the difference in cross-sectional area of the copper discs and the samples (a factor of 1.944). Assuming that no heat is lost through the exposed surface of the copper disc then the ratio of the heat flow through the standard and the sample is given by the reciprocal ratio of their cross-sectional areas. Of course heat may be lost through the outer surfaces of the upper copper disc and the upper part of the sample and heat may enter through the lower part of the sample and the lower copper disc (Fig. 6). The relative heat loss and gain will depend on the ambient temperature. Lateral heat loss was again reduced by lagging the sample. The heat flux across the upper fused silica standard was greater than that across the lower standard by less than 3% for the samples in the dry state but the difference was up to 20% in the wet state. This latter discrepancy could be attributable to heat loss by evaporation of water (which would require less than a total of 0.1 gm of water to be evaporated in 1 hour). Because the ambient temperature was closer to the cold bath temperature (18°C) during the wet measurements the lower estimate for the heat flow (Q2 in Fig. 6) is probably the better estimate of heat flow through the sample and thus should be used for the calculation of thermal conductivity. For the dry measurements the value calculated using the average of the upper and lower heat flows is illustrated (Fig. 8b) although Table 2b gives the estimates using both values of heat flow.

The results for set A and set B are shown in tables 2a and 2b respectively. Some degree of anistropy for thermal conductivity in sediments was suggested by Beck and Beck (1958) who observed a decrease in conductivity for shale measured parallel to the bedding relative to the measurement perpendicular to the bedding (4% for the wet state and 23% for the dry state). Birch and Clark's (1940) data shows the opposite effect in quartz sandstone (7% difference for the dry state). The results presented here are inconclusive regarding anisotropy.

Discussion

Tables 3a and 3b show estimates of the effective matrix conductivity using six of the different theoretical models given in Table 1 and incorporating the dry and wet observed values. The formulae can be either rearranged to give an analytical expression or numerically solved for the matrix conductivity as a function of the observed conductivity, porosity and saturant conductivity. Separate estimates, K_{md} and K_{mw}, are obtained for the air and water saturated measurements. The Nosal model (Table 1.g) requires both wet and dry observations to make an estimate of the matrix conductivity. As can be seen from Tables 3a and 3b the two estimates are often significantly different for all the theoretical models i.e. the models do not adequately describe the observations. In the past this problem has been bypassed by appealing to empirical adjustments to the original equations (e.g. Beck 1976, Robertson and Peck 1974). As can be seen from Fig. 2 and Tables 3a and 3b the models are similar ($K_{md} \simeq K_{mw}$) for low values of the effective matrix conductivity and all models considered are equally suitable. For higher values of the bulk thermal conductivity the model estimates are more variable and as can be seen from Fig. 7 the Maxwell model deviates from the $K_{md}=K_{mw}$ line because K_{mw} is greater than K_{md} but the converse is true for the geometric model. Table 4 shows the predictions using the Maxwell model and geometric mean for a range of effective matrix conductivities at 25% and 40% porosity. These two models,

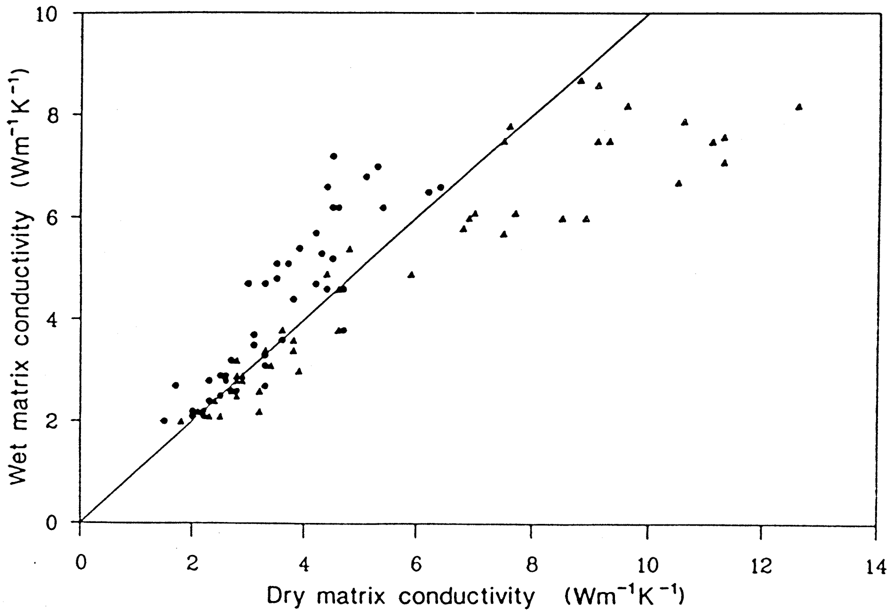

FIGURE 7

The matrix conductivity, K_{md} estimated from the dry and K_{mw} from the wet observations, using the Maxwell mode, ●, and the geometric model, ▲. The solid line represents $K_{mw}=K_{md}$.

TABLE 3a.
Estimates of effective matrix conductivity ($Wm^{-1}K^{-1}$) for sample set A, using 6 of the theoretical models given in Table 1. A—Geometric, B—Dispersive (Robertson and Peck 1974), C—Quadratic (Robertson and Peck 1974), D—Budiansky (1970), E—Maxwell (Beck 1976), F—Nosal (1981). Dry (d) and wet (w) observations were used separately, except for the Nosal (1981) formulation which requires both values.

Location	Formation	Depth	Lith.	A		B		C		D		E		F
				d	w	d	w	d	w	d	w	d	w	
Innamincka 1	Patchawarra	2080	Sd	7.5	7.5	9.7	7.8	5.5	7.1	5.3	7.0	5.3	7.0	7.5
Innamincka 1	Patchawarra	2103	Sd	6.9	6.0	6.8	5.8	3.9	5.2	3.7	5.2	3.7	5.1	5.5
Gidgealpa 2	Nappamerri	2108	Sd	8.8	8.7	8.5	8.6	4.8	7.3	4.6	7.3	4.5	7.2	8.1
Dullingari 1	Patchawarra	2592	Si	3.3	3.4	4.3	3.4	2.8	3.3	3.3	2.7	3.3	2.7	3.4
Burley 1	Toolachee	2701	Si	4.4	4.9	5.9	4.9	3.8	4.8	4.8	3.8	4.7	3.8	4.8
Burley 1	Toolachee	2704	Si	3.8	3.6	2.9	3.8	5.1	3.6	3.1	3.5	3.1	3.5	3.6
Gidgealpa 2	Toolachee	2091	Sd	7.5	5.7	6.1	5.4	3.6	4.8	3.4	4.8	3.3	4.7	5.2
				11.3	7.1	8.0	6.7	4.6	5.8	4.4	5.8	4.2	5.7	6.2
Tirrawarra 2	Patchawarra	2968	Sd	11.3	7.6	11.7	7.7	6.5	6.5	6.3	6.5	6.2	6.5	6.5
Tirrawarra 1	Basement	3068	Sd	4.8	5.4	6.6	5.4	4.4	5.3	4.3	5.3	4.3	5.3	5.4
Innamincka 1	Cadna-Owie	1201	Sh	1.8	2.0	2.1	2.0	1.6	2.0	1.5	2.0	1.5	2.0	2.1
				2.9	2.8	3.4	2.8	1.9	2.7	1.8	2.7	1.7	2.7	2.8
Innamincka 1	Nappamerri	1996	Sh	2.3	2.1	2.7	2.1	2.2	2.1	2.2	2.1	2.2	2.1	2.1
				2.8	3.2	2.7	3.2	2.7	3.2	2.7	3.2	2.7	3.2	3.2
Dullingari 1	Wallumbilla	1210	Sh	3.2	2.2	2.4	2.2	2.0	2.1	2.0	2.1	2.0	2.1	2.2
				3.9	3.0	4.1	2.9	2.5	2.8	2.4	2.8	2.3	2.8	2.8
Dullingari 1	Nappamerri	2010	Sh	2.8	2.5	3.6	2.5	2.5	2.5	2.5	2.5	2.5	2.5	2.5
				3.8	3.4	5.1	3.3	3.4	3.3	3.3	3.3	3.3	3.3	3.3
Dullingari 1	Toolachee	2106	Si	2.5	2.1	3.2	2.1	2.3	2.1	2.1	2.1	2.2	2.2	2.0
				3.2	2.6	4.2	2.6	2.8	2.6	2.8	2.6	2.8	2.6	2.5
Dullingari 1	Roseneath	2281	Sh	2.1	2.2	2.5	2.2	2.0	2.2	2.0	2.2	2.0	2.2	2.2
				2.8	2.8	3.3	2.8	2.6	2.8	2.6	2.8	2.6	2.8	2.8
Dullingari 1	Epsilon	2321	Si	2.9	2.9	3.7	2.9	2.5	2.9	2.5	2.9	2.5	2.9	2.9
				3.6	3.8	4.9	3.8	3.1	3.7	3.1	3.7	3.1	3.7	3.8
Dullingari 1	Murteree	2409	Sh	2.4	2.4	2.8	2.4	2.3	2.4	2.3	2.4	2.3	2.4	2.4
				2.8	2.9	3.4	2.9	2.6	2.9	2.6	2.9	2.6	2.9	2.9
Dullingari 1	Merrimelia	2743	Bc	2.7	2.6	3.1	2.6	2.7	2.6	2.7	2.6	2.7	2.6	2.6
				3.4	3.1	3.9	3.1	3.1	3.3	3.3	3.1	3.3	3.1	3.1

as stated in the previous section, are bounds on the model predictions. Figure 8 shows the observed wet and dry values and model curves for the geometric and Maxwell models with effective matrix conductivities of 2.5, 3.5 and 6.0 $Wm^{-1}K^{-1}$. The siltstones show considerable scatter which is due to the variation in bulk composition. The higher values observed for the sandstones are directly attributable to the high percentage of quartz present in the specimens (often up to 90%). The shales are fairly consistent at 2.0–2.7 $Wm^{-1}K^{-1}$, although the basement shales from Dullingari 1 have slightly higher values due to the fact that they are dolomitised. Although at least part of the scatter in the observed thermal conductivity, and hence the true matrix conductivity, is likely to be real, these are adopted as the preferred values of the matrix conductivity for shales, siltstones and sandstones respectively and a practical relationship for predicting thermal conductivity as a function of porosity would be the arithmetic mean of the Maxwell (or Budiansky) model and the geometric mean. Errors in the thermal conductivity will be directly reflected in heat flow estimates, but in the context of thermal history modelling the uncertainty associated with the predicted conductivity will be more important for shales as temperature gradients are inversely proportional to the thermal conductivity and the large range of observed conductivity for sandstones (Fig. 8) will be partially compensated for.

Conclusions

When making measurements of thermal conductivity using discs of rock and a divided bar apparatus the effect of an imperfect contact must be considered by incorporating a

TABLE 3b.
As Table 3a but for sample set B.

Location	Formation	Depth	Lith.	A		B		C		D		E		F
		M		d	w	d	w	d	w	d	w	d	w	
Dullingari 35	Mooga (Mu)	1495	Si	5.9	4.9	7.8	4.9	4.6	4.6	4.5	4.6	4.4	4.6	4.6
Dullingari 35	Mooga (Mu)	1498	Sd	8.5	6.0	8.4	5.8	4.8	5.3	4.5	5.2	4.5	5.2	5.4
Dullingari 29	Mooga (Na)	1500	Sd	7.0	6.1	7.2	6.0	4.1	5.4	4.0	5.4	3.9	5.3	5.7
Dullingari 29	Mooga (Na)	1504	Si	4.6	3.8	6.2	3.8	3.7	3.6	3.7	3.6	3.6	3.6	3.6
Dullingari 29	Mooga (Na)	1513	Sd	12.6	8.2	8.6	7.7	5.0	6.4	4.7	6.4	4.5	6.2	7.0
Merrimelia 16	Mooga (Na)	1612	Sd	8.9	6.0	6.5	5.6	3.8	4.9	3.6	5.0	3.5	4.8	5.3
Merrimelia 16	Mooga (Na)	1602	Sd	11.1	7.5	10.3	7.3	5.8	6.4	4.9	4.7	4.7	4.6	4.3
Merrimelia 16	Mooga (Na)	1615	Sd	6.8	5.8	5.5	5.5	3.2	4.8	3.1	4.8	3.0	4.7	5.3
Gidgealpa 17	Hutton	1836	Sd	7.7	6.1	6.5	5.8	3.8	5.1	3.6	5.1	3.5	5.1	5.6
Gidgealpa 17	Hutton	1842	Sd	9.3	7.5	8.8	7.3	5.0	6.4	4.8	6.3	4.6	6.2	6.8
Gidgealpa 17	Hutton	1847	Sd	10.5	6.7	8.0	5.6	4.6	4.8	4.4	4.8	4.2	4.7	4.8
Strzelecki 4	Hutton	1705	Sd	10.6	7.9	10.2	7.8	5.7	6.7	5.5	6.7	5.4	6.6	7.1
Strzelecki 4	Hutton	1701	Sd	11.1	7.5	10.3	7.3	5.8	6.4	5.6	6.3	5.4	6.2	6.6
Srtzelecki 4	Hutton	1710	Sd	9.1	8.6	9.9	8.5	5.6	7.4	5.4	7.4	5.3	7.3	8.0
Strzelecki 4	Birkhead	1675	Si	4.6	4.6	6.3	4.6	3.8	4.4	3.8	4.4	3.8	4.4	4.5
Strezlecki 4	Birkhead	1694	Sd	7.6	7.8	8.2	7.8	4.7	6.8	4.5	6.7	4.4	6.6	7.3
Strezlecki 4	Birkhead	1686	Sd	9.1	7.5	7.6	7.2	4.4	6.2	3.1	4.8	3.0	4.7	5.3
Strezlecki 4	Birkhead	1684	Sd	9.6	8.2	9.6	8.1	5.4	6.9	5.2	6.9	5.1	6.8	7.5

TABLE 4.
Theoretical predictions of the dry and wet bulk thermal conductivity ($Wm^{-1}K^{-1}$) for porosities of 25% and 40% for a range of effective matrix thermal conductivities (2.0–7.0 $Wm^{-1}K^{-1}$) using the geometric and Maxwell (1976) models. These two models give appropriate upper and lower bounds.

	ϕ	Sat.	Km 2.0	3.0	4.0	5.0	6.0	7.0
Geometric	25%	dry	0.68	0.92	1.14	1.35	1.55	1.73
Maxwell			1.35	2.01	2.68	3.35	4.01	4.68
Geometric		wet	1.49	2.02	2.51	2.97	3.40	3.82
Maxwell			1.58	2.26	2.93	3.60	4.27	4.93
Geometric	40%	dry	0.35	0.45	0.54	0.61	0.68	0.75
Maxwell			1.02	1.52	2.02	2.52	3.02	3.52
Geometric		wet	1.25	1.60	1.90	2.17	2.42	2.65
Maxwell			1.36	1.87	2.37	2.88	3.38	3.88

contact medium of reasonably high thermal conductivity and/or by measuring a group of discs of different thickness cut from the same sample. The errors resulting from neglecting this effect are more severe for thinner discs. The relationship between thermal conductivity of porous rocks saturated with different fluids or gases has been approximated by a variety of models but none have been proven unequivocally. For a given saturant the bulk rock thermal conductivity decreases with porosity. Of the various models considered here the data are best satisfied by a conductivity:porosity relationship that lies between the Maxwell model and the geometric mean. Although there is no rigorous physical basis for doing so taking the average of the two may be used to predict thermal conductivity. In order to generalise the results from these thermal conductivity measurements made on a restricted set of samples three lithological distinctions were considered for the sediments, sandstone, siltstone and shale. The effective matrix thermal conductivities are 6.0, 3.5 and 2.5 $Wm^{-1}K^{-1}$ respectively. Siltstones may be regarded as sandy shales or shaly sandstones and intermediate values may be more appropriate depending on their bulk composition.

Acknowledgements

I would like to thank Delhi Petroleum Pty Ltd and the Department of Resources and Energy, Canberra for permission to use core samples and the South Australian

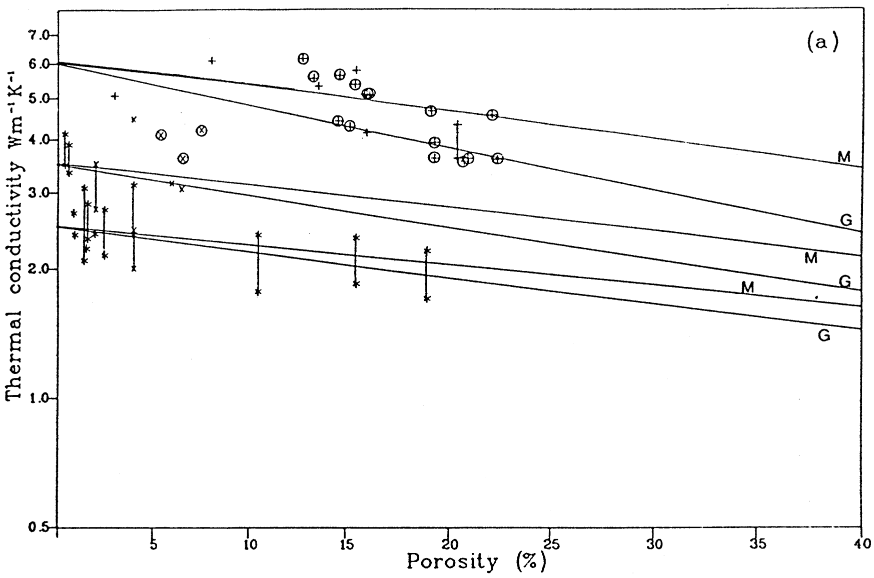

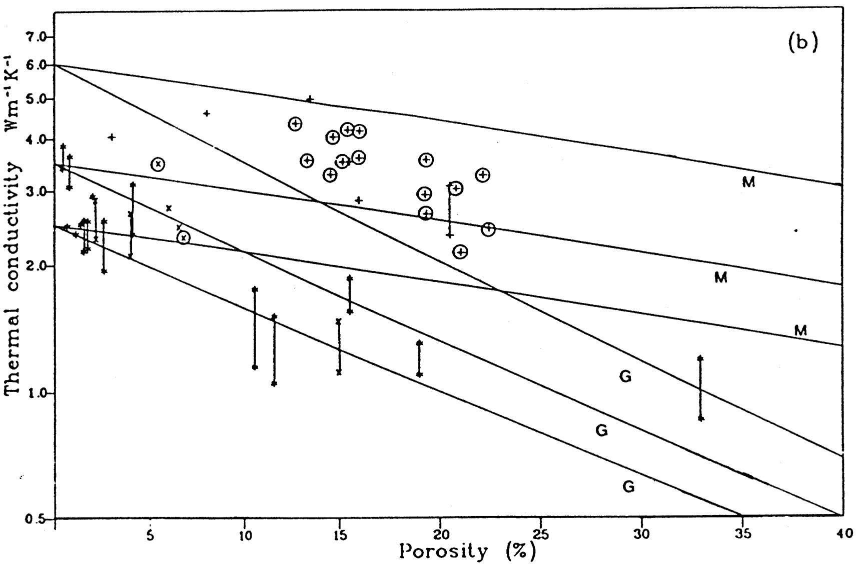

FIGURE 8

Observed thermal conductivity versus porosity (a)–wet state, (b)–dry state. 3 lithological divisions are made: sandstones (+), siltstones (x), and shales (*). Samples from set B are circled. Where a least squares regression line was not calculated the range of thermal conductivity from table 1 is shown. The 3 pairs of solid lines are the theoretical curves for the Maxwell (upper curve) and geometric mean (lower curve) models with matrix conductivities of 2.5, 3.5 and 6 $Wm^{-1}K^{-1}$.

Department of Mines and Energy for physically supplying them. Peter Moore, formerly of Delhi, and David Gravestock of SADME were particularly cooperative. Ted Lilley and Merrin Sloane gave valuable advice on the operation of the divided bar apparatus. Greg Houseman and Kurt Lambeck critically read the manuscript and made numerous improvements.

References

Battersby, D. G. (1976)—'Cooper Basin gas and oil fields', in Leslie, R. B., Evans, H. J. & Knight, C. L. (Editors), Economic geology of Australia and Papua New Guinea, 3. Petroleum, Australasian Institute of Mining and Metallurgy, Monograph 7, 321–368.

Beck, A. E. (1965)—'Techniques of measuring heat flow on land', in Lee, W. H. K. (Editor), Terrestrial Heat Flow, Geophys. Monograph 8, Am. Geophys. Union, 24–57.

Beck, A. E. (1976)—'An improved method of computing the thermal conductivity of fluid-filled sedimentary rocks', *Geophysics* **41**, 133–144.

Beck, A. E. & Beck, J. M. (1958)—'On the measurement of the thermal conductivities of rocks by observations on a divided-bar apparatus', *Trans. Am. Geophys. Union* **30**, 1111–1123.

Beck, J. M. & Beck, A. E. (1965)—'Computing thermal conductivities of rocks from chips and conventional specimens', *J. Geophys. Res.* **70**, 5227–5239.

Birch, F. & Clark, H. (1940)—'The thermal conductivity of rocks and its dependence upon temperature and composition', *Am. J. Sci.* **238**, 529–558.

Budiansky, B. (1970)—'Thermal and thermoelastic properties of isotropic composites', *J. Composite Materials* **4**, 286–295.

Cermak, V. & Rybach, L. (1982)—'Thermal properties', in Angenheister, G. (Editor), Physical Properties of Rocks (subvolume A): Numerical Data and Functional Relationships in Science and Technology', 1, Springer-Verlag, 305–371.

Gravestock, D. & Alexander, A. M., (1986)—'Porosity and permeability of reservoirs and caprocks in the Eromanga Basin, South Australia', *APEA J* **24**, 202–213.

Huang, J. H., (1971)—'Effective thermal conductivity of porous rocks', *J. Geophys. Res.* **76**, 6420–6427.

Jessop, A. M. (1970)—'The effect of environment on divided-bar measurements', *Tectonphysics* **10**, 39–49.

Lubimova, E. A., Maslennikov, V. N. & Gaviev, I. K. (1977)—'Thermal conductivity of dry, wet and oil-saturated rocks at slightly high temperatures and pressures', *Geophys. Res. Bull.* **15**, 59–66.

Moore, P. S. & Mount, T. J., (compilers), (1982)—'Eromanga Basin Symposium, summary papers', Geol Soc. Aust. & Pet. Explor. Soc. Aust., Adelaide.

Nosal, E. A. (1981)—'Predicting thermal conductivity of sandstones and carbonates', *EOS* **62**, 392.

Ratcliffe, E. M. (1959)—'Thermal conductivities of fused and crystalline quartz', *Brit. J. Appl. Phys.* **10**, 22–25.

Robertson, D. E. & Peck, D. L., (1974)—'Thermal conductivity of vesicular basalt from Hawaii', *J. Geophys. Res.* **79**, 4875–4888.

Sass, J. H., Lachenbruch, A. H., Munroe, R. J., Greene, G. W. & Moses, T. H., Jnr. (1971)—'Heat flow in the western United States', *J. Geophys. Res.* **76**, 6376–6413.

Sass, J. H., Stone, C. & Munroe, R. J., (1984)—'Thermal conductivity determinations on solid rock — a comparison between a steady state divided-bar apparatus and a commercial transient line source device', *J. Vulc. Geothermal Res.* **20**, 145–153.

Scharli, U. & Rybach, L., (1984)—'On the thermal conductivity of low-porosity crystalline rocks', in Cermak, V., Rybach, L. & Chapman, D. S. (Editors), Terrestrial Heat Flow Studies and the Structure of the Lithosphere, *Tectonophysics* **103**, 307–313.

Sekiguchi, K. (1984)—'A method for determining terrestrial heatflow in oil basinal areas', in Cermak, V., Rybach, L. & Chapman, D. S. (Editors), Terrestrial Heat Flow Studies and the Structure of the Lithosphere, *Tectonphysics* **103**, 67–79.

Walsh, J. B. & Decker, E. R., (1966)—'Effect of pressure and saturating fluid on the thermal conductivity of compact rock', *J. Geophys. Res.*, **71**, 3053–3061.

Woodside, W. H. & Messmer, J. H., (1961)—'Thermal conductivity of porous media 1: unconsolidated sands', *J. Appl. Phys.* **32**, 1688–1699.

Appendix 2

Results from backstripping and decompaction calculations

The observed thickness of each stratigraphic formation and the age assigned to its top are given with three estimates of each of the following :

Tectonic subsidence (m, basement depth, with sediment loading, palaeobathymetry and sea level corrections),

Total decompacted sediment thickness (m),

Deposition, or solid influx, rate (m/m.y.).

The first estimate for each is that obtained with the best fit porosity/depth curve, and the other two are using the maximum and minimum curves, in order to obtain bounding values. A thickness of zero indicates an unconformity. An age of zero means the sediments are thought to be post-Winton Formation and note that the tectonic subsidence estimate does not include the fact that the upper surface of the youngest sediments is generally above sea level at the present day, effectively assuming post-depositional uplift.

Macumba 1 26.44 138.27 Height above present day sea level 41 m

Observed Thickness (m)	Age (Ma)	Basement Depth (m)			Total Decompacted Thickness (m)			Deposition Rate (m/m.y.)		
160	0	1096	1183	1022	2438	2437	2438	1.04	0.95	1.14
620	91	882	969	807	2343	2350	2336	90.34	83.48	96.51
369	96	808	893	731	1882	1911	1850	79.11	74.66	82.48
30	100	757	834	682	1550	1585	1510	27.39	26.22	28.00
244	101	730	807	656	1519	1554	1480	18.57	17.77	19.05
57	113	596	661	530	1261	1291	1225	3.72	3.56	3.84
623	127	569	630	506	1195	1223	1162	11.46	10.73	12.12
175	175	260	292	231	489	513	466	14.90	14.34	15.40
0	186	142	160	125	252	266	239	0.02	0.01	0.02
160	205	142	159	125	252	266	238	5.07	4.91	5.20

Age at base of sediments 235 Ma

Poonarunna 1 27.41 137.92 Height above present day sea level 1 m

Observed Thickness (m)	Age (Ma)	Basement Depth (m)			Total Decompacted Thickness (m)			Deposition Rate (m/m.y.)		
95	0	822	882	772	1630	1630	1630	0.6	0.56	0.67
572	91	616	676	567	1574	1577	1570	80.40	73.94	85.89
299	96	545	598	498	1135	1155	1114	50.22	47.18	52.25
199	101	453	497	413	841	862	819	14.58	13.82	15.08
46	113	317	350	286	615	632	598	2.77	2.60	2.95
201	127	294	326	265	564	581	547	15.84	14.94	16.69
126	138	182	202	162	325	339	312	19.43	18.65	19.99
37	144	81	89	73	140	145	135	16.53	15.57	17.40
55	146	50	55	45	86	89	82	4.07	3.84	4.25

Age at base of sediments 158 Ma

Kuncherinna 1 26.71 138.27 Height above present day sealevel 51 m

Observed Thickness (m)	Age (Ma)	Basement Depth (m)			Total Decompacted Thickness (m)			Deposition Rate (m/m.y.)		
150	0	1213	1308	1134	2832	2832	2832	0.97	0.89	1.06
530	91	1002	1097	922	2746	2752	2738	94.34	86.97	101.0
597	95	954	1051	869	2368	2397	2336	102.4	96.66	106.7
45	100	861	950	775	1848	1891	1800	42.05	40.47	42.85
237	101	829	918	744	1802	1845	1754	18.31	17.60	18.73
59	113	704	783	626	1555	1594	1510	3.91	3.75	4.02
746	127	678	753	602	1488	1525	1445	13.95	13.12	14.68
179	175	339	382	300	666	699	634	15.44	14.92	15.88
0	186	234	265	207	438	464	414	0.02	0.01	0.02
179	205	234	265	207	437	463	414	5.73	5.57	5.85
111	235	107	121	93	185	198	173	6.77	6.65	6.86

Age at base of sediments 251 Ma

Walkandi 1 26.56 137.47 Height above present day sea level 25 m

Observed Thickness (m)	Age (Ma)	Basement Depth (m)			Total Decompacted Thickness (m)			Deposition Rate (m/m.y.)		
85	0	1268	1366	1189	3027	3027	3027	0.54	0.50	0.59
1316	91	1083	1181	1003	2980	2984	2976	115.9	108.5	121.9
47	100	892	986	801	1936	1983	1882	44.02	42.55	44.74
240	101	860	953	770	1888	1935	1834	18.79	18.13	19.16
48	113	734	817	651	1635	1679	1585	3.19	3.08	3.28
802	127	713	793	632	1581	1623	1533	15.17	14.31	15.91
196	175	352	397	311	694	730	659	17.04	16.52	17.47
0	186	237	269	209	444	471	419	0.02	0.01	0.02
190	205	237	269	209	443	470	418	6.13	5.98	6.24
102	235	100	114	87	172	185	161	6.28	6.18	6.35

Age at base of sediments 251 Ma

Putamurdie 1	26.28 139.78				Height above present day sea level			37 m		
Observed Thickness (m)	Age (Ma)	Basement Depth (m)			Total Decompacted Thickness (m)			Deposition Rate (m/m.y.)		
75	0	904	973	846	1856	1856	1856	0.48	0.44	0.52
629	91	703	772	645	1812	1815	1809	88.67	81.60	94.68
267	96	631	694	573	1343	1365	1318	56.43	53.06	58.66
52	100	579	635	525	1092	1116	1064	46.88	44.66	48.07
172	101	540	594	488	1034	1058	1008	12.69	12.04	13.10
41	113	424	468	379	844	864	822	2.49	2.33	2.65
190	127	405	448	363	800	820	779	8.72	8.23	9.18
43	146	305	337	273	580	596	563	3.15	2.97	3.31
265	158	279	308	250	527	541	511	10.51	9.8	11.14
0	180	107	120	96	188	197	179	0.01	0.01	0.01
121	215	107	120	96	188	197	179	3.09	2.95	3.20
Age at base of sediments		251 Ma								

Pandieburra 1	26.76 139.42				Height above present day sea level			31 m		
Observed Thickness (m)	Age (Ma)	Basement Depth (m)			Total Decompacted Thickness (m)			Deposition Rate (m/m.y.)		
110	0	983	1059	920	2103	2103	2103	0.71	0.65	0.77
690	91	777	853	714	2040	2044	2035	100.1	92.41	106.6
227	96	694	764	629	1518	1545	1489	39.07	36.85	40.50
248	101	642	707	580	1304	1333	1272	18.41	17.49	18.98
57	113	505	560	451	1044	1071	1015	3.49	3.28	3.71
63	127	483	536	431	987	1014	957	5.02	4.74	5.28
87	138	457	507	407	921	947	891	13.30	12.75	13.69
58	144	410	455	366	816	840	791	25.40	23.90	26.78
96	146	382	423	340	751	773	726	7.14	6.75	7.47
288	158	329	364	294	636	655	614	15.05	14.16	15.88
117	175	154	172	137	276	290	263	9.83	9.43	10.20
0	186	63	71	55	106	113	100	0.01	0.01	0.02
63	205	62	70	55	106	113	99	1.99	1.94	2.04
Age at base of sediments		235 Ma								

Kalladeina 1	27.65 139.4				Height above present day sea level			28 m		
Observed Thickness (m)	Age (Ma)	Basement Depth (m)			Total Decompacted Thickness (m)			Deposition Rate (m/m.y.)		
111	0	922	993	863	1911	1911	1911	0.71	0.65	0.78
767	91	715	786	656	1846	1850	1842	113.0	104.5	120.1
213	96	597	659	540	1243	1269	1215	37.21	35.14	38.41
200	101	539	594	487	1030	1056	1002	14.94	14.22	15.39
55	113	409	452	365	806	827	784	3.38	3.18	3.60
212	127	383	424	342	746	767	724	9.85	9.32	10.34
111	146	266	294	239	494	509	478	8.28	7.83	8.65
243	158	192	212	172	348	358	337	7.72	7.26	8.14
Age at base of sediments		186 Ma								

Fly Lake 1 27.63 139.95 Height above present day sea level 34 m

Observed Thickness (m)	Age (Ma)	Basement Depth (m)			Total Decompacted Thickness (m)			Deposition Rate (m/m.y.)		
107	0	1232	1323	1161	2949	2949	2949	0.69	0.63	0.75
937	91	1029	1121	956	2889	2894	2884	142.0	131.7	150.3
300	96	908	1002	826	2179	2222	2134	54.22	51.73	55.74
340	101	846	935	765	1900	1947	1850	26.35	25.35	26.94
71	113	693	769	616	1552	1597	1504	4.54	4.31	4.77
276	127	665	741	593	1480	1526	1432	13.34	12.74	13.86
86	146	553	618	491	1184	1228	1140	6.62	6.33	6.85
284	158	513	574	456	1087	1129	1045	9.35	8.88	9.75
0	186	382	430	338	766	805	730	0.01	0.01	0.01
162	215	382	430	338	766	805	729	4.31	4.18	4.41
35	251	296	334	261	567	599	537	4.13	3.99	4.25
5	259	276	313	244	524	554	495	0.37	0.36	0.37
6	272	273	309	241	517	547	489	1.21	1.20	1.21
268	277	269	304	237	508	538	481	32.47	31.76	33.01
73	285	73	83	64	124	132	116	14.13	13.77	14.37

Age at base of sediments 290 Ma

Tirrawarra 1 27.68 140.12 Height above present day sea level 357 m

Observed Thickness (m)	Age (Ma)	Basement Depth (m)			Total Decompacted Thickness (m)			Deposition Rate (m/m.y.)		
17	90	1255	1347	1181	3021	3021	3021	1.17	1.07	1.28
831	91	1039	1133	964	2917	2925	2908	127.4	118.3	134.7
299	96	941	1036	857	2282	2324	2238	53.69	51.15	55.24
326	101	881	972	797	2006	2054	1956	25.19	24.20	25.78
69	113	731	813	654	1675	1721	1626	4.44	4.21	4.67
57	127	706	786	632	1605	1652	1556	8.64	8.24	9.00
240	133	684	762	612	1545	1592	1497	16.81	15.95	17.55
67	146	590	659	526	1292	1339	1246	5.20	4.96	5.38
245	158	560	626	500	1218	1263	1173	8.03	7.62	8.39
0	186	456	513	406	951	996	909	0.02	0.01	0.02
259	205	456	513	405	950	995	909	5.38	5.22	5.51
46	251	331	374	293	646	682	613	5.51	5.32	5.66
0	259	308	349	272	591	626	559	0.03	0.03	0.03
26	269	308	349	272	591	626	559	8.48	8.35	8.55
41	272	293	332	258	557	590	526	8.22	8.15	8.25
223	277	264	299	233	499	528	471	27.15	26.58	27.59
109	285	105	119	92	182	194	170	21.20	20.67	21.54

Age at base of sediments 290 Ma

Gidgealpa 1 27.96 140.08 Height above present day sea level 37 m

Observed Thickness (m)	Age (Ma)	Basement Depth (m)			Total Decompacted Thickness (m)			Deposition Rate (m/m.y.)		
160	0	1165	1248	1102	2776	2776	2776	1.04	0.95	1.14
780	91	954	1039	889	2686	2693	2678	119.2	110.8	125.7
300	96	865	952	793	2089	2128	2050	66.97	63.72	68.96
8	100	819	902	748	1813	1858	1769	7.39	7.11	7.53
340	101	801	884	730	1805	1850	1761	26.31	25.29	26.90
73	113	646	719	581	1458	1502	1415	4.72	4.49	4.90
281	127	618	689	556	1382	1426	1340	13.45	12.78	14.01
124	146	513	575	459	1092	1137	1050	9.99	9.74	10.13
123	158	452	507	404	944	984	907	5.14	4.88	5.37
0	180	398	448	355	808	847	772	0.0	0.01	0.01
154	230	398	448	355	807	847	772	7.02	6.83	7.15
88	251	318	358	283	620	653	591	10.47	10.11	10.77
22	259	269	304	239	511	540	484	4.26	4.16	4.32
210	264	256	289	227	482	510	456	9.64	9.40	9.82
112	285	108	123	95	188	201	176	21.86	21.41	22.16

Age at base of sediments 290 Ma

Moomba 1 28.15 140.28 Height above present day sea level 33 m

Observed Thickness (m)	Age (Ma)	Basement Depth (m)			Total Decompacted Thickness (m)			Deposition Rate (m/m.y.)		
263	0	1184	1268	1120	2841	2841	2841	1.76	1.60	1.93
824	91	954	1040	888	2685	2697	2672	131.9	123.3	138.3
198	96	846	932	774	2023	2067	1981	44.77	42.75	45.97
38	100	828	911	756	1839	1885	1793	36.05	34.77	36.66
289	101	799	881	728	1799	1846	1754	22.44	21.61	22.92
78	113	658	732	594	1500	1546	1458	5.09	4.85	5.28
279	127	629	700	566	1419	1464	1377	13.39	12.73	13.95
29	146	519	581	466	1125	1170	1084	2.30	2.24	2.33
144	158	504	565	453	1090	1134	1051	5.98	5.67	6.25
0	180	446	502	399	937	981	898	0.01	0.01	0.01
174	230	446	502	399	936	981	898	7.96	7.73	8.10
103	251	365	411	325	734	772	700	12.23	11.81	12.58
59	259	316	358	281	615	651	583	11.41	11.16	11.58
74	264	286	324	253	543	576	513	14.66	14.50	14.72
80	269	238	270	210	442	469	417	25.94	25.42	26.28
62	272	186	211	163	333	355	312	12.33	12.22	12.37
146	277	133	151	117	235	250	221	17.60	17.16	17.94

Age at base of sediments 285 Ma

Mcleod 1 27.82 140.76 Height above present day sea level 70 m

Observed Thickness (m)	Age (Ma)	Basement Depth (m)			Total Decompacted Thickness (m)			Deposition Rate (m/m.y.)		
91	0	1463	1566	1386	3747	3747	3747	0.59	0.53	0.64
765	91	1262	1366	1184	3696	3701	3692	139.5	128.8	148.4
93	95	1174	1285	1086	3148	3190	3107	79.00	74.25	82.42
278	96	1174	1285	1084	3072	3117	3027	61.99	58.94	63.87
6	100	1143	1253	1051	2824	2878	2771	5.68	5.46	5.78
397	101	1125	1235	1033	2818	2872	2765	30.38	29.10	31.15
89	113	971	1075	883	2437	2496	2380	5.80	5.54	6.03
60	127	942	1044	856	2349	2409	2292	9.16	8.74	9.51
230	133	921	1022	836	2288	2348	2231	15.86	14.92	16.68
85	146	846	943	766	2064	2130	2005	6.59	6.29	6.82
45	175	791	886	714	1897	1966	1836	3.75	3.56	3.89
0	186	777	871	701	1853	1923	1791	0.01	0.01	0.02
407	205	777	871	701	1853	1923	1791	8.53	8.31	8.68
174	251	630	711	565	1421	1485	1365	20.80	20.03	21.31
95	259	566	640	504	1235	1298	1181	18.61	18.21	18.84
80	264	529	599	470	1131	1190	1078	15.84	15.65	15.93
140	269	492	558	437	1037	1093	987	45.63	44.68	46.24
83	272	429	488	380	875	925	829	16.38	16.23	16.45
361	277	384	436	339	769	814	729	44.24	43.37	44.81
47	285	161	184	142	290	310	272	22.43	21.52	22.98
134	287	130	149	114	226	244	210	44.22	43.78	44.45

Age at base of sediments 290 Ma

Burley 2	27.8 140.64				Height above present day sea level			48 m		
Observed Thickness (m)	Age (Ma)	Basement Depth (m)			Total Decompacted Thickness (m)			Deposition Rate (m/m.y.)		
107	0	1441	1544	1363	3664	3664	3664	0.69	0.62	0.75
777	91	1238	1342	1159	3604	3610	3599	143.0	132.2	152.0
92	95	1146	1257	1057	3043	3085	3000	78.41	73.78	81.73
275	96	1142	1252	1051	2966	3013	2921	61.48	58.51	63.30
5	100	1115	1225	1023	2720	2774	2667	4.84	4.66	4.92
393	101	1098	1207	1006	2715	2769	2662	30.21	28.96	30.96
89	113	943	1046	855	2335	2393	2279	5.79	5.54	6.01
58	127	914	1014	827	2246	2305	2190	8.90	8.49	9.23
263	133	892	991	808	2186	2245	2131	18.18	17.11	19.10
58	146	804	898	726	1927	1991	1869	4.46	4.26	4.61
132	158	783	875	706	1867	1931	1810	6.99	6.52	7.36
32	175	741	831	667	1740	1808	1680	2.68	2.55	2.78
0	186	731	821	657	1708	1776	1648	0.01	0.01	0.02
422	205	731	821	657	1708	1776	1647	8.87	8.65	9.02
129	251	573	647	511	1253	1314	1200	15.45	14.88	15.81
86	259	522	592	464	1114	1172	1062	16.78	16.42	16.98
60	264	487	553	432	1017	1073	968	11.80	11.67	11.87
138	269	458	520	406	946	998	899	45.03	44.09	45.64
80	272	393	447	346	782	829	740	15.83	15.69	15.90
375	277	346	394	305	678	718	641	45.88	44.98	46.47
41	285	89	101	78	154	165	144	19.94	19.13	20.43
51	287	55	63	48	91	99	84	16.71	16.55	16.81
Age at base of sediments		290 Ma								

Innamincka 1	27.49 140.92				Height above present day sea level			123 m		
Observed Thickness (m)	Age (Ma)	Basement Depth (m)			Total Decompacted Thickness (m)			Deposition Rate (m/m.y.)		
610	91	806	882	743	2146	2146	2146	81.66	74.99	87.99
198	96	758	832	693	1727	1750	1702	40.95	38.35	42.61
3	100	739	810	675	1553	1580	1524	2.63	2.49	2.72
389	101	722	793	658	1550	1577	1521	28.27	26.77	29.28
56	113	548	607	493	1167	1194	1138	3.57	3.39	3.71
305	127	523	580	471	1105	1133	1078	13.85	12.94	14.64
112	146	397	442	354	789	817	760	8.74	8.44	8.95
137	158	334	371	298	650	673	626	5.58	5.27	5.83
0	180	257	286	229	484	504	464	0.01	0.01	0.01
243	220	257	286	229	483	504	463	6.37	6.09	6.63
94	255	91	102	80	156	166	147	6.00	5.84	6.12
Age at base of sediments		270 Ma								

McKinlay 1	28.47 140.47				Height above present day sea level			39 m		
Observed Thickness (m)	Age (Ma)	Basement Depth (m)			Total Decompacted Thickness (m)			Deposition Rate (m/m.y.)		
200	0	804	865	750	1524	1524	1524	1.29	1.17	1.41
705	91	603	662	549	1396	1402	1390	50.70	46.99	53.79
42	100	433	473	394	775	789	759	65.27	59.29	70.80
190	101	422	460	383	735	750	718	14.92	14.10	15.59
52	113	275	301	248	511	521	500	3.14	2.95	3.35
52	127	244	267	220	448	456	439	7.37	6.94	7.79
232	133	210	229	190	382	388	375	14.90	13.77	15.97
23	146	46	51	42	79	81	76	1.75	1.67	1.83
28	158	24	26	22	41	42	41	1.40	1.30	1.50
Age at base of sediments		175 Ma								

Kidman 2 28.24 140.78 Height above present day sea level 73 m

Observed Thickness (m)	Age (Ma)	Basement Depth (m)			Total Decompacted Thickness (m)			Deposition Rate (m/m.y.)		
213	0	1008	1082	953	2253	2253	2253	1.38	1.25	1.50
631	91	781	856	724	2124	2133	2115	95.14	88.16	100.7
226	96	714	786	655	1636	1669	1604	50.14	47.60	51.58
9	100	685	754	627	1426	1462	1391	8.49	8.09	8.72
291	101	667	735	609	1417	1453	1382	22.51	21.63	22.96
68	113	520	579	470	1112	1145	1080	4.50	4.34	4.60
57	127	489	544	441	1035	1066	1005	8.80	8.48	9.00
234	133	460	511	416	967	996	940	15.78	14.76	16.65
33	146	354	397	319	713	743	687	2.51	2.41	2.60
78	158	338	378	304	675	704	649	3.13	2.91	3.31
0	180	302	340	271	590	620	563	0.01	0.01	0.01
116	230	302	340	271	589	619	563	5.27	5.10	5.37
105	251	240	270	213	446	471	423	12.63	12.29	12.87
6	259	171	193	151	305	323	287	1.16	1.12	1.19
27	264	167	189	148	297	315	279	5.25	5.16	5.29
36	269	146	165	129	256	272	241	11.58	11.33	11.77
43	272	118	133	103	203	215	190	8.46	8.34	8.51
61	277	76	85	67	130	138	123	7.20	6.94	7.43
17	285	20	22	17	32	34	30	3.37	3.30	3.42

Age at base of sediments 290 Ma

Toolachee 9 28.36 140.84 Height above present day sea level 69 m

Observed Thickness (m)	Age (Ma)	Basement Depth (m)			Total Decompacted Thickness (m)			Deposition Rate (m/m.y.)		
781	91	848	924	792	2347	2347	2347	138.7	128.2	147.2
276	95	759	835	698	1784	1815	1754	47.54	44.93	49.32
23	100	722	794	662	1534	1570	1499	20.96	19.93	21.55
240	101	699	771	640	1511	1548	1477	18.26	17.46	18.72
67	113	574	638	520	1264	1300	1231	4.35	4.16	4.49
67	127	546	608	495	1192	1228	1160	10.26	9.82	10.57
212	133	516	575	468	1117	1152	1087	14.36	13.48	15.11
36	146	429	481	388	896	931	865	2.78	2.67	2.86
84	158	412	462	372	855	889	825	2.66	2.51	2.80
0	186	378	425	340	766	801	736	0.01	0.01	0.01
80	230	377	425	340	765	801	735	3.61	3.49	3.69
153	251	339	381	304	672	704	643	18.00	17.33	18.44
0	259	261	295	233	489	517	465	0.29	0.28	0.29
6	260	261	295	232	48	517	464	1.45	1.41	1.49
64	264	258	291	229	482	509	457	12.49	12.28	12.58
62	269	214	242	190	392	415	372	19.89	19.30	20.28
54	272	174	196	154	309	327	291	10.53	10.36	10.60
140	277	128	145	114	225	238	213	16.69	16.12	17.07

Age at base of sediments 285 Ma

Durham Downs 1 27.08 145.33 Height above present day sea level 112 m

Observed Thickness (m)	Age (Ma)	Basement Depth (m)			Total Decompacted Thickness (m)			Deposition Rate (m/m.y.)		
549	91	975	1060	905	2704	2704	2704	89.91	82.36	97.52
213	95	918	1005	847	2331	2355	2308	163.9	152.0	175.3
287	96	892	979	819	2167	2199	2134	60.96	57.36	63.41
12	100	856	941	783	1918	1958	1877	11.07	10.58	11.34
370	101	836	921	763	1906	1946	1865	27.86	26.59	28.69
96	113	681	758	613	1545	1589	1503	6.19	5.89	6.42
78	127	648	722	582	1450	1494	1407	11.73	11.17	12.19
69	133	620	692	556	1370	1414	1327	12.22	11.48	12.86
126	138	598	668	535	1304	1349	1260	19.86	19.21	20.30
34	144	544	608	486	1163	1206	1122	14.91	13.99	15.70
63	146	531	595	474	1129	1172	1088	4.97	4.80	5.07
249	158	503	563	448	1057	1098	1018	10.49	10.04	10.86
0	180	388	436	344	775	811	741	0.01	0.01	0.01
327	230	388	436	344	775	811	740	14.82	14.36	15.17
100	251	196	221	173	357	377	333	11.93	11.51	12.23
111	259	121	137	107	213	227	201	4.11	3.98	4.20
21	285	23	27	20	38	41	35	4.06	3.99	4.10

Age at base of sediments 290 Ma

Naccowlah 1 27.48 142.1 Height above present day sea level 80 m

Observed Thickness (m)	Age (Ma)	Basement Depth (m)			Total Decompacted Thickness (m)			Deposition Rate (m/m.y.)		
61	0	960	1035	899	2020	2020	2020	0.39	0.35	0.42
849	91	761	836	700	1985	1988	1983	68.96	63.76	73.32
17	100	661	727	603	1324	1351	1296	15.12	14.35	15.54
319	101	638	704	581	1305	1332	1278	23.24	21.97	24.09
92	113	476	528	429	978	1003	953	5.77	5.47	6.05
85	127	434	481	391	877	900	853	12.51	11.89	13.12
77	133	391	434	353	780	801	758	12.82	11.70	13.78
48	138	356	397	321	699	722	677	7.27	6.92	7.54
69	144	329	367	297	640	662	620	30.32	28.46	32.05
59	146	293	327	264	560	581	540	4.41	4.16	4.61
50	158	259	289	233	487	507	469	2.53	2.32	2.69
66	175	232	260	208	430	449	411	5.58	5.33	5.75
0	186	189	212	169	342	359	326	0.01	0.01	0.01
40	230	189	212	169	342	358	326	1.79	1.73	1.83
84	251	160	179	143	285	299	272	9.78	9.44	10.06
0	259	94	105	84	163	170	155	0.02	0.01	0.02
103	277	94	104	84	162	169	155	11.83	11.24	12.25

Age at base of sediments 285 Ma

Naryilco 1 28.45 141.71 Height above present day sea level 132 m

Observed Thickness (m)	Age (Ma)	Basement Depth (m)			Total Decompacted Thickness (m)			Deposition Rate (m/m.y.)		
37	0	762	818	720	1477	1477	1477	0.22	0.20	0.24
408	91	567	622	524	1456	1457	1455	52.99	48.46	57.01
191	96	552	604	509	1175	1189	1158	37.31	34.68	39.09
36	100	532	580	490	1010	1028	989	29.23	27.30	30.49
306	101	505	553	463	977	996	956	21.97	20.75	22.70
89	113	340	375	307	658	675	639	5.63	5.34	5.81
80	127	292	322	263	552	567	536	11.91	11.32	12.29
79	133	242	266	219	450	462	438	13.26	12.35	14.08
20	138	196	216	177	357	368	346	2.98	2.85	3.08
75	144	181	200	164	329	339	319	31.64	29.36	33.65
42	146	133	147	120	235	244	226	3.11	2.96	3.25
38	158	101	112	91	176	183	169	1.44	1.33	1.54
0	180	74	82	66	126	132	119	0.01	0.01	0.01
78	230	73	82	65	125	132	119	3.40	3.25	3.50

Age at base of sediments 251 Ma

Orientos 1 28.05 141.42 Height above present day sea level 144 m

Observed Thickness (m)	Age (Ma)	Basement Depth (m)			Total Decompacted Thickness (m)			Deposition Rate (m/m.y.)		
20	0	994	1066	9402	2172	2172	2172	0.12	0.11	0.13
650	91	801	874	748	2206	2207	2205	89.55	82.33	95.72
248	96	747	820	689	1752	1779	1724	52.92	49.85	54.77
323	100	699	769	641	1534	1568	1501	22.59	21.58	23.13
91	113	559	622	506	1214	1249	1180	5.97	5.73	6.12
140	127	523	582	472	1117	1151	1084	11.77	11.31	12.06
65	138	459	511	414	958	990	929	9.46	8.87	9.97
40	144	431	481	389	890	922	861	17.56	16.39	18.55
36	146	414	462	373	847	879	818	2.71	2.59	2.82
74	158	397	444	357	807	838	778	3.77	3.50	4.01
5	175	366	411	328	729	762	700	0.40	0.38	0.42
0	186	364	408	326	724	756	694	0.01	0.01	0.01
265	230	363	408	326	723	756	694	11.91	11.52	12.15
260	251	212	238	189	390	410	372	7.23	6.98	7.41

Age at base of sediments 285 Ma

Wareena 1 26.89 142.30 Height above present day sea level 107 m

Observed Thickness (m)	Age (Ma)	Basement Depth (m)			Total Decompacted Thickness (m)			Deposition Rate (m/m.y.)		
406	91	728	797	670	1897	1896	1896	51.47	47.04	55.86
117	96	721	789	663	1628	1642	1612	21.75	20.06	23.04
29	100	719	785	660	1536	1554	1516	23.08	21.48	24.15
333	101	704	769	646	1510	1528	1490	22.57	21.10	23.65
92	113	557	615	505	1204	1228	1181	5.47	5.12	5.77
29	127	524	579	474	1115	1140	1091	4.04	3.78	4.26
114	133	512	567	464	1086	1111	1062	18.62	17.25	19.91
126	138	474	525	427	980	1007	953	18.85	17.94	19.50
17	144	415	461	373	839	864	815	6.99	6.47	7.47
68	146	408	453	367	822	848	798	5.10	4.85	5.27
138	158	374	415	336	744	767	721	7.15	6.74	7.50
52	175	304	339	273	586	608	565	9.30	8.77	9.73
0	180	276	307	247	523	544	504	0.01	0.01	0.01
341	205	275	307	247	523	544	503	10.41	9.95	10.79
32	235	32	36	29	54	57	51	1.24	1.19	1.27

Age at base of sediments 259 Ma

Mt. Howitt 1 26.62 142.47 Height above present day sea level 144 m

Observed Thickness (m)	Age (Ma)	Basement Depth (m)			Total Decompacted Thickness (m)			Deposition Rate (m/m.y.)		
440	91	857	935	793	2264	2263	2263	56.16	51.37	60.92
229	96	834	911	768	1976	1994	1957	43.91	40.68	46.33
28	100	816	892	749	1795	1820	1769	23.35	21.90	24.24
308	101	792	867	725	1769	1795	1742	21.64	20.35	22.56
102	113	658	728	596	1485	1516	1454	6.20	5.82	6.50
126	127	624	691	564	1388	1420	1356	9.71	9.09	10.30
114	138	584	648	526	1270	1305	1236	17.18	16.41	17.72
43	144	537	596	482	1148	1182	1115	18.06	16.77	19.25
90	146	522	581	468	1107	1141	1073	6.85	6.54	7.05
153	158	482	537	432	1008	1041	976	8.02	7.60	8.39
82	175	416	464	372	843	875	812	6.79	6.49	7.05
0	186	376	420	336	748	779	719	0.01	0.01	0.01
393	230	376	420	336	748	778	719	17.40	16.73	17.95
136	251	138	156	123	246	259	233	3.77	3.63	3.87
21	285	23	26	20	38	41	35	4.01	3.92	4.07

Age at base of sediments 290 Ma

Ingella 1 25.53 142.79 Height above present day sea level 125 m

Observed Thickness (m)	Age (Ma)	Basement Depth (m)			Total Decompacted Thickness (m)			Deposition Rate (m/m.y.)		
899	91	978	1072	904	2668	2668	2668	159.	147.1	170.8
8	95	843	936	765	2014	2050	1978	67.81	63.66	71.54
314	96	843	936	765	1946	1984	1907	69.56	66.06	71.95
21	100	792	878	716	1656	1698	1613	19.46	18.77	19.79
261	101	769	854	693	1634	1676	1591	20.11	19.32	20.60
80	113	634	709	566	1362	1400	1322	5.14	4.89	5.35
26	127	601	673	537	1277	1314	1238	3.77	3.53	3.96
119	133	591	662	527	1251	1288	1212	21.12	19.79	22.19
116	138	544	609	484	1127	1163	1088	18.13	17.45	18.61
23	144	486	544	433	991	1022	957	10.20	9.57	10.76
90	146	476	532	424	965	997	932	6.90	6.58	7.14
197	158	428	478	382	857	885	827	10.29	9.52	10.88
140	175	326	366	289	628	656	601	11.79	11.17	12.24
0	186	243	273	215	452	475	429	0.02	0.01	0.02
11	205	243	273	215	451	474	429	0.42	0.40	0.43
292	230	236	265	209	436	459	415	13.21	12.75	13.56

Age at base of sediments 251 Ma

Galway 1 25.08 142.56 Height above present day sea level 207 m

Observed Thickness (m)	Age (Ma)	Basement Depth (m)			Total Decompacted Thickness (m)			Deposition Rate (m/m.y.)		
11	0	1163	1255	1088	2655	2655	2655	0.07	0.06	0.08
915	91	972	1065	897	2649	2649	2648	131.0	120.79	140.2
333	96	853	944	774	1979	2016	1942	73.35	69.55	75.97
18	100	796	882	720	1674	1715	1631	16.53	15.92	16.82
226	101	774	859	698	1655	1696	1612	17.31	16.60	17.76
86	113	653	730	584	1421	1460	1381	5.49	5.22	5.73
182	127	620	693	554	1332	1370	1293	14.92	14.16	15.59
75	138	546	611	487	1139	1175	1101	11.67	11.22	11.99
37	144	509	569	454	1051	1085	1017	16.63	15.58	17.58
94	146	493	551	439	1011	1044	976	7.23	6.88	7.48
233	158	444	495	396	899	928	868	12.14	11.22	12.85
107	175	329	370	291	635	665	605	9.22	8.92	9.45
0	186	265	298	235	497	522	473	0.01	0.01	0.01
337	230	265	298	234	497	521	473	15.26	14.72	15.67

Age at base of sediments 251 Ma

Bodalla 1 26.43 143.44 Height above present day sea level 152 m

Observed Thickness (m)	Age (Ma)	Basement Depth (m)			Total Decompacted Thickness (m)			Deposition Rate (m/m.y.)		
40	0	916	985	860	1910	1910	1910	0.25	0.23	0.27
714	91	721	790	665	1887	1889	1886	55.85	51.42	59.67
468	100	642	705	587	1352	1377	1327	31.21	29.52	32.39
48	113	432	480	390	881	906	857	3.03	2.87	3.17
56	127	411	456	370	829	853	805	8.17	7.72	8.54
98	133	384	426	345	766	789	743	16.81	15.69	17.82
69	138	340	378	305	661	685	638	10.70	10.27	10.99
71	144	299	332	268	573	594	554	30.67	28.59	32.54
98	146	262	293	235	493	514	473	7.58	7.28	7.78
78	158	199	222	178	363	379	348	4.14	3.94	4.31
63	175	146	163	130	259	272	248	5.31	5.10	5.48
0	186	96	107	86	167	175	159	0.01	0.01	0.01
71	230	96	107	86	167	175	159	3.12	2.99	3.22
35	251	34	38	30	57	60	55	0.95	0.90	0.98

Age at base of sediments 285 Ma

Chandos 1 25.84 143.33 Height above present day sea level 225 m

Observed Thickness (m)	Age (Ma)	Basement Depth (m)			Total Decompacted Thickness (m)			Deposition Rate (m/m.y.)		
4	0	1098	1186	1026	2436	2436	2436	0.02	0.02	0.03
726	91	909	997	837	2434	2434	2434	124.8	114.6	134.0
182	95	809	896	735	1916	1945	1888	147.9	138.2	156.6
201	96	784	869	711	1765	1798	1731	43.60	41.21	45.26
36	100	765	845	692	1583	1619	1545	33.33	31.94	34.04
260	101	736	815	664	1545	1581	1507	19.67	18.79	20.23
85	113	601	670	537	1276	1309	1241	5.38	5.10	5.63
151	127	567	632	506	1187	1220	1153	12.20	11.54	12.78
80	138	502	561	448	1026	1057	994	12.40	11.89	12.77
65	144	461	514	412	931	958	902	28.38	26.53	30.09
101	146	431	480	385	859	886	831	7.72	7.33	8.00
233	158	374	416	335	736	758	711	7.32	6.75	7.76
0	186	246	276	219	459	481	438	0.01	0.01	0.01
249	230	246	276	219	459	481	438	11.15	10.71	11.50
62	251	62	70	54	105	112	99	1.76	1.71	1.80

Age at base of sediments 285 Ma

Canaway 1   29.93 143.96   Height above present day sea level 239 m

Observed Thickness (m)	Age (Ma)	Basement Depth (m)			Total Decompacted Thickness (m)			Deposition Rate (m/m.y.)		
324	91	603	664	550	1480	1480	1480	49.74	45.32	53.94
143	95	582	640	531	1259	1268	1249	100.42	92.37	108.1
213	96	564	619	514	1148	1161	1134	41.21	38.23	43.51
219	100	508	557	463	957	971	940	13.95	13.07	14.57
87	113	377	415	341	727	739	714	5.08	4.74	5.39
160	127	334	367	302	633	644	621	12.08	11.28	12.83
41	138	246	269	223	448	456	439	5.98	5.65	6.24
37	144	217	237	198	394	399	387	14.99	13.85	16.15
67	146	195	212	178	350	355	343	4.81	4.50	5.05
19	158	146	157	134	259	260	256	9.20	8.38	9.91

Age at base of sediments 175 Ma

Yongola 1   25.5 143.93   Height above present day sea level 208 m

Observed Thickness (m)	Age (Ma)	Basement Depth (m)			Total Decompacted Thickness (m)			Deposition Rate (m/m.y.)		
5	0	981	1054	918	2095	2095	2095	0.03	0.03	0.03
635	91	791	865	728	2092	2092	2092	106.89	98.08	115.3
190	95	702	773	641	1638	1661	1614	148.7	138.1	158.8
229	96	677	746	615	1485	1513	1454	49.97	47.31	51.62
11	100	640	703	581	1267	1297	1234	9.70	9.27	9.93
234	101	620	683	561	1255	1286	1223	17.56	16.76	18.11
86	113	486	539	435	1006	1034	977	5.42	5.13	5.68
112	127	448	498	401	913	940	885	16.56	15.68	17.35
67	133	397	441	355	789	815	763	11.79	11.14	12.41
56	138	365	407	326	715	740	690	8.67	8.32	8.93
29	144	334	371	298	646	669	623	12.79	11.95	13.53
72	146	319	355	285	613	636	590	5.49	5.27	5.69
180	158	277	308	247	522	542	503	9.56	9.05	9.98
87	175	163	182	145	291	305	278	7.45	7.18	7.67
0	186	93	104	83	162	170	155	0.01	0.01	0.01
76	230	93	104	83	162	169	154	3.32	3.16	3.46
0	251	27	30	24	45	48	43	0.04	0.03	0.04
27	259	27	30	24	45	47	42	0.96	0.92	0.99

Age at base of sediments 285 Ma

Cothalow 1   25.73 144.4   Height above present day sea level 241 m

Observed Thickness (m)	Age (Ma)	Basement Depth (m)			Total Decompacted Thickness (m)			Deposition Rate (m/m.y.)		
18	0	820	881	767	1600	1600	1600	0.12	0.11	0.13
554	91	628	689	575	1589	1590	1589	73.64	67.50	79.50
192	96	572	627	521	1191	1208	1172	39.03	36.48	40.76
6	100	543	593	496	1013	1032	992	5.21	4.90	5.38
251	101	525	574	478	1006	1025	985	17.95	16.94	18.67
79	113	375	413	338	738	754	720	4.77	4.48	5.04
143	127	336	370	303	650	666	634	20.08	18.79	21.31
40	133	261	289	235	489	503	474	3.26	3.09	3.38
43	144	236	260	213	437	449	424	17.91	16.60	19.12
52	146	211	233	190	387	399	374	3.84	3.65	4.01
165	158	176	194	159	318	328	308	8.46	7.95	8.91
0	175	54	60	48	92	96	88	0.00	0.00	0.00
58	259	54	60	48	92	96	87	2.00	1.91	2.09

Age at base of sediments 285 Ma

Quilberry 1 145.5 26.4 Height above present day sea level 324 m

Observed Thickness (m)	Age (Ma)	Basement Depth (m)			Total Decompacted Thickness (m)			Deposition Rate (m/m.y.)		
23	91	463	506	424	1067	1067	1067	2.54	2.31	2.77
184	96	519	562	479	1053	1054	1052	27.02	24.58	29.34
1	100	507	54	469	927	931	921	9.81	8.97	10.54
287	101	486	526	449	915	919	908	16.90	15.55	18.02
84	113	338	369	309	657	664	649	4.44	4.10	4.78
108	127	301	328	275	574	582	566	7.42	6.84	8.00
84	138	250	273	227	464	472	455	11.24	10.48	11.86
44	144	200	218	183	366	372	359	16.94	15.54	18.33
64	146	176	192	160	317	323	310	4.36	4.08	4.62
137	158	133	145	122	236	241	231	6.53	6.06	6.98
0	175	33	37	30	56	58	54	0.00	0.00	0.00
36	251	33	36	30	55	57	53	0.91	0.85	0.95

Age at base of sediments 285 Ma

Dartmouth 1 26.14 145.30 Height above present day sea level 341 m

Observed Thickness (m)	Age (Ma)	Basement Depth (m)			Total Decompacted Thickness (m)			Deposition Rate (m/m.y.)		
162	91	743	816	680	1910	1910	1910	23.40	21.30	25.52
123	95	770	842	706	1812	1818	1806	79.25	72.40	86.08
148	96	763	834	698	1733	1743	1721	26.25	24.15	27.91
12	100	769	838	704	1622	1636	1605	9.17	8.48	9.66
319	101	749	819	685	1612	1626	1595	20.98	19.54	22.09
97	113	612	674	553	1329	1349	1308	5.52	5.14	5.89
108	127	578	638	522	1239	1260	1217	7.93	7.37	8.48
107	138	541	597	487	1139	1161	1114	15.24	14.36	15.92
69	144	495	547	446	1027	1048	1004	27.94	25.78	29.97
84	146	469	519	422	960	982	936	6.07	5.74	6.37
512	158	430	476	387	868	889	846	26.37	24.78	27.77
63	175	146	163	130	260	272	248	5.29	5.07	5.48
0	186	97	109	87	169	178	160	0.01	0.01	0.01
71	230	97	109	86	168	177	160	3.13	3.01	3.23
35	251	34	38	31	58	61	55	0.96	0.92	0.99

Age at base of sediments 285 Ma

Gilmore 1 25.36 144.8 Height above present day sea level 327 m

Observed Thickness (m)	Age (Ma)	Basement Depth (m)			Total Decompacted Thickness (m)			Deposition Rate (m/m.y.)		
58	0	939	1010	878	1964	1964	1964	0.37	0.34	0.40
582	91	741	812	680	1931	1933	1928	79.59	73.08	85.72
209	96	688	756	627	1515	1536	1490	43.63	40.93	45.41
9	100	661	724	602	1325	1350	1297	7.98	7.55	8.23
262	101	642	705	583	1316	1341	1288	19.07	18.06	19.78
78	113	502	556	452	1047	1072	1021	4.76	4.48	5.01
115	127	470	520	422	966	991	941	8.94	8.38	9.46
59	138	421	467	377	846	870	821	8.82	8.40	9.13
55	144	391	433	350	778	800	754	23.32	21.67	24.83
91	146	366	406	328	719	742	696	6.87	6.55	7.15
248	158	316	351	283	609	629	589	13.02	12.28	13.65
0	175	167	186	149	300	314	286	0.00	0.00	0.00
198	259	166	186	148	299	313	286	7.05	6.77	7.29

Age at base of sediments 285 Ma

Log Creek 1 25.27 144.91 Height above present day sea level 295 m

Observed Thickness (m)	Age (Ma)	Basement Depth (m)			Total Decompacted Thickness (m)			Deposition Rate (m/m.y.)		
46	0	969	1042	906	2056	2056	2056	0.29	0.26	0.32
507	91	772	845	709	2029	2031	2028	84.61	77.55	91.33
106	95	717	788	654	1673	1693	1652	80.37	74.33	86.24
175	96	714	784	651	1593	1616	1567	36.42	34.17	37.90
6	100	699	766	637	1436	1463	1407	5.30	5.01	5.47
297	101	681	748	620	1430	1457	1401	21.57	20.43	22.37
84	113	535	592	480	1133	1160	1105	5.14	4.85	5.42
75	127	501	556	450	1047	1075	1019	10.85	10.23	11.43
30	133	470	522	422	969	996	941	5.14	4.82	5.44
59	138	458	509	411	938	966	910	8.87	8.46	9.19
51	144	430	477	385	871	897	845	21.80	20.26	23.20
154	146	408	454	365	818	845	791	11.61	11.08	12.07
226	158	329	365	294	637	659	615	11.92	11.26	12.48
0	175	197	220	175	359	376	342	0.00	0.00	0.00
35	251	196	220	175	358	375	342	4.05	3.89	4.19
205	259	172	193	153	311	326	296	7.35	7.06	7.58

Age at base of sediments 285 Ma

Stafford 1 25.29 145.43 Height above present day sea level 357 m

Observed Thickness (m)	Age (Ma)	Basement Depth (m)			Total Decompacted Thickness (m)			Deposition Rate (m/m.y.)		
170	91	647	710	591	1626	1626	1626	24.83	22.60	27.05
104	95	671	733	614	1522	1528	1516	66.90	61.15	72.67
197	96	671	733	614	1455	1463	1443	35.38	32.59	37.48
3	100	654	713	599	1299	1312	1283	2.33	2.16	2.45
276	101	638	696	582	1296	1310	1280	18.24	16.99	19.17
91	113	500	551	452	1038	1054	1021	5.15	4.78	5.52
101	127	466	513	421	951	968	933	7.31	6.79	7.84
99	138	427	471	384	854	871	835	14.08	13.26	14.71
26	144	380	418	342	745	761	728	10.33	9.48	11.16
148	146	369	407	332	719	736	702	10.61	10.02	11.17
197	158	289	318	261	547	560	534	7.62	7.13	8.10
0	180	170	187	154	307	316	298	0.01	0.00	0.01
144	230	170	187	154	306	315	297	6.91	6.43	7.33
70	248	68	75	60	114	120	108	9.23	8.85	9.51

Age at base of sediments 255 Ma

Bury 1 25.04 145.6 Height above present day sea level 333 m

Observed Thickness (m)	Age (Ma)	Basement Depth (m)			Total Decompacted Thickness (m)			Deposition Rate (m/m.y.)		
55	91	648	711	591	1609	1609	1609	6.34	5.79	6.91
207	96	715	777	657	1578	1579	1576	31.73	28.90	34.29
3	100	704	764	647	1438	1446	1430	2.04	1.87	2.19
275	101	687	747	630	1436	1443	1427	16.46	15.18	17.59
56	113	564	618	512	1207	1219	1194	2.98	2.76	3.21
152	127	545	597	495	1157	1171	1143	19.49	18.04	20.91
93	133	488	536	443	1016	1031	1001	5.62	5.19	6.02
101	146	452	496	409	927	942	911	6.85	6.41	7.29
235	158	407	448	369	822	838	807	8.73	8.08	9.34
0	180	296	327	268	573	589	557	0.00	0.00	0.01
126	230	296	327	268	572	589	557	5.80	5.36	6.21
98	248	234	260	210	435	452	418	12.57	11.99	13.02
207	255	172	191	154	309	322	296	7.56	7.24	7.83

Age at base of sediments 280 Ma

Gumbardo 1 25.04 145.60 Height above present day sea level 86 m

Observed Thickness (m)	Age (Ma)	Basement Depth (m)			Total Decompacted Thickness (m)			Deposition Rate (m/m.y.)		
29	0	766	822	716	1441	1441	1441	0.18	0.17	0.20
255	91	572	628	522	1424	1425	1423	38.99	35.58	42.36
116	95	572	625	522	1254	1263	1244	79.21	72.66	85.69
164	9	566	617	516	1172	1183	1157	31.35	29.06	32.96
5	100	551	598	503	1029	1044	1012	4.14	3.85	4.32
282	101	533	580	486	1025	1039	1007	19.42	18.20	20.26
8	113	373	409	337	733	747	719	5.11	4.76	5.45
105	127	332	364	299	640	653	626	7.78	7.25	8.35
8	138	279	307	252	526	538	512	12.54	11.80	13.22
50	144	227	250	205	419	429	408	20.52	18.95	22.09
94	146	199	219	179	361	372	350	6.90	6.54	7.22
164	158	132	144	119	234	240	228	6.40	6.01	6.80

Age at base of sediment 180 Ma

Eastwood 1 24.77 145.35 Height above present day sea level 277 m

Observed Thickness (m)	Age (Ma)	Basement Depth (m)			Total Decompacted Thickness (m)			Deposition Rate (m/m.y.)		
264	91	673	740	616	1700	1700	1700	39.78	36.21	43.17
83	95	675	740	618	1531	1539	1521	55.72	51.09	60.56
208	96	672	736	615	1473	1484	1460	38.82	35.85	40.98
4	100	653	713	599	1300	1316	1283	2.91	2.71	3.04
269	101	636	696	582	1297	1312	1280	17.92	16.70	18.87
62	113	502	553	454	1044	1061	1026	3.56	3.31	3.79
216	127	478	527	432	983	1001	965	16.09	14.93	17.09
41	138	389	430	350	767	786	747	6.15	5.86	6.34
7	144	366	405	330	717	735	699	2.87	2.65	3.08
75	146	363	401	327	710	727	692	5.50	5.22	5.72
278	158	322	354	290	620	635	605	10.81	10.08	11.48
0	180	161	178	144	287	298	276	0.01	0.01	0.01
12	220	160	178	144	287	298	276	1.10	1.06	1.12
73	230	150	166	135	269	279	259	3.50	3.26	3.71
109	248	101	112	90	174	183	165	14.38	13.81	14.83

Age at base of sediments 255 Ma

Ban Ban 1 24.13 143.7 Height above present day sea level 21 m

Observed Thickness (m)	Age (Ma)	Basement Depth (m)			Total Decompacted Thickness (m)			Deposition Rate (m/m.y.)		
122	91	550	604	504	1362	1362	1362	17.38	15.81	18.96
72	95	582	635	536	1288	1291	1283	44.09	40.15	47.80
335	96	577	629	531	1241	1247	1234	59.43	54.69	63.17
33	100	527	572	483	972	984	957	25.80	24.02	26.99
200	101	498	542	455	940	953	925	13.41	12.52	14.08
55	113	373	409	339	736	748	723	3.15	2.93	3.36
155	127	348	382	316	679	691	666	11.30	10.49	12.09
65	138	273	301	247	514	527	502	9.20	8.66	9.62
41	144	235	258	213	436	446	425	16.60	15.30	17.84
80	146	213	234	192	390	400	379	5.70	5.38	5.99
150	158	160	176	145	287	295	280	7.50	7.00	7.95
0	175	51	56	46	86	89	82	0.00	0.00	0.01
54	230	50	56	45	85	89	82	0.88	0.83	0.91

Age at base of sediments 285 Ma

Fermoy 1	23.14 143.05				Height above present day sea level			245 m		
Observed Thickness (m)	Age (Ma)	Basement Depth (m)			Total Decompacted Thickness (m)			Deposition Rate (m/m.y.)		
335	91	608	666	557	1536	1536	1536	51.75	47.22	56.20
155	95	587	643	538	1309	1320	1298	109.0	100.2	117.7
301	96	570	624	521	1194	1209	1177	60.61	56.58	63.40
34	100	506	551	462	918	936	897	29.74	28.08	30.70
197	101	474	519	432	881	899	861	14.12	13.34	14.68
53	113	341	376	308	662	677	646	3.20	3.01	3.39
27	127	314	346	284	602	617	587	3.72	3.49	3.94
65	133	300	330	271	572	586	558	10.92	10.21	11.63
35	138	265	292	239	498	511	484	5.10	4.83	5.30
100	144	243	268	220	453	465	441	41.50	38.44	44.37
107	146	186	206	167	336	348	325	7.90	7.51	8.25
109	158	108	119	98	190	196	184	5.61	5.27	5.91
19	175	19	21	17	31	33	30	1.71	1.63	1.78

Age at base of sediments 185 Ma

Appendix 3

Solution to the heat conduction problem in an semi-infinite half-space and a slab with constant heat flux and constant temperature lower boundary conditions

The simplified governing equation in 1-D is given as

$$\frac{\partial^2 T}{\partial z^2} = \kappa \frac{\partial T}{\partial t} \qquad \text{(A.3.1)}$$

and the initial and upper boundary conditions are given as

$$T(z,0) = 0 \qquad z < L \qquad \text{(A.3.2a)}$$

$$= G(z - L) \qquad z > L$$

and $T(0,t) = 0$ (A.3.2b)

(i) semi-infinite half-space

The general solution for the temperature is given as (Carslaw and Jaeger, 1959, section 2.4)

$$T(z,t) = \frac{1}{2\sqrt{\kappa t \pi}} \int_0^{\infty} f(z') \left(e^{-(z-z')^2/4\kappa t} - e^{-(z+z')^2/4\kappa t} \right) dz' \qquad \text{(A.3.3)}$$

where f(z') is the initial condition (A.3.2a). The integral is solved in two parts. Making the substitution

$$z' = z + 2u\sqrt{(\kappa t)}$$

The first exponential term in (A.3.3) is then expressed, with the initial condition (A.3.2a), as

$$\frac{G}{\sqrt{\pi}} \int_{\frac{L-z}{2\sqrt{\kappa t}}}^{\infty} (z - L + 2u\sqrt{(\kappa t)})\, e^{-u^2}\, du$$

$$= \frac{G}{\sqrt{\pi}}(z - L)\left[\int_0^{\infty} e^{-u^2}\, du + \int_{\frac{L-z}{2\sqrt{\kappa t}}}^{0} e^{-u^2}\, du\right] + 2G\sqrt{\frac{\kappa t}{\pi}} \int_{\frac{L-z}{2\sqrt{\kappa t}}}^{\infty} u\, e^{-u^2}\, du$$

(A.3.4)

The error function, erf (u) is given as (Carslaw and Jaeger, 1959, appendix ii)

$$\mathrm{erf}(u) = \frac{2}{\sqrt{\pi}} \int_0^{u} e^{-\xi^2}\, d\xi$$

and erf (u) = -erf(-u), erf(0) = 0 and erf(∞) = 1, the solution to (A.3.4) is then written as

$$\frac{G\,(z - L)}{2}\left[1 + \mathrm{erf}\left(\frac{z - L}{2\sqrt{\kappa t}}\right)\right] + G\sqrt{\frac{\kappa t}{\pi}}\left[e^{-(z - L)^2/4\kappa t}\right]$$

(A.3.5a)

The second exponential term in (A.3.3) is solved with the substitution

$$z' = -z + 2u\sqrt{(\kappa t)}$$

to give , after including the minus sign in front of the second exponential term in A.3.3

$$\frac{G\,(z + L)}{2}\left[1 - \mathrm{erf}\left(\frac{z + L}{2\sqrt{\kappa t}}\right)\right] - G\sqrt{\frac{\kappa t}{\pi}}\left[e^{-(z + L)^2/4\kappa t}\right]$$

(A.3.5b)

Then adding A.3.5a and A.3.5b,

$$T(z,t) = G\left[z + \sqrt{\frac{\kappa t}{\pi}} \left(e^{-(L-z)^2/4\kappa t} - e^{-(L+z)^2/4\kappa t} \right) + \frac{z-L}{2} \operatorname{erf}\left(\frac{z-L}{2\sqrt{\kappa t}}\right) - \frac{z+L}{2} \operatorname{erf}\left(\frac{z+L}{2\sqrt{\kappa t}}\right) \right] \tag{A.3.6a}$$

and with the complementary error function, erfc(u) = 1 - erf(u), then

$$T(z,t) = G\left[(z-L) + \sqrt{\frac{\kappa t}{\pi}} \left(e^{-(L-z)^2/4\kappa t} - e^{-(L+z)^2/4\kappa t} \right) + \frac{z+L}{2} \operatorname{erfc}\left(\frac{z+L}{2\sqrt{\kappa t}}\right) - \frac{z-L}{2} \operatorname{erfc}\left(\frac{z-L}{2\sqrt{\kappa t}}\right) \right] \tag{A.3.6b}$$

As erfc(0) = 1, then as $t \rightarrow \infty$, $T(z,t) \rightarrow Gz$, the steady state solution.

(ii) A slab of thickness a with constant gradient at the base equal to the steady state value, G. The additional lower boundary condition is then

$$\left.\frac{dT}{dz}\right|_a = G \tag{A.3.7}$$

Following Carlsaw and Jaeger (1959), sections 1.14.I, 3.4 and 3.8, the solution is considered in two parts i.e.

$$T(z,t) = u(z) + w(z,t)$$

where u(z) is the steady state term and w(z,t) is the transient contribution. With (A.3.2a,b) and (A.3.7), then

$$u(z) = Gz$$

For w(z,t), the initial and boundary conditions are expressed as

$$w(0,t) = 0, \quad \left.\frac{dw}{dz}\right|_a = 0 \text{ and } w(z,0) = f(z) - u(z), \text{ where } f(z) \text{ is given by (A.3.2a)}$$

These conditions are satisfied by a solution of the form

$$w(z,t) = \sum_{n=0}^{\infty} A_n \, e^{-\kappa\left(\frac{(2n+1)\pi}{2a}\right)^2 t} \sin\left(\frac{(2n+1)\pi z}{2a}\right) \tag{A.3.8a}$$

with
$$A_n = \frac{2}{a}\int_0^a [f(z') - u(z')] \sin\left(\frac{(2n+1)\pi z}{2a}\right) dz' \tag{A.3.8b}$$

Then, as $T(z,t) = u(z) + w(z,t)$,

$$T(z,t) = Gz - \frac{8Ga}{\pi^2}\sum_{n=0}^{\infty}\frac{1}{(2n+1)^2} e^{-\kappa\left(\frac{(2n+1)\pi}{2a}\right)^2 t} \sin\left(\frac{(2n+1)\pi z}{2a}\right)\sin\left(\frac{(2n+1)\pi L}{2a}\right) \tag{A.3.9}$$

(iii) a slab of thickness a with constant temperature $T_b = Ga$ at the base. The same approach as (ii) is taken, .i.e.

$$T(z,t) = u(z) + w(z,t)$$

with
$$u(z) = T_b \frac{z}{a}$$

and for $w(z,t)$ the initial and boundary conditions are expressed as

$$w(0,t) = w(a,t) = 0 \text{ and } w(z,0) = f(z) - u(z), \text{ where } f(z) \text{ is given by (A.3.2a)}$$

These conditions are satisfied by a solution of the form

$$w(z,t) = \sum_{n=1}^{\infty} A_n \, e^{-\kappa\left(\frac{n\pi}{a}\right)^2 t} \sin\left(\frac{n\pi z}{a}\right) \tag{A.3.10a}$$

with
$$A_n = \frac{2}{a}\int_0^a [f(z') - u(z')] \sin\left(\frac{n\pi z'}{a}\right) dz' \tag{A.3.10b}$$

then

$$T(z,t) = T_b \frac{z}{a} + \frac{2T_b}{\pi a} \sum_{n=1}^{\infty} \frac{1}{n} e^{-\kappa\left(\frac{n\pi}{a}\right)^2 t} \sin\left(\frac{n\pi z}{a}\right)\left[(-1)^n L - \frac{a}{n\pi}\sin\left(\frac{n\pi L}{a}\right)\right]$$

(A.3.11)

Appendix 4
Inversion procedure for palaeo-heat flow from vitrinite reflectance

The methods outlined here are basically standard optimization techniques and more detail can be found in Adby and Dempster (1974), Lee and Stewart (1981, chapter 5) and Lines and Treitel (1984).

If we have a heat flow model with discrete unknown parameters Q_j, j=1,M and reflectance observations, or data, M_i , i = 1,N, given as

$$M_i = \sum_{j=1}^{M} F_i(Q_j) \qquad i = 1, N \qquad \text{(A.4.1a)}$$

where the known functions F_i relate the heat flow and the reflectance observations, then for a small perturbation δQ_j in each parameter Q_j we obtain the corresponding change in the observations, which are then written as

$$M_i + \delta M_i = \sum_{j=1}^{M} F_i(Q_j + \delta Q_j) \qquad \text{(A.4.1b)}$$

We want to define a misfit function of the model parameters, E(Q) where Q is the vector of model parameters, which will be a measure of the difference between the observed and calculated data, i.e. $M_i^{obs}-M_i^{calc}$ and obviously we want to make this as small as possible.

The misfit function can be expanded as a Taylor's series to second order,

$$E(Q + \delta Q) = E(Q) + \sum_{j=1}^{M} \delta Q_j \frac{\partial E(Q)}{\partial Q_j} + \frac{1}{2} \sum_{j=1}^{M} \sum_{k=1}^{M} \delta Q_j \, \partial Q_k \frac{\partial^2 E(Q)}{\partial Q_j \delta Q_k} \qquad \text{(A.4.2)}$$

Differentiating this with respect to the model parameters and setting the result equal to zero we obtain, again to second order

$$\frac{\partial E(Q)}{\partial Q_m} + \sum_{j=1}^{M} \delta Q_j \frac{\partial^2 E(Q)}{\partial Q_j \delta Q_m} = 0 \qquad \text{for m = 1, M} \qquad \text{(A.4.3)}$$

or in matrix form

$$\mathbf{g} = -\mathbf{H}\,\delta\mathbf{Q} \tag{A.4.4}$$

and then

$$\delta\mathbf{Q} = -\mathbf{H}^{-1}\,\mathbf{g} \tag{A.4.5}$$

where g is the (M x 1) gradient vector and **H** is the (M x M) matrix of second derivatives or Hessian of the misfit function with respect to the model parameters. For a least squares approach we define the misfit function as

$$E = \delta\mathbf{M}^T\delta\mathbf{M} \tag{A.4.6}$$

where $\delta M_i = (M_i^{obs} - M_i^{calc})$, the difference between the observed value and the value calculated from the current heat flow model. Differentiating this with respect to the model parameters gives

$$\frac{dE}{dQ_j} = -\sum_{i=1}^{N} 2\delta M_i \frac{\partial M_i^{calc}}{\partial Q_j} \tag{A.4.7}$$

or $$\mathbf{g} = -2\mathbf{G}^T\delta\mathbf{M} \tag{A.4.8}$$

with $$G_{ji} = \frac{\partial}{\partial Q_j}\left(M_i^{calc}\right)$$

and a second differentiation gives

$$\frac{\partial^2 E}{\partial Q_j \delta Q_k} = 2\sum_{i=1}^{N} \frac{\partial M_i^{calc}}{\partial Q_k}\frac{\partial M_i^{calc}}{\partial Q_j} - 2\sum_{i=1}^{N} \delta M_i \frac{\partial^2\left(M_i^{calc}\right)}{\partial Q_j \delta Q_k} \tag{A.4.9a}$$

$$\approx 2\sum_{i=1}^{N} \frac{\partial M_i^{calc}}{\partial Q_k}\frac{\partial M_i^{calc}}{\partial Q_j} \tag{A.4.9b}$$

or $$H \approx 2G^TG \qquad \text{(A.4.9c)}$$

Substituting eqns. A.4.9c and A.4.8 into A.4.5 gives

$$\delta Q = [\, G^TG]^{-1}\, G^T\, \delta M \qquad \text{(A.4.10)}$$

The discrepancies between the observed and predicted reflectances (M_i^{obs} - M_i^{calc}) may be readily determined and the derivative terms G_{ij} are found from the prescribed relationship between Q and M. Eqn. A.4.10 then gives an improvement to an initial heat flow model (Q_j, j=1,M). This is known as the Gauss-Newton method and, for a non-linear problem, is solved iteratively, updating all the matrices at each pass. However it was found that the solutions rarely converged when the initial model was not close to the true answer (the minimum of the misfit function) so a damped least squares or Levenberg-Marquardt (Marquardt 1963) method was used which minimizes a function of the form

$$E' = E + \lambda\, \delta M^T \delta M$$

and then the improvement to the initial model is

$$\delta Q = [G^TG + \lambda\, I]^{-1}\, G^T\, \delta M \qquad \text{(A.4.11)}$$

As λ becomes large a near steepest descent direction is followed which should always approach a minimum although at a prohibitive rate for this problem. As $\lambda \rightarrow 0$ then the solution is simply the least squares direction. Fletcher (1971) gives a method for choosing λ and this is also summarized in Adby and Dempster (1974). I set the initial value at the size of the biggest eigenvalue of G^TG and at subsequent iterations the ratio P is calculated where

$$P = \frac{E(Q+\delta Q)-E(Q)}{2\delta M^T G \delta Q - \delta Q^T G^T G \delta Q}$$

This is the ratio of the actual reduction in the misfit function to that predicted by the first order approximation, $\delta M + G\delta Q$, to δM at $Q + \delta Q$. If P is close to 1 then the least squares direction is safe and λ should be reduced. Otherwise if P is small a more steepest descent direction is preferred and λ should be increased. We follow the recommended procedure given in Adby and Dempster (1974, pg 105-106) where λ is reduced if $P \geq 0.75$, increased if $P \leq 0.25$ and otherwise it is unchanged. In the first case λ is halved unless it falls below a value λ_c which I take as the sum of the diagonal of $(G^TG)^{-1}$. In this case λ is set to zero and a new λ_c is calculated. If λ is to be increased then a factor ω is calculated as

$$\omega = -\delta M^T G\delta Q \, [\, -2\delta M^T G\delta Q + E(Q) - E(Q+\delta Q)]^{-1}$$

which is derived in Adby and Dempster from the methods used to estimate the optimum step length for the steepest descent technique. If ω^{-1} is between 2 and 10 then $\lambda_{new} = \omega^{-1} \lambda$ otherwise the limit of 2 or 10 is used to multiply λ. Additional stability was provided by using the second derivative terms in eqn. A.4.9a to approximate the Hessian. As these terms form a diagonal matrix, this is equivalent to using a variable λ in eqn. A.4.11 for each model parameter.

In practice it was also found desirable to selectively damp the changes in the model parameters between iterations by applying a damping factor ψ, such that

$$Q_j^{new} = Q_j^{old} + \psi(j)\delta Q_j^{new}$$

and ψ was calculated as

$$\psi(j) = \sigma \left[\frac{j}{M}\right]^p$$

where σ and p were in the range 0.9-1.0 and 1.0-1.5 respectively. The least well constrained parameters were most heavily damped as they were the most unstable.

Appendix 5

Results of palaeo-heat flow inversions with synthetic vitrinite reflectance data

The results of inversion runs are presented in the following format (all heat flows are in mWm^{-2}) -

Solid straight line - assumed heat flow model.

Dashed line - starting heat flow model for inversion (40 mWm^{-2} in all cases).

Solid line (step functions) - heat flow model obtained after inversion with 40 iterations.

Upper panel : Ritter maturation integral (Ri),

Middle panel : Waples maturation integral (Wa),

Lower panel : Royden maturation integral (Ro),

Bottom panel : reflectance values, solid line = values from forward calculation, '+' - inversion generated values.

All models were run for 250 m.y. and the heat flow histories were

(i) $Q(t) = 50$ $mW\,m^{-2}$

(ii) $Q(t) = 100$ $mW\,m^{-2}$

(iii) $Q(t) = 50 + \frac{(250 - t)}{5}$ $(50 \rightarrow 100)$ $mW\,m^{-2}$

(iv) $Q(t) = 100 - \frac{(250 - t)}{5}$ $(100 \rightarrow 50)$ $mW\,m^{-2}$

The sediment thickness was either

(a) 2 km

(b) 5 km

and was deposited linearly over 250 m.y.. The 'x' at the top of the upper panel in each diagram represents the age of each vitrinite observation in the lowermost panel marked by a '+' .

The figures are labeled according to this scheme, so

Figure. number	True heat flow mWm^{-2}	Sediment thickness km
A.5.(i,a)	50	2
A.5.(i,b)	50	5
A.5.(ii,a)	100	2
A.5.(ii,b)	100	5
A.5.(iii,a)	50-100	2
A.5.(iii,b)	50-100	5
A.5.(iv,a)	100-50	2
A.5.(iv,b)	100-50	5

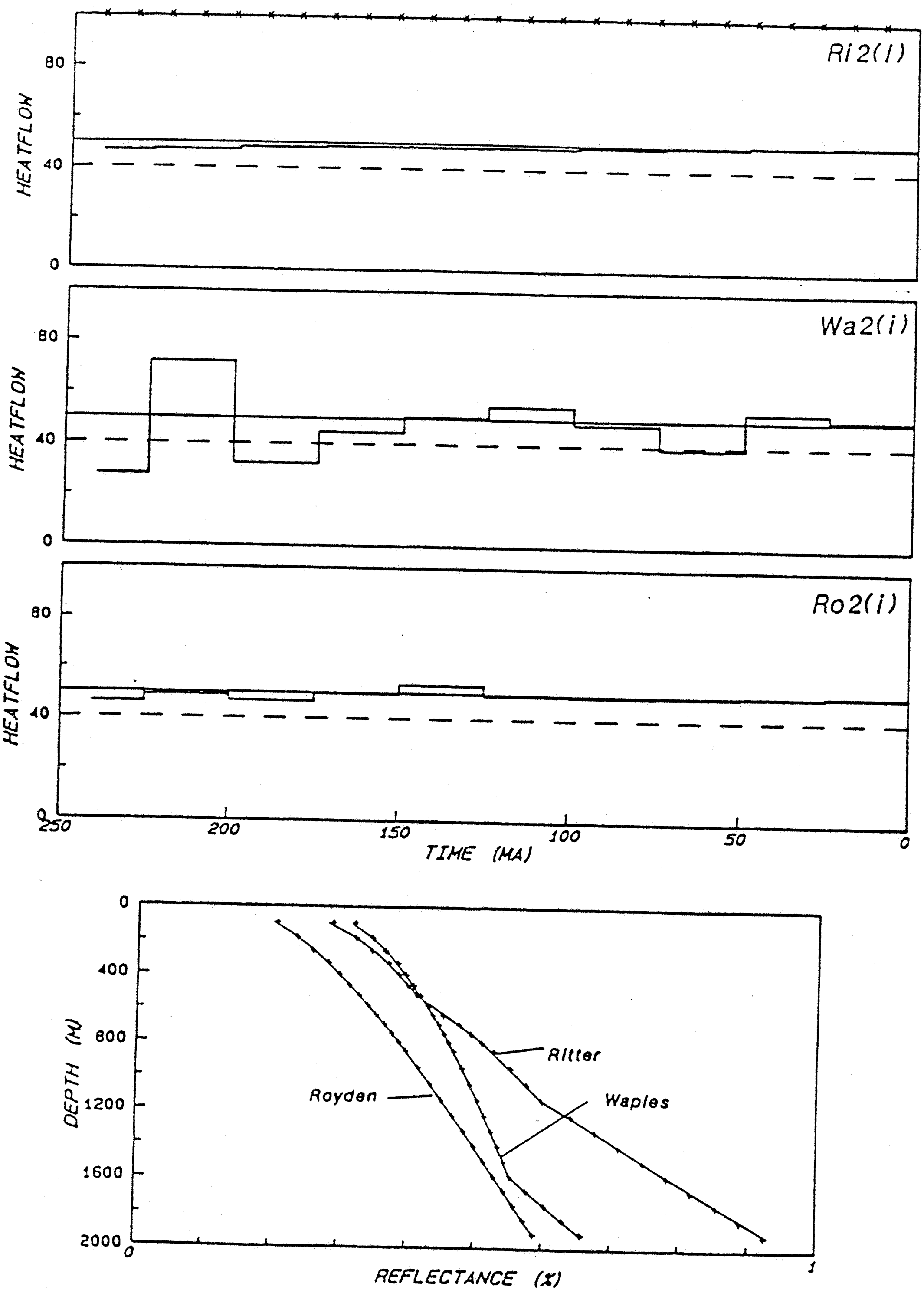
Ri2(I)
HEATFLOW
80
40
0
Wa2(i)
HEATFLOW
80
40
0
Ro2(i)
HEATFLOW
80
40
0
250
200
150
100
50
0
TIME (MA)
DEPTH (M)
0
400
800
1200
1600
2000
0
1
REFLECTANCE (%)
Ritter
Royden
Waples

Fig. A.5.(i,a)

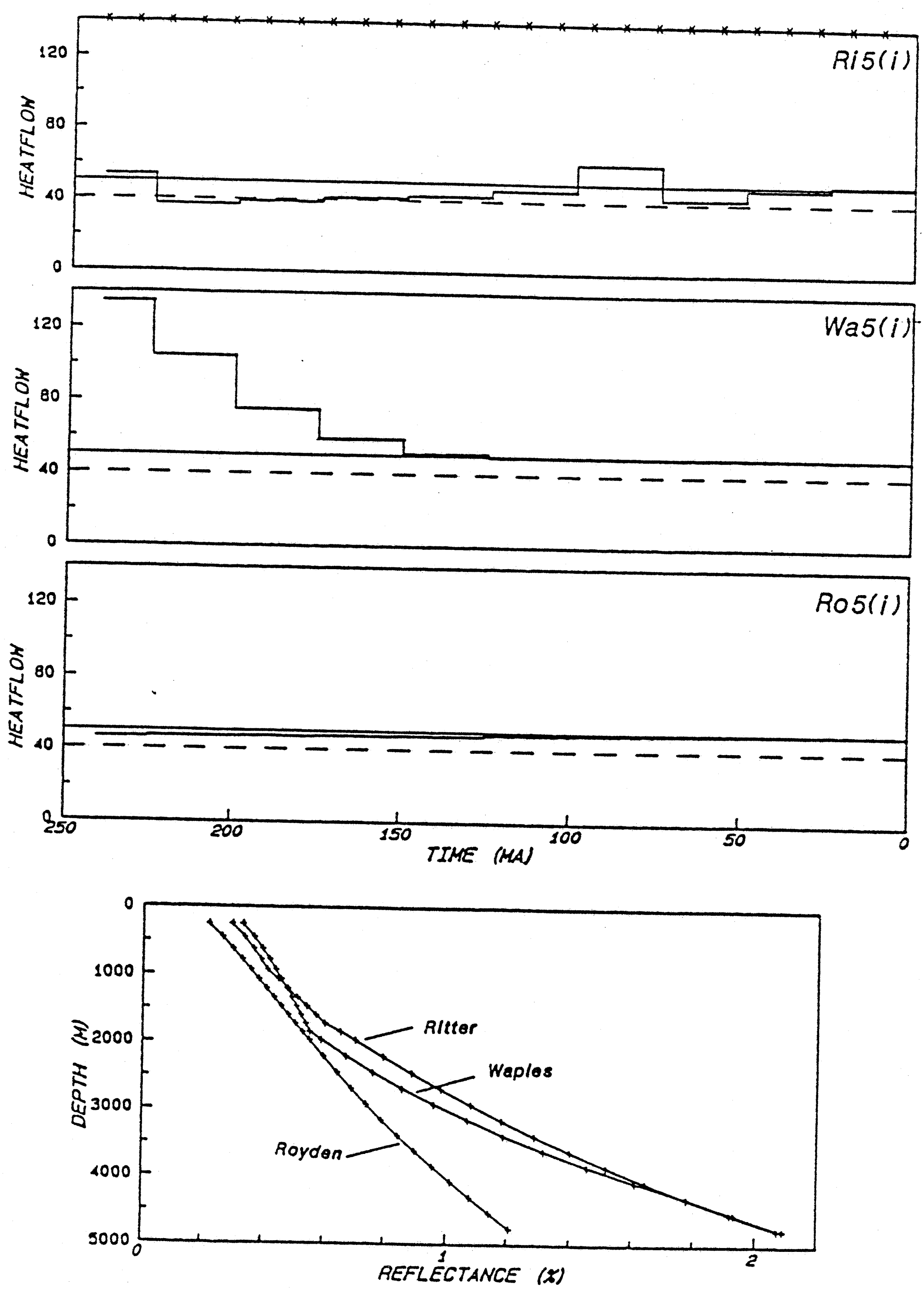
Ri5(i)
HEATFLOW
120
80
40
0
Wa5(i)
HEATFLOW
120
80
40
0
Ro5(i)
HEATFLOW
120
80
40
0
250
200
150
100
50
0
TIME (MA)
DEPTH (M)
0
1000
2000
3000
4000
5000
Ritter
Waples
Royden
0
1
2
REFLECTANCE (%)

Fig. A.5.(i,b)

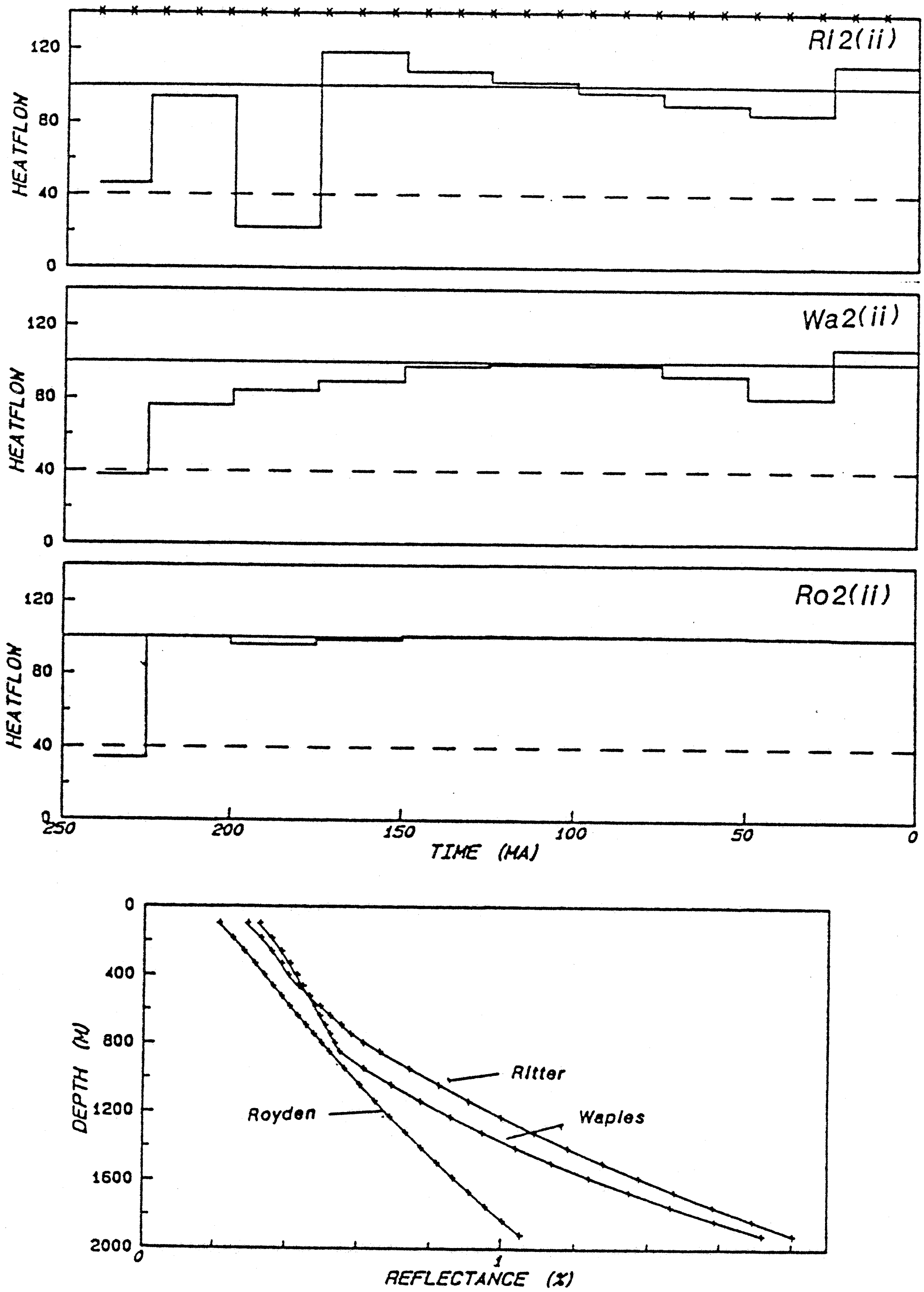

Rl2(ii)
Wa2(ii)
Ro2(ii)
HEATFLOW
0
40
80
120
250
200
150
100
50
0
TIME (MA)
DEPTH (M)
0
400
800
1200
1600
2000
REFLECTANCE (%)
0
1
Ritter
Waples
Royden

Fig. A.5.(ii.a)

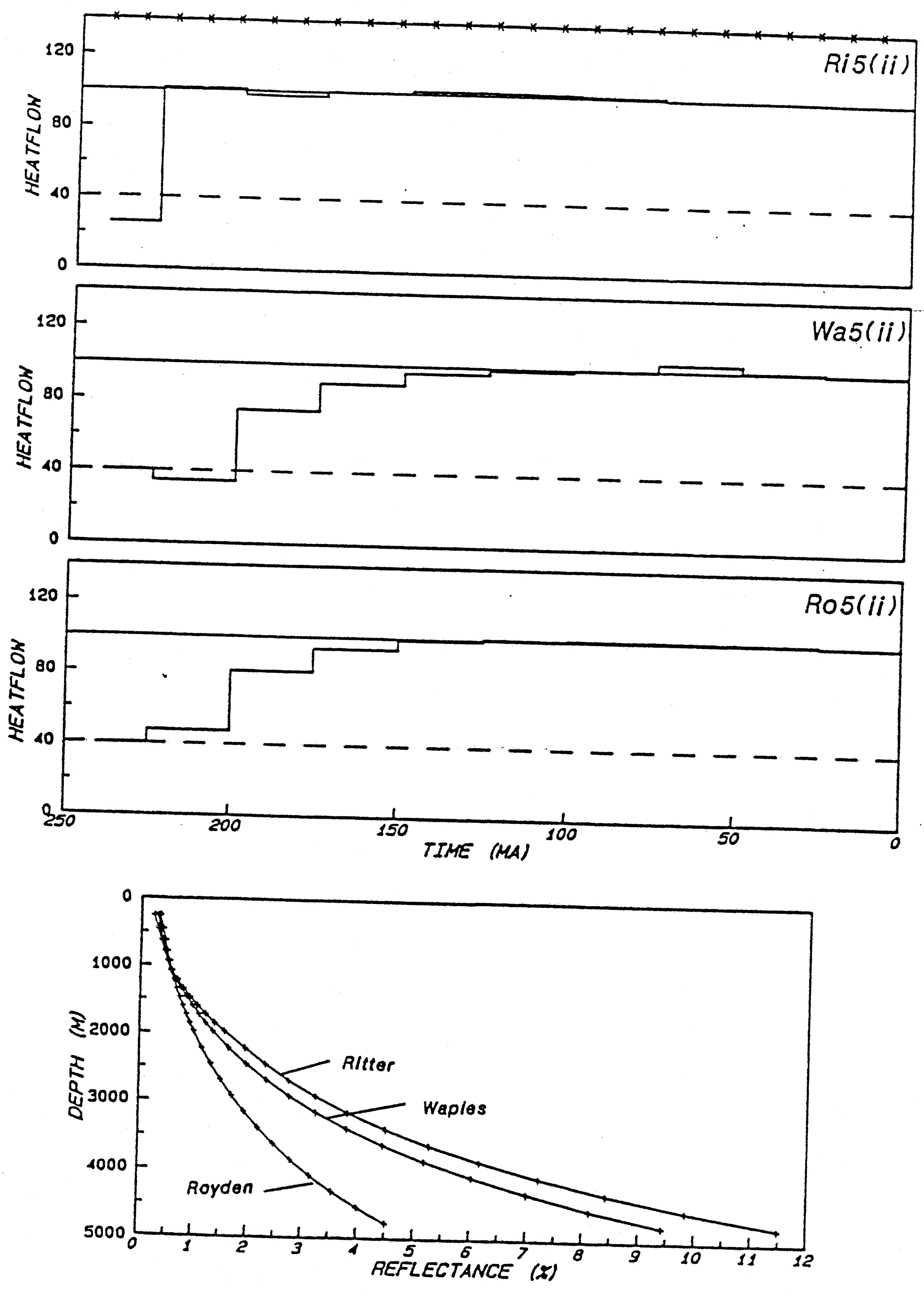

Ri5(ii)
Wa5(ii)
Ro5(ii)
HEATFLOW
120
80
40
0
250
200
150
100
50
0
TIME (MA)
DEPTH (M)
0
1000
2000
3000
4000
5000
REFLECTANCE (%)
1
2
3
4
5
6
7
8
9
10
11
12
Ritter
Waples
Royden

Fig. A.5.(ii,b)

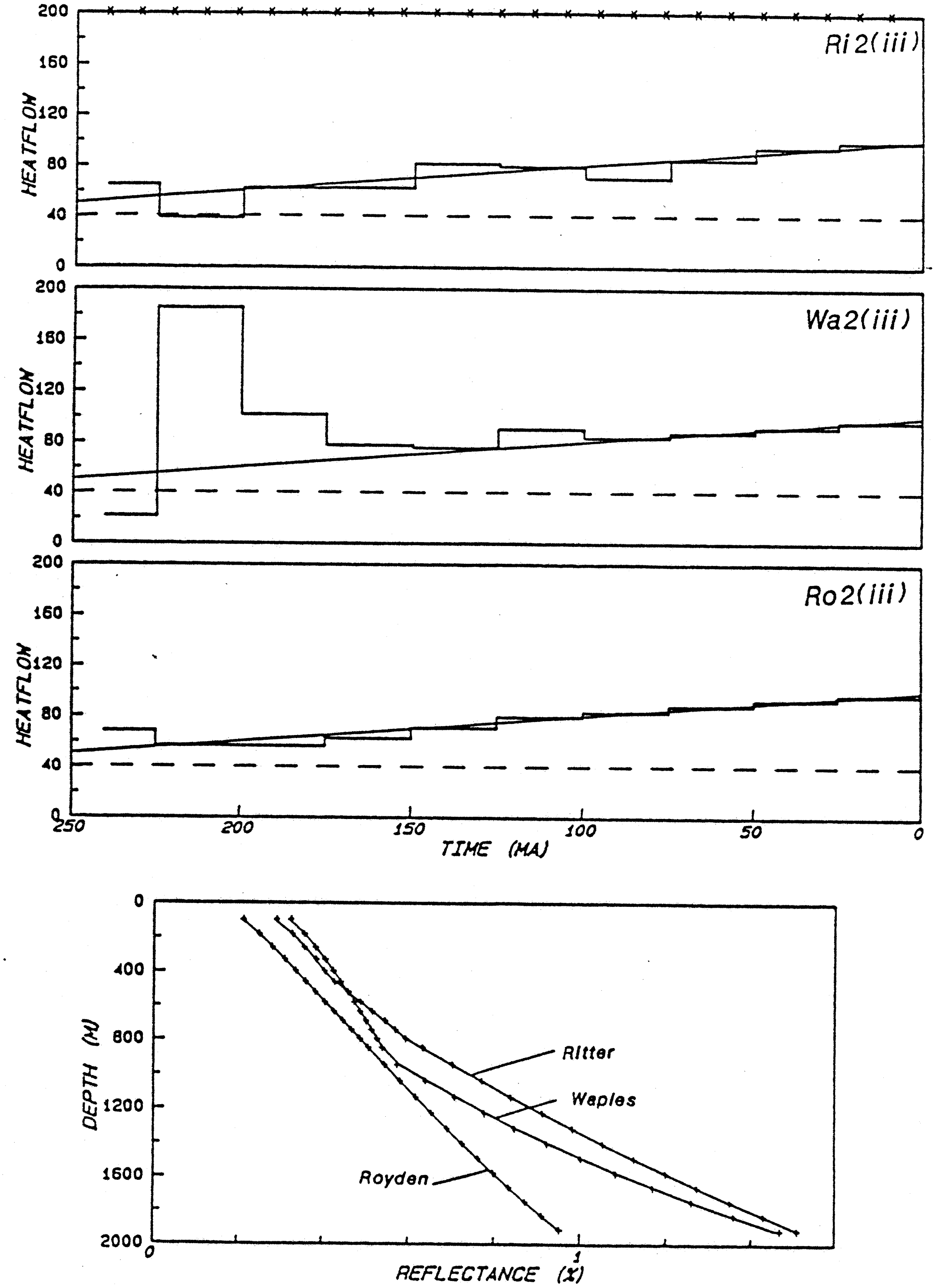
Ri2(iii)
Wa2(iii)
Ro2(iii)
HEATFLOW
200
160
120
80
40
0
250
200
150
100
50
0
TIME (MA)
DEPTH (M)
0
400
800
1200
1600
2000
REFLECTANCE (%)
1
Ritter
Waples
Royden

Fig. A.5.(iii,a)

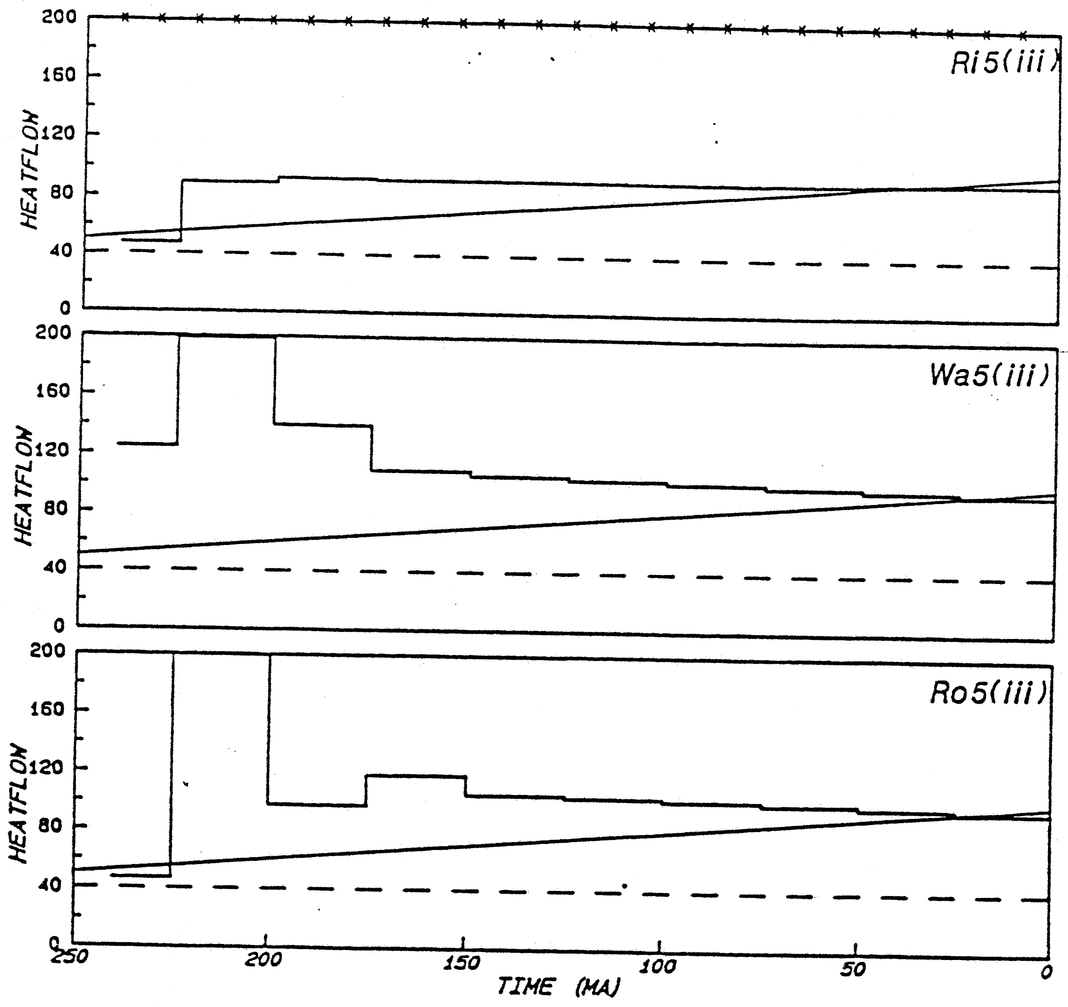

Ri5(iii)
Wa5(iii)
Ro5(iii)
HEATFLOW
TIME (MA)
250
200
150
100
50
0

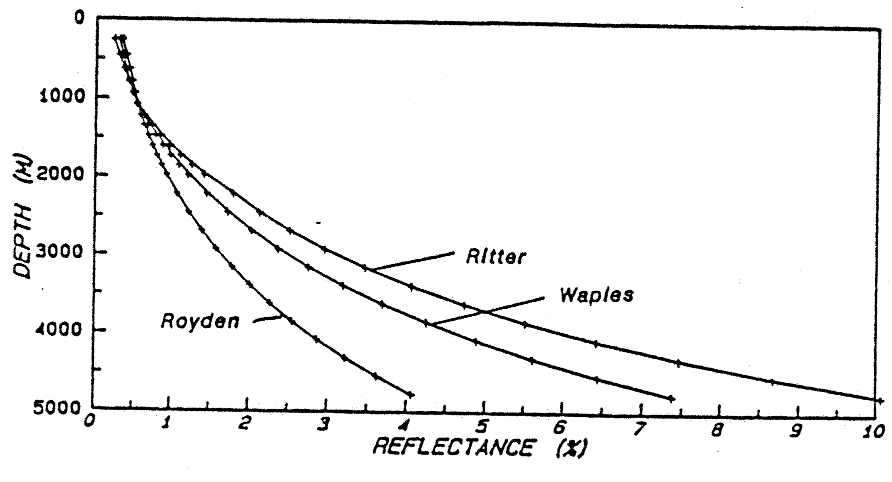

DEPTH (M)
REFLECTANCE (%)
Ritter
Waples
Royden

Fig. A.5.(iii,b)

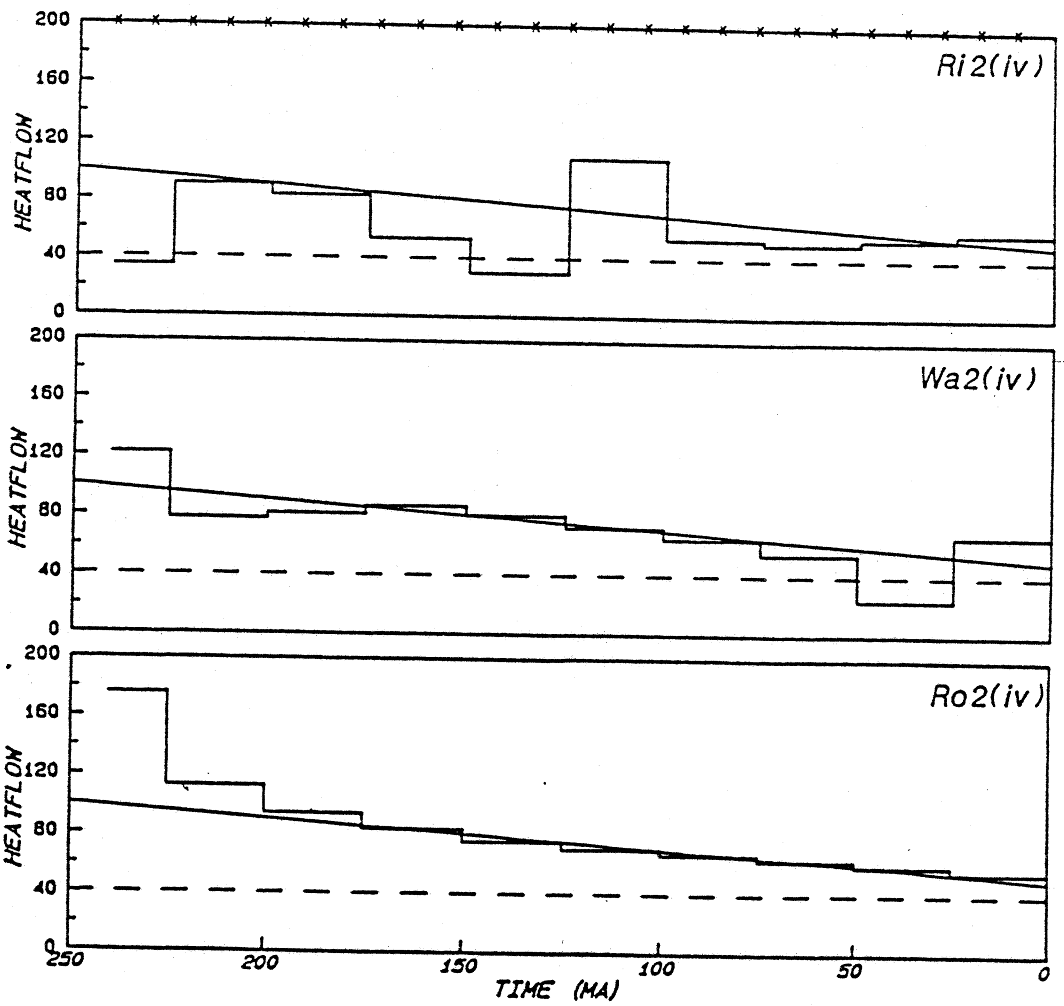

Ri2(iv)
Wa2(iv)
Ro2(iv)
HEATFLOW
TIME (MA)

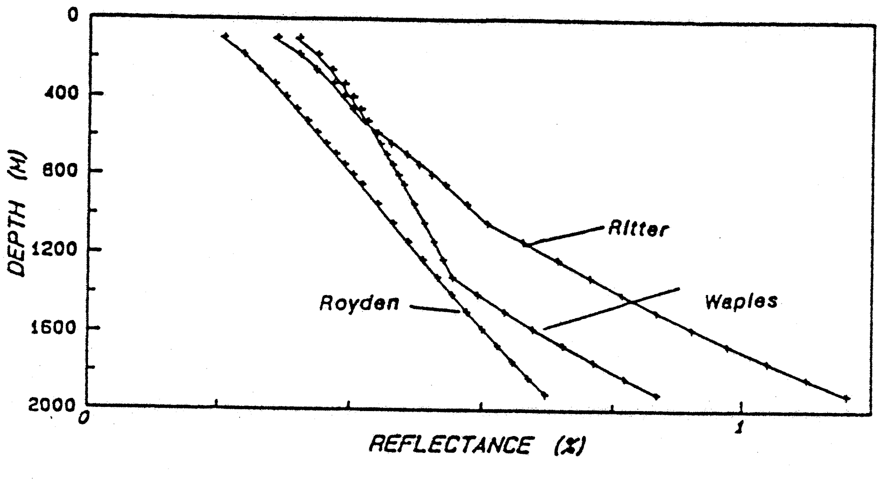

DEPTH (M)
REFLECTANCE (%)
Ritter
Waples
Royden

Fig. A.5.(iv,a)

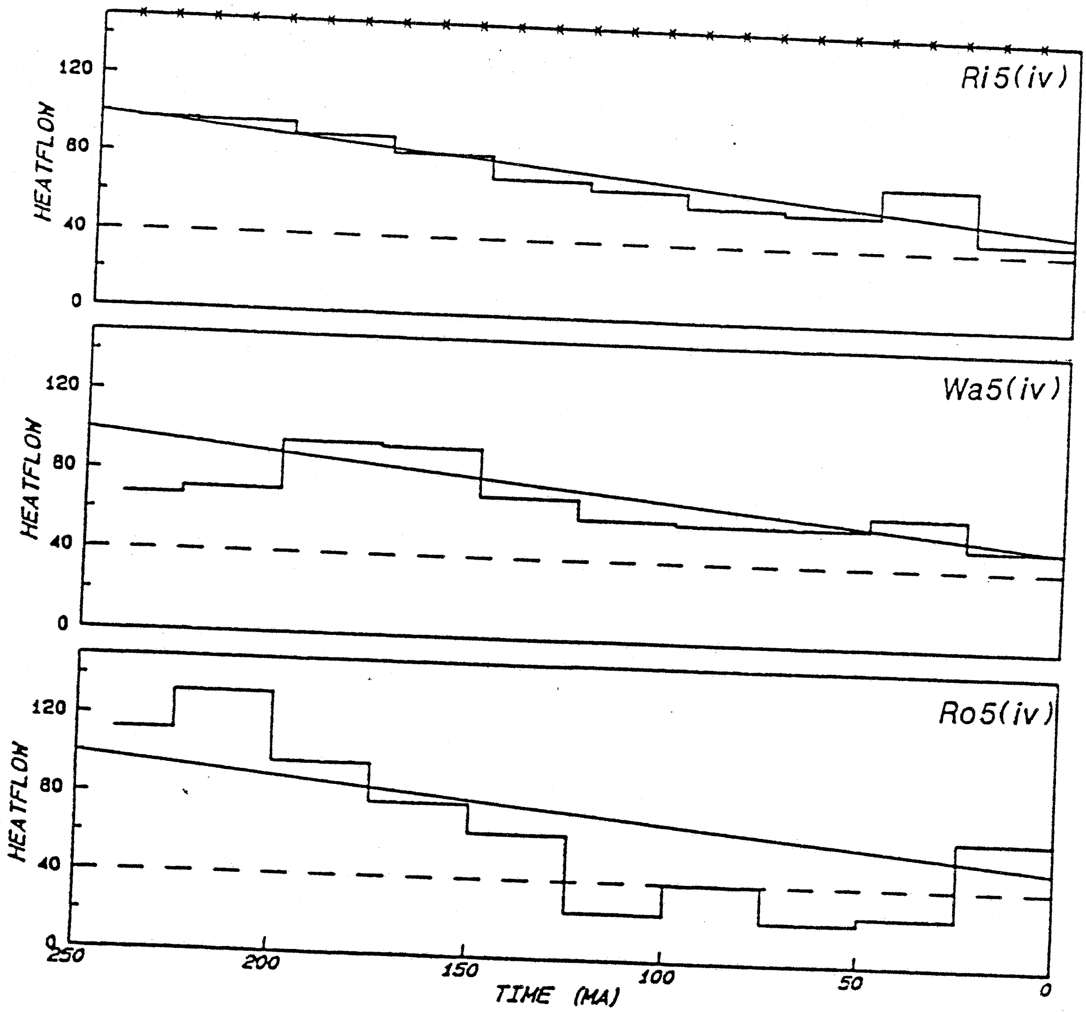
HEATFLOW
Ri5(iv)
HEATFLOW
Wa5(iv)
HEATFLOW
Ro5(iv)
TIME (MA)

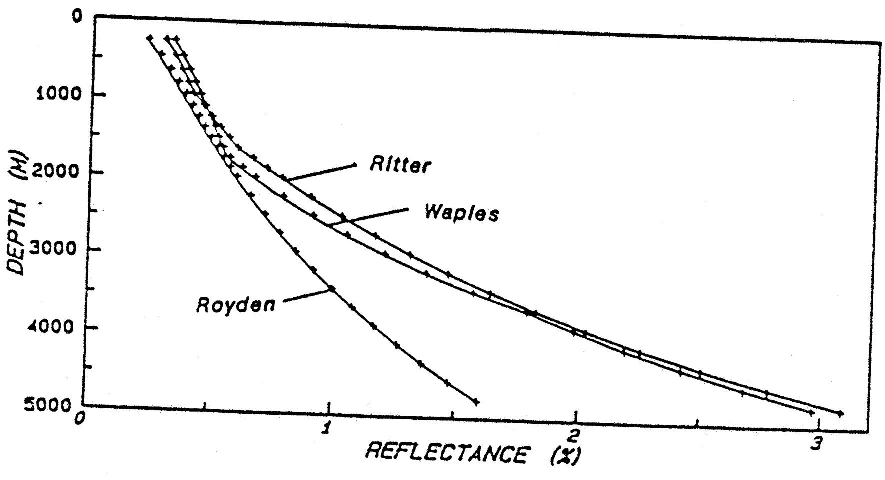
DEPTH (M)
Ritter
Waples
Royden
REFLECTANCE (%)

Fig. A.5.(iv,b)

Appendix 6

Numerical solution of the 2-D steady state heat flow equation

The general form of the heat conduction equation for a porous medium is :

$$\nabla.(k_b \nabla T) + A = \rho_b c_b \frac{\partial T}{\partial t} + \rho_f c_f v.\nabla T \qquad (A.6.1)$$

where k = thermal conductivity, c = heat capacity, b,f = bulk, fluid subscripts, v = pore fluid velocity.

The time derivative may be ignored under the assumption of steady state and A.6.1 can be written as

$$\nabla^2 T = -\frac{1}{k_b}\left[A + \nabla k_b.\nabla T - \rho_f c_f v.\nabla T\right] \qquad (A.6.2)$$

$$= C(x,y,z) \quad \text{for Poisson's equation}$$

The above equation may then be reformulated in 2 dimensions using cartesian coordinates with only horizontal flow as:

$$\frac{\partial^2 T}{\partial x^2} + \frac{\partial^2 T}{\partial z^2} = -\frac{1}{k_b}\left[A + \frac{\partial T}{\partial x}\frac{\partial k_b}{\partial x} - \rho_f c_f v \frac{\partial T}{\partial x} + \frac{\partial T}{\partial z}\frac{\partial k_b}{\partial z}\right] \qquad (A.6.3)$$

and cylindrical coordinates assuming radial symmetry and no flow:

$$\frac{\partial^2 T}{\partial r^2} + \frac{\partial^2 T}{\partial z^2} = -\frac{1}{k_b}\left[A + \frac{\partial T}{\partial r}\left(\frac{\partial k_b}{\partial r} + \frac{k_b}{r}\right) + \frac{\partial T}{\partial z}\frac{\partial k_b}{\partial z}\right] \qquad (A.6.4)$$

A finite difference scheme similar to that used by Sclater et al. (1970) was used to represent eqns. A.6.3 and A.6.4. The thermal properties values were parameterized as illustrated in fig A.6.1 and the temperature derivatives were approximated as

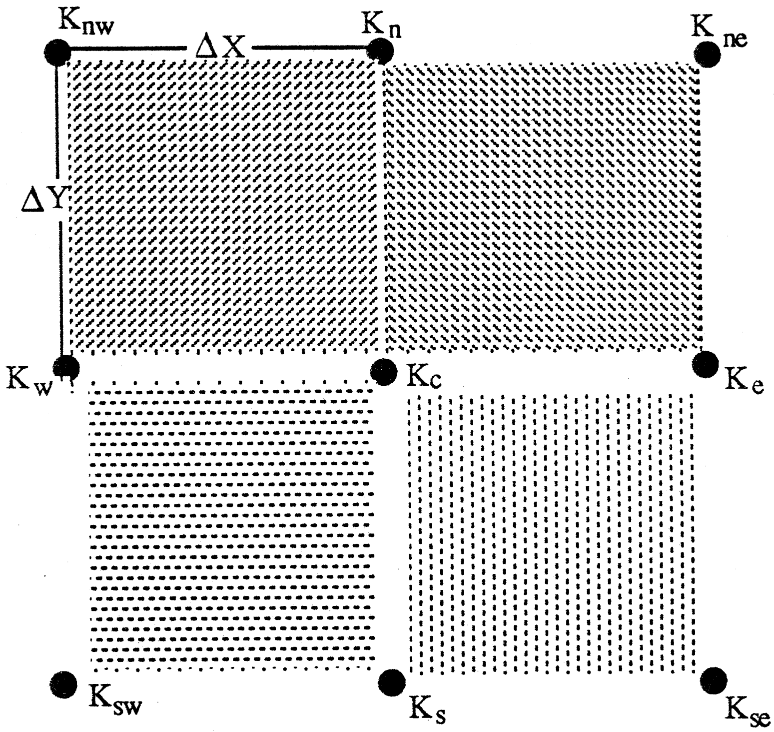

$$\frac{\partial k}{\partial x} = \frac{1}{\Delta x}\left[\frac{k_c + k_n}{2} - \frac{k_{nw} + k_w}{2} \right]$$

$$\frac{\partial k}{\partial z} = \frac{1}{\Delta z}\left[\frac{k_c + k_w}{2} - \frac{k_n + k_{nw}}{2} \right]$$

$$k = 0.25 \left(k_c + k_n + k_{nw} + k_w \right)$$

$$A = 0.25 \left(A_c + A_n + A_{nw} + A_w \right)$$

$$\rho c = 0.25 \left(\rho c_c + \rho c_n + \rho c_{nw} + \rho c_w \right)$$

Fig. A.6.1 Parameterization of thermal properties and the spatial derivatives of the thermal conductivity. The value assigned to a mesh point is assumed to be representative of the area to the bottom right of the point.

$$\frac{\partial T}{\partial x} = \frac{T_{i+1,j} - T_{i-1,j}}{2\Delta x} \quad \text{(A.6.5a)}$$

$$\frac{\partial^2 T}{\partial x^2} = \frac{T_{i+1,j} - 2T_{i,j} + T_{i-1,j}}{\Delta x^2} \quad \text{(A.6.5b)}$$

The boundary conditions were specified as no lateral temperature gradient at x =0 and x_{max}, surface temperature of zero and heat flow into the base of the model, i.e.

$$\frac{\partial T}{\partial x} = 0 \text{ at } x = 0,\ x_{max} \quad \text{(A.6.6a)}$$

$$T(x,0) = 0 \text{ and } k\left.\frac{\partial T}{\partial z}\right|_{z_{max}} = Q_b \quad \text{(A.6.6b)}$$

The vertical (z direction) boundary conditions are then

$$T_{i,0} = 0 \text{ and } \frac{T_{i,j_{max+1}} - T_{i,j_{max-1}}}{2\Delta z} = \frac{Q_b}{k} \quad \text{(A.6.6c)}$$

In a cartesian coordinate system the horizontal boundary conditions are implemented by setting $T_{i+1,j} = T_{i-1,j}$ at i =0 and i_{max}. For a cylindrical coordinate system there is a singularity at r = 0 in the term $\frac{k}{r}\frac{\partial T}{\partial r}$. However this can be expanded as Maclaurin's series given by

$$f(r) = f(0) + r f'(0) + \ldots + \frac{r^n}{n!} f^n(0)$$

and for this case

$$\frac{k}{r}\frac{\partial T}{\partial r} = \frac{k}{r}\left[\left.\frac{\partial T}{\partial r}\right|_{r=0} + r\left.\frac{\partial^2 T}{\partial r^2}\right|_{r=0} + \ldots\right]$$

and as $\left.\frac{\partial T}{\partial r}\right|_{r=0} = 0$ then it is possible to replace $\frac{k}{r}\frac{\partial T}{\partial r}$ by $k\frac{\partial^2 T}{\partial r^2}$ and use $T_{-1,j} = T_{1,j}$.

The solution was obtained by making an initial guess at the solution (the 1-D steady state solution), evaluating the R.H.S. and treating the resulting equation as a form of Poisson's equation. A damped iterative procedure was implemented to obtain a stable solution, i.e.

$$\text{(i)} \qquad \nabla^2 T^{n'} = C(T^{n-1})$$

$$\text{(ii)} \qquad T^n = \alpha T^{n'} + (1-\alpha) T^{n-1} \qquad (0 < \alpha \leq 1)$$

Here $T^{n'}$ is the actual solution to eqns. A.6.3 and A.6.4 obtained by treating the equation as Poisson's equation by using the previous iteration's solution T^{n-1}. T^n is the actual solution used for the next iteration, obtained by combining part of the previous solution T^{n-1} with part of $T^{n'}$. The convergence criterion incorporated was a maximum temperature difference of 0.05° C between iterations and convergence was reached in 4 or 5 iterations for the cartesian system and up to 15 iterations for the cylindrical case. When the advective term was included, the procedure required heavy damping with $\alpha \sim 0.02\text{-}0.2$ and, at worst, up to 500 iterations were required to obtain a stable solution. Also, to achieve convergence, it was necessary to increase the horizontal grid spacing when the advective term was incorporated and the maximum value used was 10000 m for the highest velocity (5×10^{-7} m/s). The maximum depth of any anomalous bodies was always less than half the total depth of the mesh and if necessary, the vertical grid spacing was increased. The surface heat flow for the no fluid flow case agreed to less than 0.5 mWm^{-2} (~ 1%) for all grid spacings used. Convergence rates were increased by using the temperature field previously obtained for a similar model (e.g. lower velocity or heat production values) as the initial temperature. The mesh spacing was allowed to differ for the x and z directions and the relevant values were

$$\Delta x = 100 - 10000 \text{ m}, \quad i_{max} = 190, \quad x_{max} = 19 - 1900 \text{ km}$$

$$\Delta z = 500 - 1500 \text{ m}, \quad j_{max} = 63, \quad z_{max} = 31\text{-}93 \text{ km}$$

As a test on the calculation method, I give an example in fig. A.6.2 of the surface heat flow over two half ellipsoids having a vertical symmetry axis, with a thermal conductivity ratio inside to outside the body of 2, calculated analytically (see Lee and Henyey 1974) and numerically. The agreement is to within 1% except at the boundary where the heat flow has a discontinuity.

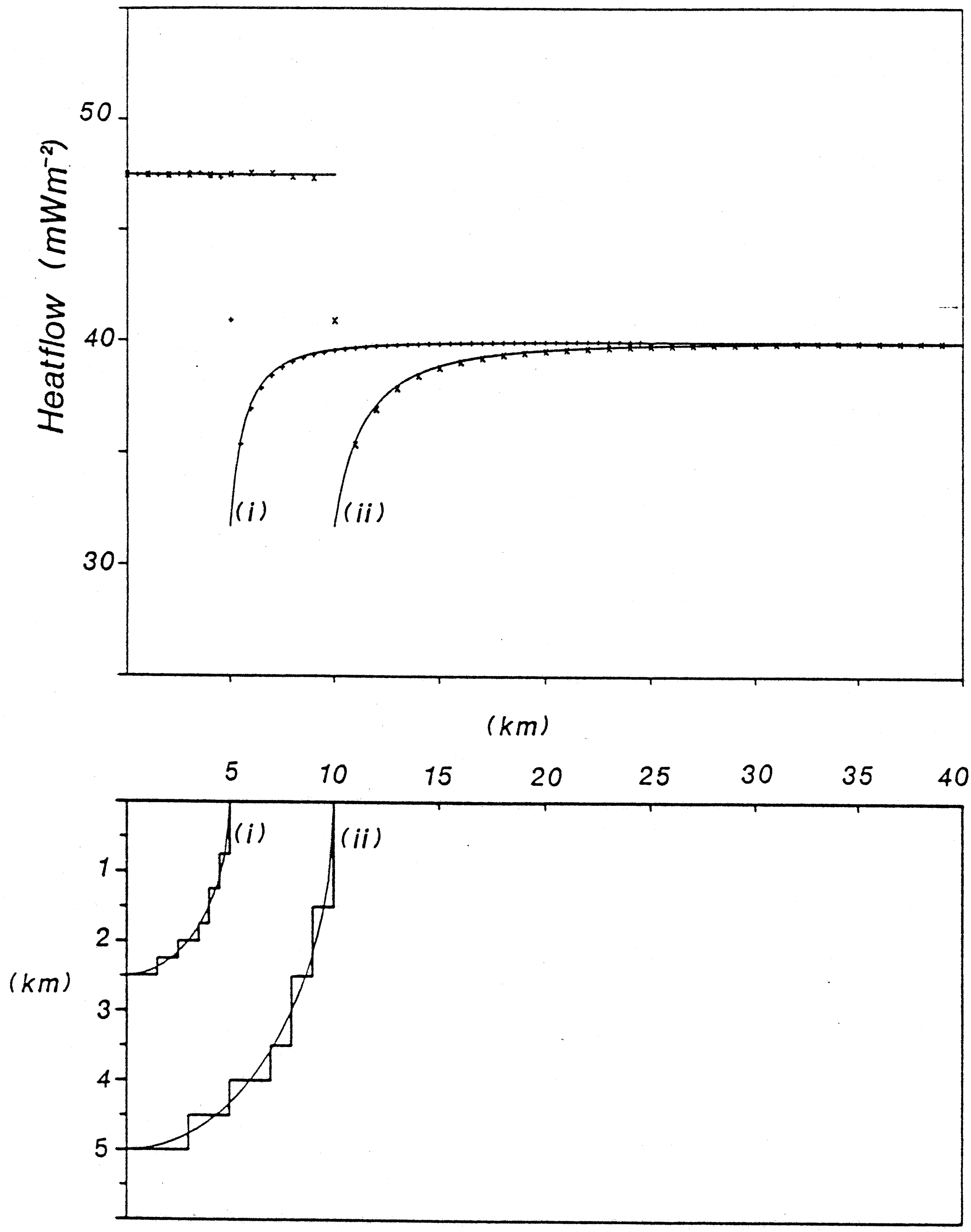

Fig. A.6.2 Comparison of the numerical (+) and analytical (line) solutions for the surface heat flow above a semi-ellipsoid where the thermal conductivity inside the body is twice that outside.

REFERENCES

Abbott, G.D., Lewis, C.A. and Maxwell, J.R., 1985. Laboratory models for aromatization and isomerization of hydrocarbons in sedimentary basins, Nature, **318**, 651-653.

Adby, P.R. and Dempster, M.A.H., 1974. Introduction to Optimization Methods, Chapman and Hall, pp. 204.

Ager, D.V., 1973. The Nature of the Stratigraphic Record, J. Wiley and Sons, pp. 114.

Ahern, J.L. and Ditmars, R.C., 1985. Rejuvenation of the continental lithosphere beneath an intracratonic basin, Tectonophysics, **120**, 21-35.

Ahern, J.L. and Mrkvicka, S.R., 1984. A mechanical and thermal model for the evolution of the Williston Basin, Tectonics, **3**, 79-102.

Alföldi, L., Gàlfi, J. and Liebe, P., 1985. Heat flow anomalies caused by water circulation, J. Geodynamics, **4**, 199-217.

Ambrose, G., Suthill, R., and Lavering, I., 1982. A review of the early Cretaceous Murta Member (Mooga Formation) in the southern Cooper Basin, in: Moore, P.S. and Mount, T.J. (compilers), Eromanga Basin Symposium, summary papers, Geol. Soc. Aust. and Pet. Expl. Soc. Aust., Adelaide, 92 - 109.

Ambrose, G., Suthill, R., and Lavering, I., 1986. The geology and hydrocarbon potential of the Murta member (Mooga Formation) in the southern Eromanga Basin, in: Gravestock, D.I., Moore, P.S., Mount, T.J. and Pitt, G.M., (Eds), Contributions to the geology and hydrocarbon potential of the Eromanga Basin, Geol. Soc. Aust., spec. publ. **12**, 71-84.

Andrews-Speed, C.P., Oxburgh, E.R., and Cooper, B.A., 1984. Temperatures and depth dependent heat flow in the western North Sea, AAPG Bull., **68**, 1764-1781.

Angevine, C.L. and Turcotte, D.L., 1983. Oil generation in overthrust belts, AAPG Bull., **67**, 235-241.

Armin, R.A. and Mayer, L., 1983. Subsidence analysis of the Cordilleran miogeosyncline: Implications for timing of late Proterozoic rifting and amount of extension, Geology, **11**, 702-705.

Armstrong, J.D. and Barr, T.M., 1986. The Eromanga Basin. An overview of exploration and potential, in: Gravestock, D.I., Moore, P.S., Mount, T.J. and Pitt, G.M., (Eds), Contributions to the geology and hydrocarbon potential of the Eromanga Basin, Geol. Soc. Aust., spec. publ. **12**, 25-38.

Artyushkov, E.V., 1973. Stress in the lithosphere caused by crustal thickness inhomogeneities, J. Geophys. Res., **78**, 7675-7708.

Artyushkov, E.V., 1981. Mechanics of continental riftogenesis, Tectonophysics, **73**, 9-14.

Artyushkov., E.V. and Baer, M.A., 1985. Mechanism of formation of deep basins in continental crust in fold belts, J. Geodynamics, **2**, 67-84.

Auchinloss, G., 1976. The Adavale Basin, in: Leslie, R.B., Evans, H.J. and Knight, C.L., (Eds), Economic Geology of Australia and Papua New Guinea, 3, Australian Institute of Mining and Metallurgy, Monograph 7, 309-315.

Audley-Charles, M.G., 1983. Reconstruction of eastern Gondwanaland, Nature, **306**, 48-50.

Bachu, S., 1985. Influence of lithology and fluid on the temperature distribution in a sedimentary basin : A case study from the Cold Lake area, Alberta, Canada, Tectonophysics, **120**, 257-284.

Baldwin, B. and Butler, C.O., 1985. Compaction curves, AAPG Bull., **69**, 622-626.

Ballard, S. and Pollack, H.N., 1987. Diversion of heat by Archean cratons : a model for southern Africa, Earth Planet. Sci. Lett., **85**, 253-264.

Bally, A.W., 1982. Musings over sedimentary basin evolution, Phil. Trans. Roy. Soc. Lond., ser. A, **305**, 325-338.

Barker, C.E., 1983. Influence of time on metamorphism of sedimentary organic matter in liquid dominated geothermal systems, western North America, Geology, **11**, 384-388.

Barroll, M.W. and Reiter, M., 1987. Influence of stress and temperature regimes on graben subsidence - a note, Tectonophysics, **133**, 157-163.

Barton, P. and Wood, R., 1984. Tectonic evolution of the North Sea basin : crustal stretching and subsidence, Geophys. J. Roy. astr. Soc., **79**, 987-1022.

Battersby, D.G., 1976. Cooper Basin gas and oil fields, in: Leslie, R.G., Evans, H.J. and Knight, C.L., (Eds), Economic Geology of Australia and Papua New Guinea, **3**, Australian Institute of Mining and Metallurgy, Monograph 7, 321-368.

Bear, J., 1972. Dynamics of Fluids in Porous Media, Elsevier, pp. 764.

Beard, D.C. and Weyl, P.K., 1973. Influence of texture on porosity and permeability of unconsolidated sand, AAPG Bull., **57**, 349-369.

Beaumont, C., 1978. The evolution of sedimentary basins on a viscoelastic lithosphere : theory and examples, Geophys. J. Roy. astr. Soc., **55**, 471-497.

Beaumont, C., 1979. On rheological zoning of the lithosphere during flexure, Tectonophysics, **59**, 347-365.

Beaumont, C., 1981. Foreland basins, Geophys. J. Roy. astr. Soc., **65**, 291-329.

Beaumont, C., Keen, C.E., and Boutilier, R., 1982. On the evolution of rifted continental margins : comparison of models and observations for the Nova Scotia margin, Geophys. J. Roy. astr. Soc., **70**, 667-715.

Beaumont, C. and Sweeney, J.F., 1978. Graben generation of major sedimentary basins, Tectonophysics, **50**, T19-23.

Beck, A.E., 1976. An improved method of computing the thermal conductivity of fluid-filled sedimentary rocks, Geophysics, **41**, 133-144.

Bejan, A., 1984. Convection Heat Transfer, J. Wiley and Sons, pp. 477.

Bethke, C.M., 1985. A numerical model of compaction driven groundwater flow and heat transfer and its application to the palaeohydrology of intracratonic sedimentary basins, J. Geophys. Res., **90**, 6817-6828.

Bhattacharji, S. and Singh, R.N., 1984. Thermo-mechanical structure of the southern part of the Indian shield and its relevance to Precambrian basin evolution. Tectonophysics, **105**, 103-120.

Bills, B.G., 1983. Thermoelastic bending of the lithosphere : implications for basin subsidence, Geophys. J. Roy. astr. Soc., **75**, 169-200.

Biot, M.A, 1941. General theory of three dimensional consolidation, J. Appl. Phys., **12**, 155-164.

Biot, M.A., 1955. Theory of elasticity and consolidation for a porous isotropic solid, J. Appl. Phys., **26**, 182-185.

Birch, F. and Clark, H., 1940. The thermal conductivity of rocks and its dependence upon temperature and composition, Am. J. Sci., **238**, 529-558.

Bird, P. and Piper, K. 1980. Plane-stress finite element models of tectonic flow in southern California, Phys. Earth Planet. Int., **21**, 158-175.

Blackwell, D.D., 1985. A transient model of the geothermal system of the Long Valley Caldera, California, J. Geophys. Res., **90**, 11229-11241.

Blackwell, D.D., Steele, J.L. and Steeples, D.W., 1981. Heat flow determinations in Kansas and their implications for midcontinent heat flow patterns, EOS, **62** ,392.

Blanche, J.B. and Whitaker, J.H.McD., 1978. Diagenesis of part of the Brent Sand Formation (Middle Jurassic) of the northern North Sea Basin, J. Geol. Soc. Lond., **135**, 73-82.

Blatt, H., Middleton, G., and Murray, R., 1976. Origin of Sedimentary Rocks, Prentice-Hall Inc., pp. 782.

Bodine, J.H., Steckler, M.S., and Watts, A.B., 1981. Observations of flexure and the rheology of the oceanic lithosphere, J. Geophys. Res., **86**, 3695-3707.

Bond, G., 1976. Evidence for continental subsidence in North America during the Late Cretaceous global submergence, Geology, **4**, 557-560.

Bond, G., 1978. Speculations on real sea-level changes and vertical motions of continents at selected times in the Cretaceous and Tertiary periods, Geology, **6**, 247-250.

Bond, G.C., 1979. Evidence for some uplifts of large magnitude in continental platforms, Tectonophysics, **61**, 285-305.

Bond, G.C., Christie-Blick, N, Kominz, M.A. and Devlin, W.J., 1985. An early Cambrian rift to post-rift transition in the Cordillera of western North America, Nature, **315**, 742-746.

Bond, G.C. and Kominz, M.A., 1984,. Construction of tectonic subsidence curves for the lower Palaeozoic miogeocline, southern Canadian Rocky Mountains : implications for subsidence mechanisms, age of breakup and crustal thinning., Geol. Soc. Am. Bull., **95**, 155-173.

Bostick, N.H., 1979. Microscopic measurement of the level of catagenesis of solid organic matter in sedimentary rocks - a review, Soc. Econ. Palaeontol. Mineral., spec. publ., **26**, 17-43.

Bott, M.H.P., 1982. Origin of the lithospheric tension causing basin formation, Phil. Trans. Roy. Soc. Lond., **305**, 319-324.

Bott, M.H.P., Day, A.A. and Masson-Smith, D., 1958. The geological interpretation of gravity and magnetic surveys in Devon and Cornwall, Phil. Trans. Roy. Soc. Lond., ser. A, **251**, 161-191.

Bott, M.H.P. and Mithen, D.P., 1983. Mechanism of graben formation - the wedge subsidence hypothesis, Tectonophysics, **94**, 11-22.

Boyd, F.R., Gurney, J.J. and Richardson, S.H., 1985. Evidence for a 150-200 km thick Archean lithosphere from diamond inclusion thermobarometry, Nature, **315**, 387-389.

Brace, W.F. and Kohlstedt, D.L., 1980. Limits on lithospheric stress imposed by laboratory experiments, J. Geophys. Res., **85**, 6248-6252.

Brailsford, A.D. and Major, K.G., 1964. The thermal conductivity of aggregates of several phases, including porous materials, Brit. J. Appl. Phys., **15**, 313-319.

Braun, J. and Beaumont, C., 1987a. Dynamical models of the role of crustal shear zones in asymmetric continental extension, pre-print.

Braun, J. and Beaumont, C., 1987b. Styles of continental rifting : results from dynamical models of lithospheric extension, in: Beaumont, C. and Tankard, A., (Eds), Sedimentary Basins and Basin-Forming Mechanisms, Canadian Society Petroleum Geologists Memoir **12**, in press.

Bray, C.J. and Karig, D.E., 1985. Porosity of sediments in accretionary prisms and some implications of dewatering processes, J. Geophys. Res., **90**, 768-778.

Bridwell, R.J. and Potzick, C., 1981. Thermal regimes, mantle diapirs and stresses in continental rifts, Tectonophysics, **73**, 15-32.

Brotchie, J.F. and Silvester, R., 1969. Crustal flexure, J. Geophys. Res., **74**, 5240-5252.

Brunet, M-F. and Le Pichon, X., 1982. Subsidence of the Paris Basin, J. Geophys. Res., **87**, 8547-8560.

Bullard, E.C., 1939. Heat flow in South Africa , Proc. Roy. Soc. Lond., Ser A, **173**, 474-502.

Buntebarth, G., 1979. The degree of metamorphism of organic matter in sedimentary rocks as a palaeo-geothermometer, applied to the upper Rhine Graben, Pageoph., **117**, 83-91.

Burger, D., 1982. Palynology of the Eromanga Basin and its applications, in: Moore, P.S. and Mount, T.J. (compilers), Eromanga Basin Symposium, summary papers, Geol. Soc. Aust. and Pet. Expl. Soc. Aust., Adelaide, 174-183.

Burger, D., 1986. Palynology, cyclic sedimentation and palaeoenvironments in the late Mesozoic of the Eromanga Basin., in: Gravestock, D.I., Moore, P.S., Mount, T.J. and Pitt, G.M., (Eds), Contributions to the Geology and Hydrocarbon Potential of the Eromanga Basin, Geol. Soc. Aust., spec. publ. **12**, 53-70.

Burger, D. and Senior, B.R., 1979. A revision of the sedimentary and palynological history of the north eastern Eromanga Basin, Queensland, J. Geol. Soc. Aust., **26**, 121-132.

Burke, K., 1976. The Chad Basin : an active intra-continental basin, Tectonophysics, **36**, 197-206.

Caldwell, J.G. and Turcotte, D.L., 1979. Dependence of the thickness of the elastic oceanic lithosphere on age, J. Geophys. Res., **84**, 7572-7576.

Calmant, S. and Cazenave, A., 1986. The effective elastic lithosphere under the Cook-Austral and Society Islands, Earth Planet. Sci. Lett., **7**, 187-202.

Carney, J.N. and MacFarlane, A., 1982. Geological evidence bearing on the Miocene to recent structural evolution of the New Hebrides arc, Tectonophysics, **87**, 147-175.

Carr, P.F., Jones, B.G., Quinn, B.G. and Wright, B.G., 1984. Towards an objective Phanerozoic time scale, Geology, **12**, 274-277.

Carslaw, H.S. and Jaeger, J.C., 1959. Conduction of Heat in Solids, Oxford Univ. Press, pp. 510.

Carter, N.L. and Tsenn, M.C., 1987. Flow properties of continental lithosphere, Tectonophysics, **136**, 27-63.

Castano, J.R., 1985, Uses of vitrinite reflectance in determining thermal history in sedimentary basins, AAPG Bull., **69**, 243.

Catala, G., 1984. Technical aspects of measurements of temperatures in boreholes : some aspects of their interpretation, in: Durand, B., (Ed), Thermal Phenomena in Sedimentary Basins, Int. Coll. Bordeaux 1983, Collection Colloques et Seminaires 41, Editions Technip, Paris, 37-43.

Cawood, P.A., 1982. Structural relations in the subduction complex of the Palaeozoic New England fold belt, Eastern Australia, J. Geology, **90**, 381 -392.

Cercone, K.R., 1984., Thermal history of the Michigan Basin, AAPG Bull., **68**, 130-136.

Cěrmak, V. and Rybach, L., 1982. Thermal properties, in: Angenheister, G., (Ed), Physical Properties of Rocks (subvolume A): Numerical Data and Functional Relationships in Science and Technology , 1, Springer-Verlag, 305-371.

Chadwick, R.A., 1986, Extension tectonics in the Wessex Basin, southern England, J. Geol. Soc. Lond., **143**, 465-488.

Chapman, D.S., Keho, T.H., Bauer, M.S. and Picard, D.S., 1984. Heat flow in the Uinta Basin determined from bottom hole temperature (BHT) data, Geophysics, **49**, 453-466.

Chilingarian, G.V. and Wolf, K.H., (Eds), 1976. Compaction of coarse-grained sediments, II, Developments in sedimentology 18b, Elsevier, pp. 808.

Chopra, P.N. and Paterson, M.S., 1984. The role of water in the deformation of dunite, J. Geophys. Res., **89**, 7861-7876.

Cloetingh, S., McQueen, H., and Lambeck, K., 1985. On a tectonic mechanism for regional sea level variations, Earth Planet. Sci. Lett., **75**, 157-166.

Cloetingh, S. and Nieuwland, F., 1984. On the mechanisms of lithospheric stretching and doming: a finite element analysis, Geol. en Mijn., **63**, 315-322.

Cloetingh, S. and Wortel, R., 1985. Regional stress field of the Indian plate, Geophys. Res. Lett., **12**, 77-80.

Cochran, J.R., 1980. Some remarks on isostasy and the long term behaviour of the continental lithosphere, Earth Planet. Sci. Lett., **46**, 266-274.

Cochran, J.R., 1983. Effects of finite rifting times on the development of sedimentary basins, Earth Planet. Sci. Lett., **66**, 289-302.

Cogley, J.C., 1984. Continental margins and the extent and number of the continents, Rev. Geophys. Space Phys. **22**, 101-122.

Cohee, G.V., Glaessner, M.F. and Hedberg, H.D., (Eds), 1978. Contributions to the geologic time scale, AAPG studies in geology, **6**, pp. 388.

Connan, J., 1974. Time-temperature relation in oil genesis, AAPG Bull., **58**, 2516-2521.

Constable, S.C., Parker, R.L. and Constable, C.G., 1987. Occam's inversion : a practical algorithm for generating smooth models from electromagnetic sounding data, Geophysics, **52**, 289-300.

Conybeare, C.E.B., 1979. Lithostratigraphic Analysis of Sedimentary Basins, Academic Press, pp. 555.

Cooper, B.J., 1981. Carboniferous and Permian sediments in South Australia and their correlation, Quart. Geol. Notes, Geol. Surv. S. Aust., **79**, 2-6.

Cooper, B.J., 1983. 'Carboniferous and Permian sediments in South Australia and their correlation.' A reply to C.B. Fisher, Quart. Geol. Notes, Geol. Surv. S. Aust., **87**, 10-15.

Courtney, R.C. and Beaumont, C., 1983. Thermally activated creep and flexure of the oceanic lithosphere, Nature, **305**, 201-204.

Coward, M.P., 1986. Heterogeneous stretching, simple shear and basin development, Earth Planet. Sci. Lett., **80**, 325-336.

Creaney, S., 1979. Petrographic texture and vitrinite reflectance variation on the Alston Block, north-east England, Proc. Yorks. Geol. Soc., **42**, 553-580.

Crough, S.T., 1983. Rifts and Swells : geophysical constraints on causality, Tectonophysics, **94**, 23-38.

Crowley, K.D., 1985. Thermal significance of fission track length distributions, Nucl. Tracks, **10**, 311-322.

Cull, J.P. and Conley, D., 1983. Geothermal gradients and heat flow in Australian sedimentary basins, Bur. Miner. Resour. J. Aust. Geol. Geophys., **8**, 329-337.

Cull., J.P., Houseman, G.A., Muir, P.M., and Paterson, H.L., Geothermal signatures and uranium ore deposits on the Stuart Shelf of South Australia, Expl. Geophys., **19**, 34-38.

Curry, D.M. and Cox, J.E., 1971. Two dimensional analysis of heat and mass transfer in porous media, in: Cremers, C.J., Kreith, F., Clark, J.A., (Eds), Environmental and Geophysical Heat Transfer, ASME, 9-19.

Davies, G.F. and Strebeck, J.W., 1982. Old continental geotherms : constraints on heat production and thickness of continental plates, Geophys. J. Roy. astr. Soc., **69**, 623-634.

De Bremaecker, J-C., 1983. Temperature, subsidence and hydrocarbon maturation in extensional basins : a finite element model, AAPG Bull., **67**, 1410-1414.

Delhi Petroleum, 1967. Delhi-Santos Kalladeina No.1., South Australian well completion report, unpubl.

Dembicki, H., Jr. , 1984. An interlaboratory comparison of source rock data, Geochim. Cosmochim. Acta, 48, 2641-2649.

Denham. D., 1983. Earthquakes, stresses and deformations of the Indo-Australian Plate, Geol. Soc. Aust. Abstr., **9**, 5-6.

DeRito, R.F., Cozzarelli, F.A. and Hodge, D.S., 1983. Mechanism of subsidence of ancient cratonic rift basins, Tectonophysics, **94**, 141-168.

DeRito, R.F., Cozzarelli, F.A. and Hodge, D.S., 1986. A forward approach to the nonlinear problem of viscoelasticity and the thickness of the mechanical lithosphere, J. Geophys. Res., **91**, 8295-8313.

Dodson, M., 1973. Closure temperature in cooling geological and petrological systems, Contrib. Mineral. Petrol., **40**, 259-275.

Dominenco, P.A. and Palciauskas, V.V., 1973. Theoretical analysis of forced convective heat transfer in regional ground-water flow, Geol. Soc. Am. Bull., **84**, 3803-3014.

Dow, W.G. and O'Connor, D.E., 1982. Kerogen maturity and type by reflected light microscopy applied to petroleum exploration, in: Staplin, F.L., (Ed). How to assess Maturation and Palaeotemperatures, Soc. Econ. Palaeontol. Mineral. short course no. 7., 133-157.

Drewry, D., 1983. Antartica : Glaciological and geophysical folio, Scott Polar Research Inst., Cambridge.

Drummond, B.J., Etheridge, M.A. and Middleton, M.F., 1987. The geometry of extensional structures in the Fitzroy Trough, Canning Basin, Western Australia, Bureau Miner. Resour. Record 1987/51, 143-147.

Duddy, I.R., 1987. Fission track thermal history assessment of the Eromanga-Cooper Basin: an initial apatite study, in: Gleadow, A.J.W., Duddy, I.R., Green, P.F. and Lovering, J.F., End of Grant Technical Report, NERDDC project no. 720.

Durand, B., (Ed), 1980. Kerogen. Insoluble Organic Matter from Sedimentary Rocks, Editions Technip, pp. 518.

Dutton, C.E., 1889. On some of the greater problems of physical geology, Bull. Wash. Phil. Soc., ser. B, **11**, 51-64.

Eckstein, Y., Maurath, G., and Ferry, R.A., 1985. Modelling the thermal evolution of an active geothermal system, J. Geodynamics, **4**, 149-163.

Elder, J.W., 1965. Physical processes in geothermal areas in: Lee, W.H.K., (Ed), Terrestrial Heat Flow, Am. Geophys. Un., Geophys. Mono. **8**, 211-239.

Ellis, P.L. and Whitaker, W.G., 1976. Geology of the Bundaburg 1:250 000 sheet area, Qld. Geol. Surv. Rep., **90**.

Ellis, P.L., 1968. Geology of the Maryborough 1:250 000 sheet area, Qld. Geol. Surv. Rep., **26**.

Embleton, B.J.J., 1984. Past global settings, continental palaeomagnetism, in; Veevers, J.J, (Ed), Phanerozoic Earth History of Australia, Clarendon Press, 11-16.

England, P.C., 1983. Constraints on extension of continental lithosphere, J. Geophys. Res., **88**, 1145-1152.

England, P.C. and McKenzie, D.P., 1982. A thin viscous sheet model for continental deformation, Geophys. J. Roy. astr. Soc., **70**, 295-322.

England, P.C. and McKenzie, D.P., 1983. Correction to : A thin viscous sheet model for continental deformation, Geophys. J. Roy. astr. Soc., **73**, 525-532.

England, P.C., Oxburgh, E.R., and Richardson, S.W., 1980. Heat refraction and heat production in and around granite plutons in north-east England, Geophys. J. Roy. astr. Soc., **62**, 439-455.

England, P.C. and Richardson, S.W., 1980. Erosion and the age dependence of continental heat flow, Geophys. J. Roy. astr. Soc., **62**, 421-437.

Erdélyi, M., 1985. Geothermics and the deep flow-system of the Hungarian Basin, J. Geodynamics, **4**, 321-330.

Etheridge, M.A, Branson, J.C., and Stuart-Smith, P.G., 1987. The Bass, Gippsland and Otway Basins in south east Australia : a branched rift system formed by continental extension, in: Beaumont, C. and Tankard, A., (Eds), Sedimentary Basins and Basin-Forming Mechanisms, Canadian Society Petroleum Geologists Memoir **12**, in press.

Evans, P.R. 1980. Geology of the Galilee Basin, in: Henderson, R.A. and Stephenson, P.J., (Eds), The geology and geophysics of north eastern Queensland, Geol. Soc. Aust. (Qld. Div.), 299-305.

Evans, P.R. and Roberts, J., 1979. Evolution of central eastern Australia during the late Palaeozoic and early Mesozoic, J. Geol. Soc. Aust., **26**, 325-340.

Exon. N.F., 1976. The geology of the Surat Basin, Bur. Miner. Resour. Geol. Geophys. Bull. **166**.

Exon, N.F. and Burger, D., 1981. Sedimentary cycles in the Surat Basin and global changes of sea level, Bur. Miner. Resour. J. Aust. Geol. Geophys., **6**, 153-159.

Exon, N.F. and Senior, B.R., 1976. The Cretaceous of the Eromanga and Surat Basins, Bur. Miner. Resour. J. Aust. Geol. Geophys., **1**, 33-50.

Falvey, D.A., 1974. The development of continental margins in plate tectonic theory, APEA J., **14**, 95-106.

Falvey, D.A., 1975. Arc reversals and a tectonic model for the North Fiji Basin, Bull. Aust. Soc. Expl. Geophys., **6**, 47-49.

Falvey, D.A., 1978. Analysis of palaeomagnetic data from the New Hebrides, Bull. Aust. Soc. Expl. Geophys., **9**, 117-123.

Falvey, D.A. and Deighton, I., 1982. Recent advances in burial and thermal geohistory analysis, APEA J., **22**, 65-81.

Falvey, D.A. and Mutter, J.C., 1981. Regional plate tectonics and the evolution of Australia's passive continental margins, Bur. Min. Resour. J. Geol. Geophys., **6**, 1-29.

Faure, G., 1977. Principles of Isotope Geology, J. Wiley and Sons, pp. 464.

Feinstein, S., 1981. Subsidence and thermal history of the Southern Okalahoma Aulacogen : Implications for petroleum generation, AAPG Bull., **65**, 2521-2533.

Fertl, W.H. and Wichmann, P.A., 1977. How to determine static BHT from well log data, World Oil, January 1977, 105-106.

Finlayson, D.M., Leven, J.M., Mathur, S.P. and Collins, C.D.N., 1987a. Geophysical abstracts and seismic profiles from the central Eromanga Basin region, eastern Australia, Bur. Miner. Resour. Geol. Geophys. Report **278.**

Finlayson, D.M., Leven, J.M. and Etheridge, M.A., 1987b. Structural styles and basin evolution in the Eromanga Basin region, eastern Australia, AAPG Bull., in press.

Fletcher, R., 1971. A modified Marquardt subroutine for non-linear squares, AERE (U.K.) Harwell Technical Report no. R6799.

Forbes, B.G., 1972. Possible post-Winton Mesozoic rocks northeast of Maree, South Australia, Quart. Geol. Notes, Geol. Surv. S. Aust., **41**, 1-3.

Forbes, B.G., 1982. Margin of the Eromanga Basin, South Australia: a review, in: Moore, P.S. and Mount, T.J. (compilers), Eromanga Basin Symposium, summary papers, Geo. Soc. Aust. Pet. Expl. Soc. Aust., 110-126.

Forman, D.J. and Wales, D.W., 1981. Geological evolution of the Canning Basin, Western Australia, Bur. Miner. Resour. Bull. 210.

Forsyth, D.W., 1985. Subsurface loading and estimates of the flexural rigidity of continental lithosphere, J. Geophys. Res., **90**, 12623-12632.

Foucher, J.P. and Le Pichon X., 1972. Comments on 'Thermal effects of the formation of Atlantic continental margins by continental break-up' by N.H. Sleep, Geophys. J. Roy. astr. Soc., **29**, 43-46.

Fowler, C.M.R. and Nisbet, E.G., 1985. The subsidence of the Williston Basin, Can. J. Earth Sci., **22**, 408-415.

Garg, S.K. and Kassoy, D.R., 1981. Convective heat and mass transfer in hydrothermal systems, in: Rybach, L. and Muffler, L.J.P., (Eds), Geothermal Systems : Principles and Case Histories, J.Wiley and Sons, 37-76.

Garner, D.L. and Turcotte, D.L., 1984. The thermal and mechanical evolution of the Anadarko Basin, Tectonophysics, **107**, 1-24.

Gasparini, P. and Mantovani, M.S.M., 1984. Heat transfer in geothermal areas, in: Rapolla, A. and Keller, G.V., (Eds), Geophysics of Geothermal Areas : State of the Art and Future Development, Colorado School of Mines Press, 9-40.

Gatehouse, C.G., 1986. The geology of the Warburton Basin in South Australia, Aust. J. Earth Sci., **33**, 161-180.

Gibbs, A.D., 1987. Basin development, examples from the United Kingdom and comments on hydrocarbon prospectivity, Tectonophysics, **133**, 189-198.

Gibbs, R.J., 1965. The geochemistry of the Amazon River Basin, Ph.D. thesis, University of California, San Diego, University microfilms Inc. Ann Arbor, Michigan, USA.

Gibson, R.E., 1958, The progress of consolidation in a clay layer increasing in thickness with time, Geotechnique, **8**, 171-182.

Gilluly, J., 1964. Atlantic sediments, erosion rates and the evolution of the continental shelf : some speculations, Geol. Soc. Am. Bull., **75**, 483-492.

Gleadow, A.J.W. and Duddy, I.R., 1981. A natural long term annealing experiment for apatite. Nucl. Tracks, **5**, 169-174.

Gleadow, A.J.W., Duddy, I.R. and Lovering, J.F., 1983. Fission track analysis : a new tool for the evaluation of thermal histories and hydrocarbon potential, APEA J., **23**, 93-102.

Gleadow, A.J.W., Duddy, I.R., Green, P.F. and Lovering, J.F., 1986. Confined fission track lengths in apatite : a diagnostic tool for thermal history analysis, Contrib. Mineral. Petrol., **94**, 405-415.

Goetze, C. and Evans, B., 1979. Stress and temperature in the bending lithosphere as constrained by experimental rock mechanics, Geophys. J. Roy. astr. Soc., **59**, 463-478.

Goldstein, A., 1984. Tectonic controls on Late Palaeozoic subsidence in south central United States, J. Geology, **92**, 217-222.

Gravestock, D.I., 1982. Jurassic to Lower Cretaceous stratigraphy of the Eromanga Basin, South Australia - Problems and progress in subsurface correlation, in: Moore, P.S. and Mount, T.J. (compilers), Eromanga Basin Symposium, summary papers, Geol. Soc. Aust. Pet. Expl. Soc. Aust., 79-91.

Gravestock, D. and Alexander, A.M., 1986. Porosity and permeability of reservoirs and caprocks from the Eromanga Basin, South Australia, APEA J., **24**, 202-213.

Gravestock, D.I. and Morton, J.G.G., 1984. Geology of the Della field, a perspective on the history of the Cooper Basin, APEA J., **24**, 266-277.

Green, P.F., 1981. 'Track-in-track' length measurements in annealed apatites, Nucl. Tracks., **5**, 121-128.

Green, P.F., Duddy, I.R., Gleadow, A.J.W., Tingate, P.R., and Laslett, G.M., 1985. Fission track annealing in apatite : track length measurements and the form of the Arrhenius plot, Nucl. Tracks, **10**, 323-328.

Green, P.F., Duddy, I.R., Gleadow, A.J.W., Tingate, P.R., and Laslett, G.M., 1986. Thermal annealing of fission tracks in apatite 1. A qualitative description, Chem. Geol. (Isotope Geosci. Sect.), **59**, 237-253.

Green, P.F., Duddy, I.R., Gleadow, A.J.W., and Lovering, J.F., 1987. Apatite fission track analysis as a palaeotemperature indicator for hydrocarbon exploration. in: Naeser, N.D., (Ed), Soc. Econ. Palaeontol. Mineral, spec. publ., in press.

Green, P.F., Duddy, I.R., and Laslett, G.M., 1988. Can fission track annealing in apatite be described by first-order kinetics?, Earth Planet. Sci. Lett., **87**, 216-228.

Green, P.F. and Durrani, S.A., 1977. Annealing studies of tracks in crystals, Nucl. Tracks, **1**, 33-39.

Greenberg, J.K. and Brown, B.A., 1984. Cratonic sedimentation during the Proterozoic : an anorogenic connection in Wisconsin and the upper Midwest, J. Geology, **92**, 159-171.

Gregory, J.W. , 1906. The Dead Heart of Australia, Murray.

Guidish, T.M., Lerche, I., Kendall, C.G. St C. and O'Brien, J.J., 1984. Relationship between eustatic sea level and basement subsidence, AAPG Bull., **68**, 164-177.

Habermehl, M.A., 1980. The Great Artesian Basin, Australia, Bur. Min. Resour. J. Geol. Geophys., **5**, 9-38.

Habermehl, M.A., 1986. Regional groundwater movement, hydrochemistry and hydrocarbon migration in the Eromanga Basin, in: Gravestock, D.I., Moore, P.S., Mount, T.J. and Pitt, G.M., (Eds), Contributions to the Geology and Hydrocarbon Potential of the Eromanga Basin, Geol. Soc. Aust., spec. publ. **12**, 353-376.

Hager, B.H., 1980. Eustatic sea level and spreading rate are not simply related, EOS, **61**, 374.

Hallam, A., 1963. Major epeirogenic and eustatic changes since the Cretaceous and their possible relationship to crustal structure, Am. J. Sci., **261**, 397-423.

Hallam, A., 1984. Pre-Quaternary sea-level changes, Ann. Rev. Earth Planet. Sci., **12**, 205-243.

Hancock, J.M., and Kauffman, E.G., 1979. The great transgressions of the Cretaceous, J. Geol. Soc. Lond., **136**, 175-186.

Harland, W.B., Cox, A.V., Llewellyn, P.G., Pickton, C.A.G., Smith, A.G., and Walters, R., 1982. A Geologic Time Scale, Cambridge University Press, pp. 131.

Harrison, C.G.A., Brass, G.W., Saltzman, E.S. and Sloan, J., Southam, J. and Whitman, J.M., 1981. Sea level variations, global sedimentation rates and the hypsographic curve, Earth Planet. Sci. Lett., **54**, 1-16.

Harrison, C.G.A., Miskell, K.J., Brass, G.W., Saltzman, E.S. and Sloan II, J.L., 1983. Continental hypsography, Tectonics, **2**, 357-377.

Harrison, J.F., and Higginbotham, G.T., 1964. Delhi-Santos Gidgealpa no. 1, South Australia, well completion report, S. Aust. Dept. Mines Energy open file Env. **283** (unpubl).

Harrison, T.M., 1983. Some observations on the interpretation of $^{40}Ar/^{39}Ar$ age spectra, Isot. Geosci., **1**, 319-338.

Harrison, T.M. and Bé, K., 1983. $^{40}Ar/^{39}Ar$ spectrum analysis of detrital microclines from the southern San Joaquin Basin, California : an approach to determining the thermal evolution of sedimentary basins, Earth Planet. Sci. Lett., **64**, 244-256.

Harrison, T.M., and McDougall, I., 1982. The thermal significance of potassium feldspar K-Ar ages inferred from $^{40}Ar/^{39}Ar$ age spectrum results, Geochim. Cosmochim. Acta, **46**, 1811-1820.

Harrison, T.M., Morgan, P. and Blackwell, D.D., 1986. Constraints on the age of heating at the Fenton Hill site, Valles Caldera, New Mexico, J. Geophys. Res., **91**, 1899-1908.

Hashin, Z. and Strickman, S., 1962. A variational approach to the theory of the effective magnetic permeability of multiphase materials, J. Appl. Phys., **33**, 3215-3131.

Haxby, W.F., Turcotte, D.L. and Bird, J.M., 1976. The thermal and mechanical evolution of the Michigan Basin, Tectonophysics, **36**, 57-75.

Hays, J.D., and Pitman III, W.C., 1973. Lithospheric plate motion, sea level changes and climatic and ecological consequences, Nature, **246**, 18-22.

Hegarty, K.A., 1985, Origin and evolution of selected plate boundaries, Ph.D. thesis, Columbia University.

Hegarty, K., Duddy, I.R., Green, P.F., Gleadow, A.J.W., Fraser, I. and Weissel, J.K., 1987. Regional evaluation of the tectonic and thermal history of the Gippsland Basin, in: Glenie, R.C., (Ed), Second south-eastern Australia oil exploration symposium, Pet. Expl. Soc. Aust., 65-74.

Hegarty, K.A. and Houseman, G.A., 1988. A model for the Tertiary evolution of the lithospheric stress field of the Gippsland Basin, Geol. Soc. Aust. Abstr., 21, 9th AGC, Brisbane, 178-179.

Heidlauf, D.T., Hsui, A.T. and Klein, G., 1986. Tectonic subsidence analysis of the Illinois Basin, J. Geology., **94**, 779-794.

Heller, P. and Angevine, C.L., 1985. Sea level changes during the growth of Atlantic-type continental oceans, Earth Planet. Sci. Lett., **75**, 417-426.

Hellinger, S.J. and Sclater, J.G., 1983. Some comments on two layer extension models for the evolution of sedimentary basins, J.Geophys. Res., **88**, 8251-8269.

Henderson, R.A., 1980., Structural outline and summary geological history for northeastern Australia, in : Henderson, R.A. and Stephenson, P.J., (Eds), The Geology and Geophysics of Northeastern Australia, Geol. Soc. Aust. (Qld. Div.), 1-26.

Héroux, Y., Chagnon, A., and Bertrand, R., 1979. Compilation and correlation of major thermal maturation indices, AAPG Bull., **63**, 2128-2144.

Hicks, W.G., 1959. Lateral velocity variations near boreholes, Geophysics, **24**, 451-464.

Hood, A., Gutjahr, C.C.M., and Heacock, R.L., 1975. Organic metamorphism and the generation of petroleum, AAPG Bull., **59**, 986-996.

Horai, K., 1971. Thermal conductivity of rock-forming minerals, J. Geophys. Res., **76**, 1278-1308.

Houseman, G.A. and England, P.C., 1986. A dynamical model of lithosphere extension and sedimentary basin formation, J. Geophys. Res., **91**, 719-729.

Houseman, G.A. and Hegarty, K.A., 1987. Did rifting on Australia's southern margin result from tectonic uplift ?, Tectonics, **6**, 515-527.

Howard, L.E., (1960). Heat flow in Australia, Ph.D. thesis, Australian National University.

Hsü, K.J., 1965. Isostasy, crustal thinning, mantle changes and the disappearance of ancient land masses, Am. J. Sci., **263**, 97-109.

Hutchinson, I., 1985. The effects of sedimentation and compaction on oceanic heat flow, Geophys. J. Roy. astr. Soc., **82**, 439-459.

Issler, D.R., 1984. Calculation of organic maturation levels for offshore eastern Canada - implications for general application of Lopatin's method, Can. J. Earth Sci., **21**, 477-488.

Issler, D.R. and Beaumont, C., 1987. A finite element model of subsidence and thermal evolution of extensional basins : application to the Labrador continental margin, pre-print.

Jackson, K.S., Horvath, Z. and Hawkins, P.J., 1981. An assessment of the petroleum potential for the Galilee Basin, Queensland, APEA J., **21**, 172-186.

Jackson, M.J. and van de Graaff, W.J.E., 1981. Geology of the Officer Basin, Bureau Miner. Resour. Geol. Geophys. Bull. **206**.

Jaeger, J.C., 1965. Application of the theory of heat conduction to geothermal measurements, in: Lee, W.H.K., (Ed), Terrestrial Heat Flow, Am. Geophys. Un., Geophys. Mono. **8**, 7-23.

Jarvis, G.T. and McKenzie, D.P., 1980. Sedimentary basin formation with finite extension rates, Earth Planet. Sci. Lett., **48**, 42-52.

Jaupart, C., 1983. Horizontal heat transfer due to radioactivity contrasts : Causes and consequences of the linear heat flow relation, Geophys. J. Roy. astr. Soc., **75**, 411-435.

John, B.H. and Almond, C.S., 1987, Lithostratigraphy of the lower Eromanga Basin sequence in south-west Queensland, APEA J., **27**, 196-214.

Jones, C.H., 1987. Is extension in Death Valley accommodated by thinning of the mantle lithosphere beneath the Sierra Nevada, California ?, Tectonics, **6**, 449-473.

Jones, J.G. and Veevers, J.J., 1983. Mesozoic origins and antecedents of Australia's Eastern Highlands, J. Geol. Soc. Aust., **30**, 305-322.

Jones, L.E.A. and Wang, H.F., 1981. Ultrasonic velocities in Cretaceous shales from the Williston Basin, Geophysics, **46**, 288-297.

Jordan, T., 1981. Thrust loads and foreland basin evolution, Cretaceous, Western United States. AAPG Bull., **65**, 2506-2520.

Kantsler, A.J., Cook, A.C. and Zwigulis, M, 1986. Organic maturation in the Eromanga Basin, in: Gravestock, D.I., Moore, P.S., Mount, T.J. and Pitt, G.M., (Eds), Contributions to the Geology and Hydrocarbon Potential of the Eromanga Basin, Geol. Soc. Aust., spec. publ. **12**, 305-322.

Kantsler, A.J., Prudence, T.J.C., Cook, A.C. and Zwigulis, M, 1983. Hydrocarbon habitat of the Cooper/Eromanga Basin, Australia, APEA J., **23**, 75-92.

Kantsler, A.J., Smith, G.C., and Cook, A.C., 1978. Lateral and vertical rank variation : implications for hydrocarbon exploration, APEA J., **18**, 143-156.

Karner, G.D., Steckler, M.S., and Thorne, J.A., 1983. Long term thermo-mechanical properties of the continental lithosphere, Nature, **304**, 250-253.

Karner, G.D. and Watts, A.B., 1983. Gravity anomalies and flexure of the lithosphere at mountain ranges, J. Geophys. Res., **88**, 10449-10477.

Keen, C.E., 1985. The dynamics of rifting : deformation of the lithosphere by active and passive driving forces, Geophys. J. Roy. astr. Soc., **80**, 95-120.

Kirby, S.H., 1980. Tectonic stresses in the lithosphere : constraints provided by the experimental deformation of rocks, J. Geophys. Res., **85**, 6353-6363.

Kirby, S.H., 1983. Rheology of the lithosphere, Rev. Geophys. Space Phys., **21**, 1458-1487.

Kirby, S.H. and Kronenberg, A.K., 1987. Rheology of the lithosphere : selected topics, Rev. Geophys., **25**, 1219-1244.

Klein, G. deV., 1982. Probable sequential arrangement of depositional systems on cratons, Geology, **10**, 17-22.

Klein, G. deV., 1984. Relative rates of tectonic uplift as determined from episodic turbidite deposition in marine basins, Geology, **12**, 48-50.

Kominz, M.A., 1984, Ocean ridge volumes and sea level changes - an error analysis, in: Schlee, J.S., (Ed), Interregional Unconformities and Hydrocarbon Accumulations, AAPG memoir **36**, 109-127.

Kominz, M.A. and Bond, G.C., 1986. Geophysical modelling of the thermal history of foreland basins, Nature, **320**, 252-256.

Korvin, G., 1984. Shale compaction and statistical physics, Geophys. J. Roy. astr. Soc., **28**, 35-50.

Krieg, G.W., 1982. Stratigraphy and tectonics of the Dalhousie anticline, southwest Eromanga Basin, in: Moore, P.S. and Mount, T.J. (compilers), Eromanga Basin Symposium, summary papers, Geol. Soc. Aust. and Pet. Explor. Soc. Aust., Adelaide, 145-158.

Krumbein, W.C. and Graybill, F.A., 1965. An Introduction to Statistical Methods in Geology, McGraw-Hill, pp. 475.

Kuang, K.S., 1985. History and style of Cooper-Eromanga Basin structures, Expl. Geophys., **16**, 245-248.

Kusznir, N.J., 1982. Lithosphere response to externally and internally derived stress : a viscoelastic stress guide with amplification, Geophys. J. Roy. astr. Soc. **70**, 399-414.

Kusznir, N.J. and Bott M.H.P., 1977. Stress concentration in the upper lithosphere caused by underlying viscoelastic creep, Tectonophysics, **43**, 247-256.

Kusznir, N.J. and Karner, G.D., 1985. Dependence of the flexural rigidity of the continental lithosphere on rheology and temperature, Nature, **316**, 138-142.

Kusznir, N.J. and Park, R.G., 1984a. Intraplate deformation and the strength of the lithosphere, Geophys. J. Roy. astr. Soc., **79**, 513-538.

Kusznir, N.J. and Park, R.G., 1984b. The strength of the intraplate lithosphere, Phys. Earth Planet. Int., **36**, 224-235.

Lachenbruch, A.H., 1970. Crustal temperature and heat production : Implications of the linear heat flow relation, J. Geophys. Res., **75**, 3291-3300.

Lambeck, K., 1983a. Structure and evolution of the intracratonic basins of central Australia, Geophys. J. Roy. astr. Soc., **74**, 843-886.

Lambeck, K., 1983b. The role of compressive forces in intracratonic basin formation and midplate orogenies, Geophys. Res. Lett., **10**, 845-848.

Lambeck, K., Cloetingh, S. and McQueen, H., 1987. Intraplate stresses and apparent changes in sea level : The basins of northwestern Europe, in : Beaumont, C. and Tankard, A.J., (Eds), Sedimentary Basins and Basin-Forming Mechanisms, Canadian Society Petroleum Geologists Memoir **12**, 259-268.

Lambeck, K. and Nakiboglu, S.M., 1980. Seamount loading and stress in the oceanic lithosphere, J. Geophys. Res., **85**, 6403-6418.

Lambeck, K. and Nakiboglu, S.M., 1981. Seamount loading and stress in the oceanic lithosphere 2. Viscoelastic and elastic-viscoelastic models, J. Geophys. Res., **86**, 6961-6984.

Lambeck, K. and Stephenson, R., 1986. The post-Palaeozoic uplift history of south-eastern Australia, Aust. J. Earth. Sci., **33**, 253-270.

Lambeck, K., Penney, C.L., Nakiboglu, S.M. and Coleman, R., 1984. Subsidence and flexure along the Pratt-Welker seamount chain, J. Geodynamics., **1**, 29-60.

Laslett, G.M., Gleadow, A.J.W., and Duddy, I.R., 1984. The relationship between fission track length and density in apatite, Nucl. Tracks, **9**, 29-38.

Laslett, G.M., Green, P.F., Duddy, I.R., and Gleadow, A.J.W., 1987. Thermal annealing of fission tracks in apatite 2. A quantitative analysis, Chem. Geol. (Isot. Geosci. Sect.), **65**, 1-13.

Le Pichon, X., 1983. Land-locked oceanic basins and continental collision : the eastern Mediterranean as a case example. In : Hsü, K.J., (Ed), Mountain Building Processes, Academic Press, 201-211.

Le Pichon, X., Angelier, J. and Sibuet, J-C., 1982. Plate boundaries and extensional tectonics, Tectonophysics, **81**, 239-256.

Le Pichon, X. and Sibuet, J-C., 1981. Passive margins : a model of formation, J. Geophys. Res., **86**, 3708-3720.

Leblanc, Y., Pascoe, L.J. and Jones F.W., 1981. The temperature stabilization of a borehole, Geophysics, **46**, 1301-1303.

Leder, F. and Park, W.C., 1986. Porosity reduction in sandstone by quartz overgrowth, AAPG Bull., **70**, 1713-1728.

Lee, M.K., Brown, G.C., Webb, P.C., Wheildon, J. and Rollin, K.E., 1987. Heat flow, heat production and thermo-tectonic setting in mainland UK, J. Geol. Soc. Lond., **144**, 35-42.

Lee, T-C., 1982. Estimation of formation temperature and thermal property from dissipation of heat during drilling, Geophysics, **47**, 1577-1584.

Lee, T-C. and Henyey, T.L., 1974. Heat-flow refraction across dissimilar media, Geophys. J. Roy. astr. Soc., **39**, 319-333.

Lee, W.H.K. and Stewart, S.W., 1981. Principles and Application of Microearthquake Networks, Advances in Geophysics, suppl. 2., Academic Press, pp. 293.

Leeder, M.R., 1976. Sedimentary facies and the origins of subsidence along the northern margin of the supposed Hercynian ocean, Tectonophysics, **36**, 167-179.

Lerche, I. and Kendall, C.G., 1985. Determination of palaeoheat flux from vitrinite reflectance data : Reply, AAPG Bull., **69**, 2149.

Lerche, I., Yarzab, R.F., and Kendall, C.G., 1984. Determination of palaeoheat flux from vitrinite reflectance data, AAPG Bull., **68**, 1704-1717.

Leven, J.M. and Finlayson, D.M., 1987. Lower crustal involvement in upper crustal thrusting, Geophys. J. Roy. astr. Soc., **89**, 415-422.

Leven, J.M., Finlayson, D.M. and Etheridge, M.A., 1987. Basement involved compression and the tectonic evolution of the southern Adavale Basin, Australia, submitted to Tectonics.

Lewis, T.J. and Beck, A.E., 1977. Analysis of heat-flow data - detailed observations in many holes in a small area, Tectonophysics, **41**, 41-59.

Lines, L.R. and Treitel, S., 1984. Tutorial : a review of least-squares inversion and its application to geophysical problems, Geophys. Prospect., **32**, 159-186.

Lister, G.S., Etheridge, M.A. and Symonds, P.A., 1986. Detachment faulting and the evolution of passive continental margins, Geology, **14**, 246-250.

Lopatin, N.V., 1971. Temperature and geologic time as factors in coalification, (in Russian), Akad. Nauk. SSSR Izv. Ser. Geol., **3**, 95-106.

Lowry, D.C., 1976. The Eucla Basin, in: Leslie, R.G., Evans, H.J. and Knight, C.L., (Eds), Economic Geology of Australia and Papua New Guinea, **3**, Australian Institute of Mining and Metallurgy, Monograph **7**, 95-98.

Lubimova, E.A., Maslennikov, V.N. and Gaviev, I.K., 1977. Thermal conductivity of dry, wet and oil-saturated rocks at slightly high temperatures and pressures, Geophys. Res. Bull., **15**, 59-66.

Lucazeau, F. and Le Douaran, S., 1985. The blanketing effect of basins formed by extension : a numerical model. Application to the Gulf of Lion and Viking Graben, Earth Planet. Sci. Lett., **74**, 92-102.

Lucazeau, F. and Mailhe, D. , 1986. Heat flow, heat production and fission track data from the Hercynian basement around the Provençal Basin (Western Mediterranean), Tectonophysics, **128**, 335-356.

Ludbrook, N.H., 1961. Palaeontological report in: Ryan, J.C., Innamincka No. 1 well South Australia, Delhi-Frome-Santos, Dept. of Nat. Dev., Petroleum Search Subsidy Acts. Publ. 9.

Lyon-Caen, H. and Molnar, P., 1985. Gravity anomalies, flexure of the Indian plate, and the structure, support, and evolution of the Himalaya and Ganga Basin, Tectonics, **4**, 513-538.

Mackenzie, A.S., Beaumont, C. and McKenzie, D.P., 1984a. Estimation of the kinetics of geochemical reactions with the geophysical models of sedimentary basins and applications, Org. Geochem., **6**, 875-884.

Mackenzie, A.S., Beaumont, C., Boutilier, R., and Rullkotter, J., 1984b. Aromatization and isomerization of hydrocarbons and the thermal evolution of the Nova Scotia continental margin, in: Durand, B., (Ed), Thermal Phenomena in Sedimentary Basins, Collection Colloques et Seminaires 41, Editions Technip, 285-291.

MacKenzie, A.S., 1984, Estimation of kinetics of geochemical reactions with geophysical models and applications, in: Durand, B., (Ed), Thermal Phenomena in Sedimentary Basins, Collection Colloques et Seminaires 41, Editions Technip, 135-145.

Mackenzie, A.S., and McKenzie, D.P., 1983. Isomerization and aromatization of hydrocarbons in sedimentary basins formed by extension, Geol. Mag., **120**, 417-528.

Magara, K., 1980. Comparison of porosity/depth relationships of shale and sandstone, J. Petrol. Geol., **3**, 175-185.

Majorowicz, J.A., Jones, F.W., Lam, H.L. and Jessop, A.M., 1984a, Heat flow and geothermal gradient studies in the Alberta Basin. An essential part of geothermal potential evaluation, in: Curtis, F.A., (Ed), Energy Developments : New forms, renewables, conservation, Pergamon Press, 279-284.

Majorowicz, J.A., Jones, F.W., Lam, H.L. and Jessop, A.M., 1984b, The variability of heat flow both regional and with depth in southern Alberta, Canada : Effect of groundwater flow ?, Tectonophysics, **106**, 1-29.

Majorwicz, J.A., Marek, S. and Znosko, J., 1984c. Palaeogeothermal gradients by vitrinite reflectance data and their relation to the present day geothermal gradient patterns of the Polish lowland, Tectonophysics, **103**, 141-156.

Majorowicz, J.A., Jones, F.W., Lam, H.L. and Jessop, A.M., 1985, Terrestrial heat flow and geothermal gradients in relation to hydrodynamics in the Alberta Basin, Canada., J. Geodynamics, **4**, 265-283.

Majorowicz, J.A., Jones, F.W. and Jessop, A.M., 1986. Geothermics of the Williston Basin in Canada in relation to hydrodynamics and hydrocarbon occurrences, Geophysics, **51**, 767-779.

Mansure, A.J. and Reiter, M., 1979. A vertical groundwater correction for heat flow, J. Geophys. Res., **84**, 3490-3496.

Mareschal, J.C., 1981. Uplift by thermal expansion of the lithosphere, Geophys. J. Roy. astr. Soc., **66**, 535-552.

Mareschal, J.C., 1983. Uplift and heat flow following injection of magmas into the lithosphere, Geophys. J. Roy. astr. Soc., **73**, 109-127

Mareschal, J.C. and Gangi, A.F., 1977. Equilibrium position of a phase boundary under horizontally varying surface loads, Geophys. J. Roy. astr. Soc., **49**,757-772.

Mareschal, J.C. and Lee, C-K., 1983. Initiation of subsidence in a sedimentary basin underlain by a phase change, Geophys. J. Roy. astr. Soc., **74**, 689-712.

Marquardt, D.W., 1963. An algorithm for the least-squares estimation of nonlinear parameters, J. SIAM, **11**, 431-441.

Martin, C.A., 1967. The Gidgealpa and Merrimelia Formations in the Coopers Creek Basin, Aust. Oil and Gas Journal, **14**, 29-35.

Mathur, S.P., 1983. Deep crustal reflection results from the central Eromanga Basin, Australia, Tectonophysics, **100**, 163-173.

Mathur, S.P., 1987. Deep seismic reflection data suggest major compressional deformation of the crust in the central Eromanga Basin area during the mid-Carboniferous, Tectonophysics, **134**, 311-321.

McAdoo, D.C., Martin, C.F. and Poulouse, S., 1985. SEASAT observations of flexure : evidence for a strong lithosphere, Tectonophysics, **116**, 209-222.

McKenzie, D.P., 1967. Some remarks on heat flow and gravity anomalies, J. Geophys. Res., **72**, 6261-6273.

McKenzie, D.P., 1978. Some remarks on the development of sedimentary basins, Earth Planet. Sci. Lett., **40**, 25-32.

McKenzie, D.P., 1981. The variation of temperature with time and hydrocarbon maturation in sedimentary basins formed by extension, Earth Planet. Sci. Lett., **55**, 87-98.

McMinn, A. and Burger, D., 1986. Palynology and palaeoenvironments of the Toolebuc Formation (Sensu lato) in the Eromanga Basin, in: Gravestock, D.I., Moore, P.S., Mount, T.J. and Pitt, G.M., (Eds), Contributions to the Geology and Hydrocarbon Potential of the Eromanga Basin, Geol. Soc. Aust., spec. publ. **12**, 135-154.

McMullen, R.J., Jr. and Mohraz, B., 1987. Axisymmetric finite element analysis of an elastic lithosphere subjected to thermal loading, Geophys. J. Roy. astr. Soc., **88**, 325-343.

McNutt, M.K., 1984. Lithospheric flexure and thermal anomalies, J. Geophys. Res., **89**, 11180-11194.

McQueen, H.W.S., 1986. Geophysical inference of inplane stress in the lithosphere using numerical models, Ph.D. thesis, Australian National University.

Meissner, R. and Strehlau, J., 1982. Limits of stresses in continental crust and their relation to depth frequency distribution of shallow earthquakes, Tectonics, 1, 73-89.

Miall, A.D., 1978, Tectonic setting and syndepositional deformation of molasse and other non-marine-paralic sedimentary basins, Can. J. Earth Sci., **15**, 1613-1632.

Middleton, M.F. 1978. The genesis of the Cooper and Eromanga Basins, Ph.D. thesis, University of Sydney.

Middleton, M.F., 1979a. Heat flow in the Moomba, Big Lake and Toolachee gas fields of the Cooper Basin and implications for hydrocarbon maturation, Bull. Aust. Soc. Expl. Geophys., **10**, 149-155.

Middleton, M.F., 1979b. A model for bottom hole temperature stabilization, Geophysics, **44**, 1458-1462.

Middleton, M.F., 1980. A model of intracratonic basin formation entailing deep crustal metamorphism, Geophys. J. Roy. astr. Soc., **62**, 1-14.

Middleton, M.F., 1982a. The subsidence and thermal history of the Bass Basin, southeastern Australia, Tectonophysics, **87**, 383-397.

Middleton, M.F., 1982b. Tectonic history from vitrinite reflectance, Geophys. J. Roy. astr. Soc., **68**, 121-132.

Middleton, M.F., 1982c. Bottom hole temperature stabilization with continued circulation of drilling mud, Geophysics, **47**, 1716-1723.

Mithen, D.P., 1982. Stress amplification in the upper crust and the development of normal faulting, Tectonophysics, **83**, 259-273.

Mitrovica, J.X. and Jarvis, G.T., 1985. Surface deflections due to transient subduction in a convecting mantle, Tectonophysics, **120**, 211-237.

Moore, M.E., Gleadow, A.J.W. and Lovering, J.F., 1986. Thermal evolution of rifted continental margins : new evidence from fission tracks in basement apatites from southeastern Australia, Earth Planet. Sci. Lett., **78**, 255-270.

Moore, P.S., 1982. Mesozoic geology of the Simpson Desert region, northern South Australia, in: Moore, P.S. and Mount, T.J. (compilers), Eromanga Basin Symposium, summary papers, Geol. Soc. Aust. and Pet. Explor. Soc. Aust., Adelaide, 46-57.

Moore, P.S., 1986. Jurassic and Triassic stratigraphy and hydrocarbon potential of the Poolowanna Trough (Simpson Desert Region) northern South Australia, in : Gravestock, D.I., Moore, P.S., Mount, T.J. and Pitt, G.M., (Eds), Contributions to the Geology and Hydrocarbon Potential of the Eromanga Basin, Geol. Soc. Aust., spec. publ. **12**, 39-51.

Moore, P.S. and Pitt, G.M., 1982. Cretaceous of the southwestern Eromanga Basin, stratigraphy, facies variations and petroleum potential, in: Moore, P.S. and Mount, T.J. (compilers), Eromanga Basin Symposium, summary papers, Geol. Soc. Aust. and Pet. Explor. Soc. Aust., Adelaide, 127-144.

Moore, P.S. and Pitt, G.M., 1984. Cretaceous of the Eromanga Basin - Implications for hydrocarbon exploration, APEA J., **24**, 358-376.

Moore, P.S. and Pitt, G.M., 1985. Cretaceous subsurface stratigraphy of the southwestern Eromanga Basin: a review, S. Aust. Dept. Mines and Energy spec. publ. **5**, 269-286.

Moore, P.S., Hobday, D.K., Main, H. and Sun, Z.C., 1986a. Comparison of selected non-marine petroleum bearing basins in Australia and China, APEA J., **26**, 285-309.

Moore, P.S., Pitt., G.M. and Dettman, M.E., 1986b. The Early Cretaceous Coorikiana Sandstone and Toolebuc Formation : Their recognition and stratigraphic relationship in the southwestern Eromanga Basin, in : Gravestock, D.I., Moore, P.S., Mount, T.J. and Pitt, G.M., (Eds), Contributions to the Geology and Hydrocarbon Potential of the Eromanga Basin, Geol. Soc. Aust., spec. publ. **12**, 97-114.

Moretti, I. and Froidevaux, C., 1986. Thermomechanical models of active rifting, Tectonics, **5**, 501-511.

Morgan, P. and Baker, B.H., 1983. Introduction - processes of continental rifting, Tectonophysics, **103**, 1-10.

Morgan, P. and Sass, J.H., 1984. Thermal regime of the continental lithosphere, J. Geodynamics, **1**, 143-166.

Morgan, R., 1980. Eustasy in the Australian Early and Middle Cretaceous, Geol. Surv. N.S.W. Bull. **27**.

Muirhead, K.J. and Drummond, B.J., 1987. The seismic structure of the lithosphere under Australia and its implications for continental plate tectonics, pre-print, (Geol. Soc. Aust. spec. publ.)

Murray, C.G., Fergusson, C.L., Flood, P.G., Whitaker, W.G. and Korsch, R.J., 1987. Plate tectonic model for the Carboniferous evolution of the New England fold belt, Aust. J. Earth Sci., **34**, 213-236.

Nadai, A., 1963. Theory of flow and fracture of solids, Vol. 2., McGraw-Hill, pp. 705.

Naeser, C.W., 1979. Fission track dating and geological annealing of fission tracks, in: Jäger, E. and Hunziker, J.C., (Eds), Lectures in Isotope Geology, Springer-Verlag, 154-169.

Naeser, C.W., 1981, The fading of fission tracks in the geologic environment - data from deep drill holes, Nucl. Tracks, **5**, 248-250.

Nagtegaal, P.J.C., 1978. Sandstone framework instability as a function of burial diagenesis, J. Geol. Soc. Lond., **135**, 101-105.

Nakada, M. and Lambeck, K., 1987. Glacial rebound and relative sea-level variations : a new appraisal, Geophys. J. Roy. astr. Soc., **90**, 171-224.

Nakiboglu, S.M. and Lambeck, K., 1985. Comments on thermal isostasy, J. Geodynamics, **2**, 51-65.

Nelson, A.W., 1985. Tectonics of the Jackson-Naccowlah area, Cooper-Eromanga Basins, southwest Queensland and their implications for hydrocarbon accumulation, APEA J., **25**, 85-94.

Neugebauer, H.J., 1983. Mechanical aspects of continental rifting, Tectonophysics, **94**, 91-108.

Neugebauer, H.J. and Reuther, C., 1987. Intrusion of igneous rocks - physical aspects, Geol. Rundschau., **76**, 89-99.

Nunn, J.A. and Sleep, N.H., 1984. Thermal contraction and flexure of intracratonic basins : a three dimensional study of the Michigan Basin, Geophys. J. Roy. astr. Soc., **76**, 587-635.

Nunn, J.A., Sleep, N.H. and Moore, W.E., 1984. Thermal subsidence and generation of hydrocarbons in Michigan Basin, AAPG Bull., **68**, 298-315.

O'Connell, R.J. and Wasserburg, G.J., 1972. Dynamics of submergence and uplift of a sedimentary basin underlain by a phase change, Rev. Geophys. Space. Phys., **10**, 335-368.

Odin, G.S., (Ed), 1982. Numerical Dating in Stratigraphy, part I and II, J. Wiley and Sons, pp. 1040.

Olgers, F., 1972. The geology of the Drummond Basin, Queensland, Bur. Min. Res. Aust. Bull. **132**.

O'Nions, R.K. and Oxburgh, E.R., 1983. Heat and helium in the earth, Nature, **306**, 429-431.

Oxburgh, E.R., 1981. Heat flow and differences in lithospheric thickness, Phil. Trans. Roy. Soc. Lond, ser. A, **301**, 337-346.

Ozimic, S., 1986. The geology and petrophysics of the Toolebuc Formation and its time equivalents, Eromanga and Carpentaria Basins, in : Gravestock, D.I., Moore, P.S., Mount, T.J. and Pitt, G.M., (Eds), Contributions to the Geology and Hydrocarbon Potential of the Eromanga Basin, Geol. Soc. Aust., spec. publ. **12**, 119-137.

Pacht, J.A., 1984. Petrologic evolution and palaeogeography of the Late Cretaceous Nanaimo Basin, Washington and British Columbia : Implications for Cretaceous tectonics, Geol. Soc. Am. Bull., **95**, 766-778.

Packham, G.H., (Ed), 1969. The geology of New South Wales, J. Geol. Soc. Aust., **16**, pp. 654.

Paine, A.G.L., 1969. Palaeovulcanology of central eastern Queensland, Geol. Soc. Aust. spec. publ. **2**, 183-192.

Parasnis, D.S., 1960, The compaction of sediments and its bearing on some geophysical problems, Geophys. J. Roy. astr. Soc., **5**, 1-28.

Parker, R.L. and Oldenburg, D.W., 1973. Thermal model of ocean ridges, Nature Phys. Sci., **242**, 137-139.

Parsons, B. and Sclater, J.G., 1977. An analysis of the variation of ocean floor bathymetry and heat flow with age, J. Geophys. Res., **82**, 803-825.

Passmore, V.L. and Sexton, M.J., 1984. The structural development and hydrocarbon potential of Palaeozoic source rocks in the Adavale Basin region, APEA J., **24**, 393-411.

Paterson, M.S., 1976. Some current aspects of experimental rock deformation, Phil Trans. Roy. Soc. Lond., ser. A, **283**, 163-172.

Paterson, M.S., 1978. Experimental rock deformation - The brittle field, Springer-Verlag, pp. 254.

Paterson, M.S., 1987. Problems in the extrapolation of laboratory rheological data, Tectonophysics, **133**, 33-43.

Payton, C.E., (Ed), 1977. Stratigraphic interpretation of seismic data, AAPG memoir **26**, pp. 516.

Pecanek, H.T. and Paton, I.M., 1984. The development of the Tirrawarra oil and gas field, APEA J., **24**, 278-288.

Perrier, R. and Quiblier, J., 1974. Thickness changes in sedimentary layers during compaction history: methods for quantitative evaluation, AAPG Bull., **58**, 507-520.

Perrier, J. and Raiga-Clemenceau, J., 1984. Temperature measurements in boreholes, in: Durand, B., (Ed), Thermal Phenomena in Sedimentary Basins, Int. Coll. Bordeaux 1983, Collection Colloques et Seminaires 41, Editions Technip, Paris, 47-54.

Pigram, C.J. and Panggabean, M., 1984. Rifting of the northern margin of the Australian continent and the origin of some micro-continents in eastern Indonesia, Tectonophysics, **107**, 331-353.

Pinchin, J., 1978. A seismic investigation of the eastern margin of the Galilee Basin, Queensland, Bur. Miner. Resour. J. Aust. Geol. Geophys., **3**, 193-202.

Pinchin, J. and Senior, B.R., 1982. The Warrabin Trough, western Adavale Basin, Queensland, J. Geol. Soc. Aust., **29**, 413-424.

Piper, A.J., 1986. Notes to accompany the surface to basement geothermal gradient maps of the Cooper Sector and ATP 259P, Delhi Petroleum in-house report.

Pitman III, W.C., 1978. Relationship between eustasy and stratigraphic sequences of passive margins, Geol. Soc. Am. Bull., **89**, 1389-1403.

Pitman III, W.C. and Golovchenko, X., 1983. The effect of sealevel change on the shelf edge and slope of continental margins, Soc. Econ. Palaeontol. Mineral. spec. publ. **33**., 41-58.

Pitt, G.M., 1982. Geothermal gradients in the Eromanga-Cooper Basin, in: Moore, P.S. and Mount, T.J. (compilers), Eromanga Basin Symposium summary papers, Geol. Soc. Aust. and Pet. Explor. Soc. Aust., Adelaide, 262-283.

Pitt, G.M., 1986. Geothermal gradients, geothermal histories and the timing of thermal maturation in the Eromanga-Cooper Basins, in: Gravestock, D.I., Moore, P.S., Mount, T.J. and Pitt, G.M., (Eds), Contributions to the Geology and Hydrocarbon Potential of the Eromanga Basin, Geol. Soc. Aust., spec. publ. **12**, 232-351.

Plumb, K.A., 1979. The tectonic evolution of Australia, Earth Sci. Rev., **14**, 205-249.

Polak, E.J. and Horsfall, C.L., 1979. Geothermal gradients in the Great Artesian Basin, Australia, Bull. Aust. Soc. Expl. Geophys., **10**, 144-148.

Pollack, H.N., 1986. Cratonization and thermal evolution of the mantle, Earth. Planet. Sci. Lett., **80**, 175-182.

Porter, C.R., 1976. An empirical approach to the determination of porosity, shale percentage and permeability of Permian sandstones in the Cooper Basin, South Australia, APEA J., **16**, 111-115.

Powell, C. McA., 1984, Terminal fold belt deformation : relationship of mid-Carboniferous mega kinks in the Tasman Fold Belt to coeval thrusts in central Australia, Geology, **2**, 546-549.

Price, L.C., 1983. Geologic time as a parameter in organic metamorphism and vitrinite reflectance as a absolute palaeogeothermometer, J. Petrol. Geol., **6**, 5-38.

Price, L.C., 1985. Geologic time as a parameter in organic metamorphism and vitrinite reflectance as a absolute palaeogeothermometer : reply, J. Petrol. Geol., **8**, 223-240.

Price, L.C. and Barker, C.E., 1985. Suppression of vitrinite reflectance in amorphous rich kerogen. A major unrecognised problem, J. Petrol. Geol., **8**, 59-84.

Price, R.A., 1973. Large scale gravitational flow of supra-crustal rocks, southern Canadian Rockies, in: Gravity and Tectonics, De Jong, K.A., and Scholten, R.A., (Eds), 491-502.

Quilty, P.G., 1984. Phanerozoic climates and environments in Australia, in: Veevers, J.J., (Ed), Phanerozoic Earth History of Australia, 48-56.

Quinlan, G.M., 1987. A survey of subsidence mechanisms in intracratonic basins and their application to North American examples, in: Beaumont, C. and Tankard, A., (Eds), Sedimentary Basins and Basin- Forming Mechanisms, Canadian Society Petroleum Geologists Memoir **12**, in press.

Quinlan, G.M. and Beaumont, C., 1984. Appalachian thrusting, lithospheric flexure and the Palaeozoic stratigraphy of the eastern interior of North America, Can. J. Earth Sci., **21**, 973-996.

Rabinowicz, M., Lago, B. and Souriau, M., 1983. Landward flow in the upper mantle: effects of the heat sink and viscous coupling of the sinking slab, Earth Planet. Sci. Lett., **63**, 76-88.

Ranalli, G. and Murphy, D.C., 1987. Rheological stratification of the lithosphere, Tectonophysics, **133**, 281-295.

Reading, H.G., 1982. Sedimentary basins and global tectonics, Proc. Geol. Assoc., **93**, 321-350.

Reaves, C.M., and von Rosenberg, D.U., 1985. Determination of palaeoheat flux from vitrinite reflectance : discussion. AAPG Bull., **69**, 2148.

Reck, B.H., 1987, Implications of measured thermal gradients for water movement through the northeast Japan accretionary prism, J. Geophys. Res., **92**, 3683-3690.

Richardson, S.W. and England, P.C., 1979. Metamorphic consequences of crustal eclogite production in overthrust orogenic zones, Earth Planet. Sci. Lett., **42**, 183-190.

Rieke, H.R., and Chilingarian G.V., (Eds), 1974. Compaction of Argillaceous Sediments, Developments in sedimentology 16, Elsevier, pp. 424.

Rigby, D. and Smith, J.W., 1981. An isotopic study of gases and hydrocarbons in the Cooper Basin, APEA J., **21**, 222-229.

Ringwood, A.E., 1975. Composition and Petrology of the Earth's Mantle, McGraw-Hill, pp. 618.

Ritter, U., 1984. The influence of time and temperature on vitrinite reflectance, Org. Geochem., **6**, 473-480.

Rosenblat, S., 1985. A mathematical model of compaction-induced migration, J. Geophys. Res., **90**, 779-789.

Rowley, D.B. and Sahagian, D., 1986. Depth-dependent stretching : a different approach, Geology, **14**, 32-35.

Royden, L. and Karner, G.D., 1984. Flexure of the lithosphere beneath the Appeninne and Carpathian foredeep basins, evidence for an insufficient topographic load, AAPG Bull., **68**, 704-712.

Royden, L. and Keen, C.E., 1980. Rifting process and thermal evolution of the continental margin of eastern Canada determined from subsidence curves, Earth Planet. Sci. Lett., **51**, 343-361.

Royden, L., Sclater, J.G., and Von Herzen, R.P., 1980. Continental margin subsidence and heat flow : Important parameters in formation of petroleum hydrocarbons, AAPG Bull., **64**, 173-187.

Rumph, B., 1978. Regional gravity and magnetic data of the central Eromanga Basin: Implications on the crustal structure, regional geology and tectonic history, M. Sc. thesis, Univ. Sydney (unpubl.).

Rybach, L. 1981. Geothermal systems, conductive heat flow, geothermal anomalies, in; Rybach, L., and Muffler, L.J.P., (Eds), Geothermal Systems : Principles and Case Histories, J. Wiley and Sons, 3-36.

Sambridge, M.S. and Kennett, B.L.N., 1986. A novel method of hypocentre location, Geophys. J. Roy. astr. Soc., **87**, 679-697.

Sandiford, M. and Powell, R., 1986. Deep crustal metamorphism during continental extension : modern and ancient examples, Earth Planet. Sci. Lett., **79**, 151-158.

Sawka, W.N. and Chappell, B.W., 1986. The distribution of radioactive heat production in I- and S-type granites and residual source regions: implications to high heat flow areas in the Lachlan Fold Belt, Australia, Aust. J. Earth Sci., **33**, 107-118.

Sawyer, D.S., 1986. Effects of basement topography on subsidence history analysis, Earth Planet. Sci. Lett., **78**, 427-434.

Sawyer, D.S., Hsui, A.T. and Toksöz,. M.N., 1987, Extension, subsidence and thermal evolution of the Los Angeles Basin - a two-dimensional model, Tectonophysics, **133**, 15-32.

Sawyer, D.S., Swift, B.A., Sclater, J.G. and Toksöz, M.N., 1982. Extensional model for subsidence of the northern United States Atlantic continental margin, Geology, **10**, 134-140.

Schedl, A. and Wiltschko, D.V., 1984. Sedimentological effects of a moving terrain, J. Geology, **92**, 273-288.

Scheibnerovà, V., 1976. Cretaceous foraminifera of the Great Artesian Basin, Quart. Notes. NSW Geol. Surv., **21**,8-17

Scheibnerovà, V., 1980. Comparative foraminiferal biostratigraphy of the Santos Oodnadatta No. 1 section, South Australia Basin, Record NSW Geol. Surv., **19**, 81-139.

Scheibnerovà, V., 1986. Marine Cretaceous of the Great Australian Basin- foraminiferal and palynological zones finally reconciled, in: Gravestock, D.I., Moore, P.S., Mount, T.J. and Pitt, G.M., (Eds), Contributions to the Geology and Hydrocarbon Potential of the Eromanga Basin, Geol. Soc. Aust., spec. publ. **12**, 115-118.

Scherer, M., 1987. Parameters influencing porosity in sandstones : A model for sandstone porosity prediction, AAPG Bull.., **71**, 485-491.

Schlumberger Ltd, 1972. Log interpretation vol. 1 - Principles, Schlumberger, pp. 113.

Schmoker, J.W. and Halley, R.B., 1982. Carbonate porosity versus depth : A predictable relationship for south Florida, AAPG Bull., **66**, 2561-2570.

Schubert, G. and Reymer, A.P.S., 1985. Continental volume and freeboard through time, Nature, **316**, 336-339.

Schulz, R., 1987. Analytical model calculations for heat exchange in a confined aquifer, J. Geophys., **61**, 12-20.

Schwab, F.L., 1976. Modern and ancient sedimentary basins : comparative accumulation rates, Geology, **4**, 723-727.

Schwarzacher, W. and Schwarzacher, W., 1986. The effect of fluctuating sealevel in subsiding basins, Comp. Geosci., **12**, 225-227.

Sclater, J.G. and Christie, P.A.F., 1980. Continental stretching : an explanation of post mid-Cretaceous subsidence of the central North Sea, J. Geophys. Res., **85**, 3711-3739.

Sclater, J.G. and Francheteau, J., 1970. The implications of terrestrial heat flow on current tectonic and geochemical models of the crust and upper mantle of the earth, J. Geophys. Roy. astr. Soc., **20**, 509-542.

Sclater, J.G., Jaupart, C and Galson, D., 1980a. The heat flow through oceanic and continental crust and the heat loss of the earth, Rev. Geophys. Space Phys., **18**, 269-311.

Sclater, J.G., Jones, E.J.W. and Miller, S.P., 1970. Relationship of heat flow, bottom topography and basement relief in Peake and Freen deeps, Northeast Atlantic Tectonophysics, **10**, 283-300.

Sclater, J.G., Royden, L., Horvath, F., Burchfiel, B.C., Semken, S. and Stegena, L., 1980b. The formation of the intra-Carpathian basins as determined from subsidence curves, Earth Planet. Sci. Lett., **51**, 139-162.

Sekiguchi, K., 1984. A method for determining terrestrial heat flow in oil basinal areas, Tectonophysics, **103**, 67-79.

Selley, R.C., 1978. Porosity gradients in the North Sea oil-bearing sandstones, J. Geol. Soc. Lond., **135**, 119-132.

Sengör, A.M.C. and Burke, K., 1978. Relative timing of rifting and volcanism on Earth and its tectonic implications, Geophys. Res. Lett., **5**, 419-421.

Senior, B.R., 1971. Structural interpretation of the southern Nebine Ridge area, Queensland, Australasian Oil and Gas Review, **17**, 2-8.

Senior, B.R., 1975. Notes on the Cooper Basin in Queensland, Queensland Govt. Min. J., **76**, 260-265.

Senior, B.R., 1982. LANDSAT interpreted structure and groundwater flow within the Eromanga Basin, in: Moore, P.S. and Mount, T.J. (compilers), Eromanga Basin Symposium, summary papers, Geol. Soc. Aust. and Pet. Explor. Soc. Aust., Adelaide, 329-342.

Senior, B.R. and Habermehl, M.A., 1980. Structure, hydrodynamics and hydrocarbon potential, central Eromanga Basin, Queensland, Australia, Bur. Miner. Resour. J. Aust. Geol. Geophys., **5**, 47-55.

Senior, B.R., Mond, A. and Harrison, P.L., 1978. Geology of the Eromanga Basin, Bur. Min. Resources. Geol. Geophys. Bull. **167**.

Sevier, R., 1983. Burial history and diagenetic reaction kinetics, AAPG Bull., **67**, 684-691.

Sharp, J.M. and Dominenco, P.A., 1976. Energy transport in thick sequences of compacting sediment, Geol. Soc. Am. Bull., **87**, 390-400.

Shaw, R.D., 1987. Basement uplift and basin subsidence in central Australia, Ph.D. thesis, Australian National University.

Shi, Y. and Wang, C-Y., 1986. Pore pressure generation in sedimentary basins : overloading versus aquathermal, J. Geophys. Res., **91**, 2153-2162.

Shiboaka, M. and Bennett, A.J.R., 1977. Patterns of diagenesis in some Australian basins, APEA J., **17**, 58-64.

Sleep, N.H. 1971. Thermal effects of the formation of Atlantic continental margins by continental break-up, Geophys. J. Roy. astr. Soc., **24**, 325-350.

Sleep, N.H., 1976. Platform subsidence mechanisms and "eustatic" sea level changes, Tectonophysics, **36**, 45-56.

Sleep, N.H., Nunn, J.A., and Chou, L. 1980. Platform basins, Ann. Rev. Earth Planet. Sci., **8**, 17-34.

Sleep, N.H. and Snell, N.S., 1976. Thermal contraction and flexure of mid-continent and Atlantic margin basins, Geophys. J. Roy. astr. Soc., **45**,125-143.

Sloss, L.L. and Scherer, W., 1975. Geometry of sedimentary basins : application to Devonian of North America and Europe, Mem. Geol. Soc. Am. **142**, 71-88.

Sloss, L.L. and Speed, R.C., 1974. Relationships of cratonic and continental margin tectonic episodes, in: Dickinson, W.R., (Ed), Tectonics and Sedimentation, Soc. Econ. Palaeontol. Mineral. spec. publ **22**, 98-119.

Smart, J., Grimes, K.G., Doutch, H.F. and Pinchin, J., 1980. The Carpentaria and Karumba Basins, north Queensland, Bur. Miner. Resour. Geol. Geophys. Bull. **202**.

Smart, J. and Senior, B.R., 1980. Jurassic-Cretaceous basins of northeastern Australia, in: Henderson, R.A. and Stephenson, P.J. (Eds), The geology and geophysics of north eastern Queensland, Geol. Soc. Aust. (Qld. Div.), 315-328.

Smith B.L. 1983. Seismic investigations of the Merrimelia field, APEA J., **23**, 192-202.

Smith, G.A., 1987. The influence of explosive volcanism on fluvial sedimentation : the Deschutes Formation (Neogene) in central Oregon, J. Sed. Petrol., **57**, 613-629.

Smith, L. and Chapman, D.S., 1983. On the thermal effects of groundwater flow 1. Regional scale systems, J. Geophys. Res., **88**, 593-608.

Smith, R.B. and Bruhn, R.L., 1984. Intraplate extensional tectonics of the eastern Basin-Range : inferences on structural style from seismic reflection data, regional tectonics and thermal-mechanical models of brittle-ductile deformation, J. Geophys. Res., **89**, 5733-5762.

Snelling, N.J., (Ed), 1985. The Chronology of the Geological Record, Geol. Soc. Lond. Memoir **10**, pp. 343.

Snyder, D.B. and Barazangi, M., 1986. Deep crustal structure and flexure of the Arabian plate beneath the Zagros collisional mountain belt as inferred from gravity observations, Tectonics, **5**, 361-373.

Sørensen, K. 1986. Danish Basin subsidence by Triassic rifting on a lithosphere cooling background, Nature, **319**, 660-663.

Sonder, L.J. and England, P.C., 1986. Vertical averages of rheology of the continental lithosphere : relation to thin sheet parameters, Earth Planet. Sci. Lett., **77**, 81-90.

Sonder, L.J., England, P.C., and Houseman, G.A., 1986. Continuum calculations of continental deformation in transcurrent environments, J. Geophys. Res., **91**, 4797-4810.

Speed, R.C. and Sleep., N.H., 1982. Antler orogeny and foreland basin : a model, Geol. Soc. Am. Bull., **93**, 815-828.

Spohn, T. and Neugebauer, H.J., 1978. Metastable phase transition models and their bearing on the development of Atlantic-type geosynclines, Tectonophysics, **50**, 387-412.

Spohn, T. and Schubert, G., 1982. Convective thinning of the lithosphere : a mechanism for the initiation of continental rifting, J. Geophys. Res., **87**, 4669-4681.

Sprigg, R.C., 1978. Proterozoic, Permo-Carboniferous, and Pleistocene glacial cycles in relation to oil search, APEA J., **18**, 83-92.

Stach, E., Mackowsky, M-Th, Teichmüller, M., Taylor, G., Chandra, D. and Teichmüller, R., 1975. Stach's Textbook of Coal Petrology, Gerbrüder Borntraeger, pp. 428.

Steckler, M.S. and ten Brink, U.S., 1986. Lithospheric strength variations as a control on new plate boundaries : an example from the northern Red Sea Region, Earth Planet. Sci. Lett., **79**, 120-132.

Steckler, M.S. and Watts, A.B., 1978. Subsidence of the Atlantic-type continental margin off New York, Earth Planet. Sci. Lett., **41**, 1-13.

Steckler, M.S. and Watts, A.B., 1980. The gulf of Lion : subsidence of a young continental margin, Nature, **287**, 425-429.

Stegena, L., 1982. Water migration influences on the geothermics of basins, Tectonophysics, **83**, 91-99.

Stephenson, R., 1984. Flexural model of continental lithosphere based on the long term decay of topography, Geophys. J. Roy. astr. Soc., **77**, 385-413.

Stockmal, G.S., Beaumont, C. and Boutilier, R., 1986. Geodynamic models of convergent margin tectonics : transition from rifted margin to overthrust belt and consequences for foreland basin development, AAPG Bull., **70**, 181-190.

Strauss, J.M., and Schubert, G., 1977. Thermal convection of water in a porous medium : Effects of temperature and pressure dependent thermodynamics and transport properties, J. Geophys. Res., **82**, 325-33.

Stuart, W.J., Jr., 1976. The genesis of Permian and Lower Triassic reservoir sandstones during phases of southern Cooper Basin development, APEA J., **16**, 37-46.

Suess, E., 1906. The Face of the Earth, vol. 2. Clarendon Press, pp. 759.

Taylor, J.C.M., 1978. Sandstone diagenesis, state of the art, 1977, J. Geol. Soc. Lond., **135**, 3-5.

Taylor, S.R. and McLennan, S.M., 1985. The Continental Crust: Its Composition and Evolution , Blackwell Scientific Publications, pp. 312.

Telford, W.M., Geldart, L.P., Sheriff, R.E. and Keys, D.A., 1976. Applied Geophysics, Cambridge University Press, pp. 860.

Thorne, J. and Watts, A.W., 1984. Seismic reflection and unconformities at passive continental margins, Nature, **311**, 365-368.

Thornton, R.C.N. , 1979. Regional stratigraphic analysis of the Gidgealpa Group, southern Cooper Basin, Australia, Geol. Surv. S. Aust. Bull., **49**, pp. 140.

Thornton, R.C.N., 1978, Regional lithofacies and palaeogeography of the Gidgealpa Group, APEA J., **18**, 52- 63.

Timoshenko, S. and Woinowsky-Krieger, S., 1959. Theory of Plates and Shells, McGraw-Hill, pp. 580.

Tipper, J.C., 1987. Estimating stratigraphic completeness, J. Geology, **95**, 710-715.

Tissot, B. and Welte, D.H., 1978. Petroleum Occurrence and Formation, Springer-Verlag, pp. 538.

Toksöz, M.N., Cheng, C.H. and Timur, A., 1976. Velocities of seismic waves in porous rock, Geophysics, **41**, 621-645.

Torgersen, T. and Clarke, W.B., 1987. Helium accumulation in groundwater,. III. Limits on helium transfer across the mantle crust boundary beneath Australia and the magnitude of mantle degassing, Earth Planet. Sci. Lett., **84**, 345-355.

Tsenn, M.C. and Carter, N.L., 1987. Upper limits of power law creep of rocks, Tectonophysics, **136**, 1-26.

Tuach, J., Davenport, P.H., Dickson, W.L. and Strong, D.F., 1986. Geochemical trends in the Ackley Granite, southeast Newfoundland : Their relevance to magmatic-metallogenic processes in high-silica granitoid systems, Can. J. Earth Sci., **23**, 747-765.

Turcotte, D.L., 1980. Models for the evolution of sedimentary basins, in: Bally, A.W., Bender, P.L., McGetchin, J.R. and Walcott, R.I., (Eds), Dynamics of Plate Interiors, Am. Geophys. Un. Geodynamics ser., **1**, 21-27.

Turcotte D.L., 1983. Mechanisms of crustal deformation, J. Geol. Soc. Lond., **140**, 701-724.

Turcotte, D.L. and Angevine, C.L., 1982. Thermal mechanisms of basin formation, Phil. Trans. Roy. Soc. Lond., ser. A, **305**, 283-294.

Turcotte, D.L. and Emerman, S.H., 1983. Mechanisms of active and passive rifting, Tectonophysics, **94**, 39-50.

Turcotte, D.L. and McAdoo, D.C., 1979. Thermal subsidence and petroleum generation in the south western block of the Los Angeles Basin, J. Geophys. Res., **84**, 3460-3464.

Turcotte, D.L. and Schubert, G., 1982. Geodynamics. Applications of Continuum Physics to Geological Problems, J. Wiley and Sons, pp. 450.

Turcotte, D.L. and Willemann, R.J., 1983. Synthetic cyclic stratigraphy, Earth Planet. Sci. Lett., **63**, 89-96.

Ungerer, P. and Pelet, R. 1987. Extrapolation of the kinetics of oil and gas formation from laboratory experiments to sedimentary basins, Nature, **327**, 52-54.

Vail, P.R., Mitchum, R.M. and Thompson, S., 1977a. Relative changes of sea level from coastal onlap, in : Payton, C.E., (Ed), Stratigraphic Interpretation of Seismic Data, AAPG memoir **26**, 63-81.

Vail, P.R., Mitchum, R.M. and Thompson, S., 1977b. Seismic stratigraphy and global changes of sea level , in : Payton, C.E., (Ed), Stratigraphic Interpretation of Seismic Data, AAPG memoir **26**, 83-97.

Vail, P.R. and Todd, R.G., 1981. Northern North Sea Jurassic unconformities, chronostratigraphy and sea-level changes from seismic stratigraphy, in: Illing, L.V. and Hobson, G.D., (Eds), Petroleum Geology of the Continental Shelf of North-western Europe, Inst. Petrol., 216-235.

Van Hinte, J.E., 1978. Geohistory analysis - application of micropalaeontology in exploration geology, AAPG Bull.., **62**, 201-222.

Van Hinte, J.H., 1976a. A Jurassic time scale, AAPG Bull., **60**, 489-497.

Van Hinte, J.H., 1976b. A Cretaceous time scale, AAPG Bull., **60**, 498-516.

van Gijzel, P., 1982. Characterization and identification of kerogen and bitumen and determination of thermal maturation by means of qualitative and quantitative microscopical techniques., in Staplin, F.L. (Ed). How to assess Maturation and Palaeotemperatures, Soc. Econ. Palaeontol. Mineral. short course no. 7., 159-216.

Veevers, J.J. (Ed), 1984. Phanerozoic Earth History of Australia, Clarendon Press, pp. 418.

Veevers, J.J., 1986. Breakup of Australia and Antartica estimated as mid-Cretaceous (95±5 Ma) from magnetic and seismic data at the continental margin, Earth Planet. Sci. Lett., **77**, 91-99.

Veevers, J.J., Jones, J.G., and Powell, C. McA., 1982, Tectonic framework of Australia's sedimentary basins, APEA J., **22**, 283-300.

Vincent, P.W., Mortimer, I.R. and McKirdy, D.M., 1985. Hydrocarbon generation, migration and entrapment in the Jackson-Naccowlah area, ATP 259P, southwestern Queensland, APEA J., **25**, 62-84.

Vine, R.R., 1976. The Galilee Basin, 1976, in: Leslie, R.B., Evans, H.J. and Knight, C.L., (Eds), Economic Geology of Australia and Papua New Guinea, 3, Australian Institute of Mining and Metallurgy, Monograph **7**, 316-320.

Vollmayr, T., 1985. Temperature in the subsurface of the Swiss and German Alpine foreland, J. Geodynamics, **4**, 305-319.

Voorhoeve, H. and Houseman, G., 1987. The thermal evolution of lithosphere extending on a low angle detachment zone, Basin Research, in press.

Wake-Dyster, K.D., Moss, F.J., and Sexton, M.J., 1983. New seismic reflection results in the central Eromanga Basin : the key to understanding its tectonic evolution, Tectonophysics, **100**, 147-162.

Walcott, R.I., 1976. Lithospheric flexure, analysis of gravity anomalies and the propagation of seamount chains,in: Sutton, G.H., Manghnani, M.H. and Moberly, R., (Eds), The Geophysics of the Pacific basin and its margins, Am. Geophys. Un. monograph **19**, 431-439.

Waples, D.W. 1980. Time and temperature in petroleum formation : Application of Lopatin's method to Petroleum Exploration, AAPG Bull.., **64**, 916-926.

Watts, A.B. 1978. An analysis of isostasy in the world's oceans 1 : Hawaiian-Emperor seamount chain, J. Geophys. Res., **83**, 5989-6004.

Watts, A.B., 1982. Tectonic subsidence, flexure and global changes of sea level, Nature, **297**, 469-474.

Watts, A.B., Karner, G.D. and Steckler, M.S., 1982. Lithospheric flexure and the evolution of sedimentary basins, Phil. Trans. Roy Soc. Lond., ser. A, **305**, 249-281.

Watts, A.B. and Ryan, W.B.F., 1976. Flexure of the lithosphere and continental margin basins, Tectonophysics, **36**, 25-44.

Watts, A.B. and Steckler, M.S., 1979. Subsidence and eustasy at the continental margin of eastern North America, AGU Maurice Ewing series, 3, 218-234.

Watts, A.B. and Talwani, M., 1974. Gravity anomalies seaward of deep sea trenches and their tectonic implications. Geophys. J. Roy. astr. Soc., **36**, 57-90.

Watts, K.J., 1987, The Hutton Sandstone-Birkhead Formation transition, ATP 269P(1), Eromanga Basin, APEA J., **27**, 215-229.

Webb, A.W., 1974. Geochronology of stratigraphically significant rocks from South Australia, Progress report 7, South. Aust. Dept. Mines Energy, open file Env. **1689**.

Wells, A.T., Forman, D.J., Ranford, L.C., and Cook, P.J., 1970. Geology of the Amadeus Basin, central Australia., Bur. Miner. Resour. Geol. Geophys. Bull. **100**.

Wernicke, B., 1985. Uniform sense normal simple shear of the continental lithosphere, Can. J. Earth Sci., **22**, 108-125.

Willett, S.D., Chapman, D.S. and Neugebauer, H.J., 1985. A thermomechanical model of the continental lithosphere, Nature, **314**, 520-523.

Williams, B.P.J. and Wild, E.K., 1984. The Tirrawarra Sandstone and Merrimelia Formation of the southern Cooper Basin, S. Australia - the sedimentation and evolution of a glaciofluvial system, APEA J., **24**, 377-392.

Williams, B.P.J., Wild, E.K., and Suthill, R.J., 1985. Paraglacial aeolianites : potential new hydrocarbon reservoirs, Gidgealpa Group, southern Cooper Basin, APEA J., **25**, 291-310.

Wiltshire, M.J., 1982a, Revision of Eromanga Basin limits, in: Moore, P.S. and Mount, T.J. (compilers), Eromanga Basin Symposium, summary papers, Geol. Soc. Aust. and Pet. Explor. Soc. Aust., Adelaide, 69-75.

Wiltshire, M.J., 1982b, Late Triassic and Early Jurassic sedimentation in the Great Artesian Basin, in: Moore, P.S. and Mount, T.J. (compilers), Eromanga Basin Symposium, summary papers, Geol. Soc. Aust. and Pet. Explor. Soc. Aust., Adelaide, 58-67.

Withjack, M., 1979. A convective heat transfer model for lithospheric thinning and crustal uplift, J. Geophys. Res., **84**, 3008-3022.

Wolf, D., 1984, Isostatic compensation and continental lithosphere thickness, J. Geophys., **54**, 110-113.

Wood, R.J., 1981. The subsidence history of Conoco well 15/30-1, central North Sea, Earth Planet. Sci. Lett., **54**, 306-316.

Woodbury, A.D. and Smith, L., 1985., On the thermal effects of three-dimensional groundwater flow, J. Geophys. Res., **90**, 759-767.

Wopfner, H., 1963. Post-Winton sediments of probable Upper Cretaceous age in the central Great Artesian Basin, Trans. Roy. Soc. South Aust., **86**, 247-253.

Wopfner, H., Callen, R.A. and Harris, W.K., 1974. The Lower Tertiary Eyre Formation of the southwestern Great Artesian Basin, J. Geol. Soc. Aust., **21**, 17-51.

Wright, N.J.R., 1980. Time, temperature and organic maturation - the evolution of rank within a sedimentary pile, J. Pet. Geol. , **2**, 411-425.

Wyatt, A.R., 1984. Relationship between continental area and elevation, Nature, **311**, 370-372.

Wyatt, A.R., 1986. Post-Triassic continental hypsometry and sea level, J. Geol. Soc. Lond., **143**, 907-910.

Wyllie, M.R.J., Gregory, A.R., and Gardener, G.H.F., 1958. An experimental investigation of factors affecting elastic wave velocities in porous media, Geophysics, **23**, 459-493.

Yorath, C.J. and Hyndman, R.D., 1983. Subsidence and thermal history of the Queen Charlotte Basin, Can. J. Earth Sci., **20**, 135-159.

York, D., 1984. Cooling histories from $^{40}Ar/^{39}Ar$ age spectra : Implications for Precambrian plate tectonics, Ann. Rev. Earth Planet. Sci., **12**, 383-409.

Youngs, B.C., 1975. The Early Permian Purni Formation of the Pedirka Basin, Quart. Geol. Notes, Geol. Surv. S. Aust., **54**, 5-12.

Youngs, B.C., 1976. The Pedirka Basin, in: Leslie, R.B., Evans, H.J. and Knight, C.L., (Eds), Economic Geology of Australia and Papua New Guinea, 3, Australian Institute of Mining and Metallurgy, Monograph **7**, 372-373.

Youngs, B.C. and Boothby, P.G., 1985. The Nappamerri Formation in the Cooper Basin, South Australia and southwestern Queensland, in: Lindsay, J.M., (Ed), Stratigraphy, Palaeontology, Malacology : Papers in honour of Dr. Nell Ludbrook, South. Aust. Dept. Mines and Energy spec. publ. 5, 373-387.

Yuen, D.A. and Fleitout, L., 1985. Thinning of the lithosphere by small scale convective destabilization, Nature, **313**, 125-129.

Zeigler, P.A., 1983. Crustal thinning and subsidence in the North Sea, Nature, **304**, 561.

Ziagos, J.P. and Blackwell, D.D., 1986. A model for the transient temperature effects of horizontal fluid flow in geothermal systems, J. Volcan. Geotherm. Res., **27**, 371-397.